PJNM

Philippine Journal of Nuclear Medicine

Vol. 20 No. 2 July to December 2025

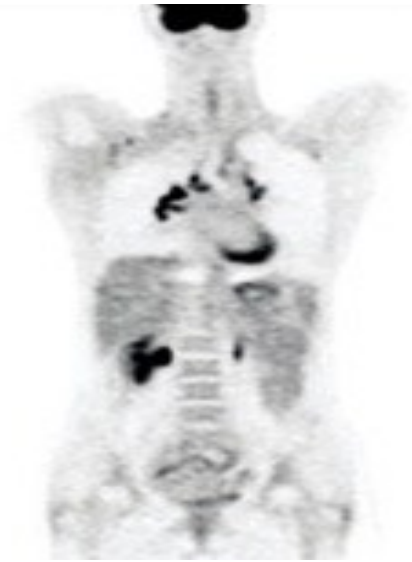

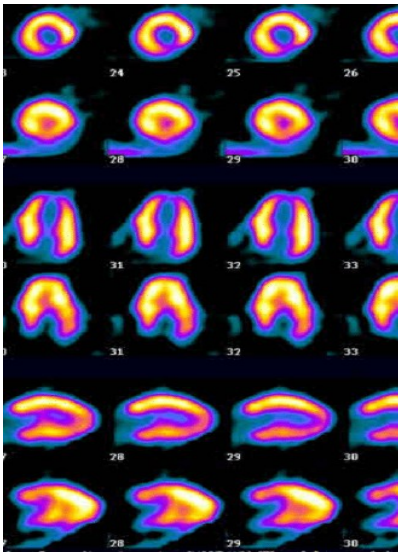

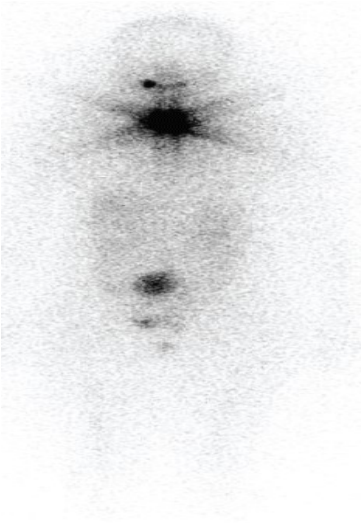

Contents:

Philippine Journal of Nuclear Medicine

Volume 20 No. 2
July to December 2025

Official Publication of the Philippine Society of Nuclear Medicine

The Philippine Journal of Nuclear Medicine is a peer-reviewed journal published by the Philippine Society of Nuclear Medicine. Subscription is free to all PSNM members in good standing as part of their membership privileges.

The Journal will be primarily of interest to medical and paramedical personnel working in nuclear medicine and related fields. Original works in clinical nuclear medicine and allied disciplines in physics, dosimetry, radiation biology, computer science, radiopharmacy, and radiochemistry are welcome. Review articles are usually solicited and published together with related reviews. Case reports of outstanding interest are likewise welcome. PSNM documents and position papers of interest to the reader will also be published as necessary.

Manuscripts for consideration should be sent to:

The Editor, Vincent Peter C. Magboo, MD
Philippine Journal of Nuclear Medicine
c/o Philippine Society of Nuclear Medicine
Unit 209 One Beatriz Tower Condo
4 Lauan St. cor. Aurora Blvd
Project 3, Quezon City 1102, Philippines
Contact. No.: +63 (966) 976 5676
Email: vcmagboo@up.edu.ph
philnucmed@gmail.com

All business communications and requests for complimentary copies should be addressed to the above.

ISSN 1655-9266

INFORMATION FOR AUTHORS

EDITORIAL POLICY

The Philippine Journal of Nuclear Medicine is the official peer-reviewed publication of the Philippine Society of Nuclear Medicine. The Journal accepts original articles pertinent to the field of nuclear medicine. Articles may be on any of the following: clinical and basic sciences, case reports, technical notes, special contributions, and editorials.

Submission of manuscripts

The submitted manuscript package should consist of: (1) the full text (including tables) in Microsoft Word, plain text or ConTeXt document format; and (2) high-resolution JPEG files of all images used in the manuscript. The complete manuscript package may be submitted as a compressed (.ZIP) file by email to philnucmed@gmail.com, or in an optical disc (CD/DVD) and mailed to

> The Editor: Philippine Journal of Nuclear Medicine, c/o Philippine Society of Nuclear Medicine, Unit 209 One Beatriz Tower Condo, 4 Lauan St. cor. Aurora Blvd., Project 3, Quezon City 1102, Philippines.

Manuscripts should be accompanied by a cover letter signed by the author responsible for correspondence regarding the manuscript. The cover letter should contain the following statement:

"All copyright ownership is transferred to the Philippine Journal of Nuclear Medicine upon acceptance of the article _____. This manuscript has been seen and approved by all the authors. The authors stipulate that the material submitted to the Philippine Journal of Nuclear Medicine is an original work and has not been submitted to another publication for concurrent consideration. Any human and/or animal studies undertaken as part of the research are in compliance with regulations of our in stitution(s) and with generally accepted guidelines governing such work."

The cover letter should also give any additional information that may be helpful to the Editor. Signed cover letters sent by email should be in PDF format.

MANUSCRIPT FORMAT

Manuscripts must be written in English, and printed on letter-sized white bond paper, 8.5 in x 11 in (21.6 cm x 27.9 cm). The text should be on one side of the paper only, single-spaced, with at least 1.5 in (4 cm) margins on all sides. Each of the following sections must begin on separate pages and in the following order: title page, abstract, text, acknowledgments, references, tables (each on a separate page), and legends. Pages should be consecutively numbered beginning with the title page. The first line of paragraphs should be indented by at least five spaces.

Title page

The title page should include: (1) a concise but informative title; (2) a short running head or footline of no more than 40 characters; (3) a complete byline, with first name, middle initial, and last name of each author and highest adacemic degrees; (4) the complete affiliation for each author, with the name of departments and institutions to which the work should be attributed; (5) disclaimers, if any; (6) the name, address, and telephone number of the author responsible for correspondence about the manuscript; and (7) the name and address of author to whom reprint requests should be directed.

Abstract and key words
An abstract of no more than 300 words should state the purpose of the study or investigation, summary of methodology, major findings, and principal conclusions. New and important aspects of the study or observations should be emphasized. No figures, abbreviations or reference citations are to be used in the abstract.

Text

The text of original scientific and technical articles is usually divided into the following sections: Introduction, Materials and Methods, Results, Discussion, and Summary or Conclusion.

Case reports are divided into the following sections: Introduction, Case Report, Discussion, and Conclusion. They should contain a concise description of one to three patients, emphasizing the nuclear medicine aspects and include methodology, data and correlative studies. Procedures should be described in sufficient detail to allow other investigators to reproduce the results.

Other articles, e.g. review articles, position papers, or editorials, should introduce a problem or question, present evidence, and conclude with an answer. Generally, review articles should have extensive documentation. Literature citations should represent the breadth and depth of the subjects being reviewed. The organization of review articles will depend greatly on the subject matter and material.
Generic names must be used throughout the text. Instruments and radiopharmaceuticals must be identified by manufacturer name and address in parentheses.

Acknowledgments

Persons or agencies contributing substantially to the work, including any grant support, must be acknowledged.

References

References must be cited in consecutive numerical order at first mention in the text and designated by the reference number in parentheses. References appearing in a table or figure should be numbered sequentially with those in the text.

The reference list must be numbered consecutively as in the text. The journal follows Index Medicus style for references and abbreviates journal names according to the List of Journals Indexed in Index Medicus. 'Unpublished observations' and 'personal communications' should not be used as references, although written—not verbal—communications may be noted as such in the text. The author is responsible for the accuracy of all references and must verify them against the original document.

For journal articles with six or less authors, all authors must be listed. For those with seven or more authors, only the first three are listed, and "et al." is added to the end of the list.

> Seabold JE, Conrad GR, Kimball DA, Ponto JA and Cricker JA. Pitfalls in establishing the diagnosis of deep venous thrombophlebitis by indium-111 platelet scintigraphy. J Nucl Med 1988;29:1169–1180.

For book and book chapters:

> Williams LJ. Evaluation of parathyroid function. In: Brock LJ, Stein JB, eds. The parathyroid and its diseases. 4th ed. New York: Wiley; 1985:196–248.
>
> Goodyear B. Bone marrow transplantation in severe combined immunodeficiency syndrome. In: Gree HJ, Blackscmith R, eds. Proceedings of the fourth biennial meeting of the International Society of Transplantation. Houston: International Society of Transplantation; 174: 44–46.

For journal article in electronic format:

> Author. Title. Journal name. Online publishing date. Available from: URL address.

Tables

Each table should be typed double-spaced on a separate page. Do not submit tables as photographs. Tables should be self-explanatory and should supplement, not duplicate, the text. Each table must be cited in consecutive numerical order in the text. Tables should be numbered consecutively with a Roman number following the word TABLE.

Illustrations

Illustrations should clarify and augment the text. Figures should be sharp and of high quality. Glossy photographs of line drawings rendered professionally on white drawing paper in black India ink, with template or typeset lettering, should be submitted. High quality computer-generated art is also acceptable. Letters, numbers, and symbols should be clear and of sufficient size to retain legibility after reduction.

Each illustration must be numbered and cited in consecutive order in the text. Illustrations should be identified on a gummed label. Legends should be typed double-spaced on a separate page. Figures should be numbered with an Arabic number following the word FIGURE.

Units of measurement

Use of the International System of Units (SI) is standard. Measurements of length, height, weight, and volume must be reported in metric units. Other measurements must be reported in the units in which they were made. Alternative units (non-SI units) should be added in parentheses by the author, if indicated.

Abbreviations and symbols

Only standard abbreviations and symbols should be used in the text. At first mention, the complete term, followed by its abbreviations in parentheses, must be used in the text. Standard units of measure should not be expanded at first mention. Consult a style manual, if necessary.

REVIEW PROCEDURE

Submitted manuscripts are peer-reviewed for originality, significance, adequacy of documentation, reader interest, composition, and adherence to the guidelines. Manuscripts are returned to the author for revision if suggestions and criticisms have been made. All accepted manuscripts are subject to editing for scientific accuracy, clarity, and style.

Author Disclosure of Interest

Authors are required to disclose any interest, relationship/s, or potential conflicts of interest upon submission of their manuscript.

Each of the authors must accomplish and submit the ICMJE Disclosure of Interest. (https://www.icmje.org/downloads/coi_disclosure.docx).

GE HealthCare

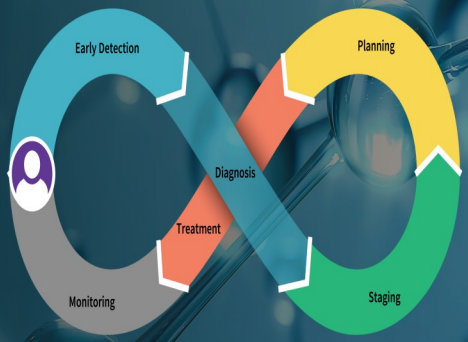

It's time for a Theranostics revolution

Cyclotron Solutions
PETtrace™ 800 Cyclotron
^{68}Ga Liquid Target
^{68}Ga Solid Target

Radiochemistry
FASTlab™ 2 New Edition Developer

Discovery PET/CT
Solutions with high sensitivity, Precision DL, Q.Clear & MotionFree to image ^{68}Ga for diagnosis, staging or restaging

Digital SPECT/CT
Solutions to image and quantitate ^{177}Lu imaging accurately to personalise patient treatment

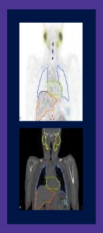

Digital AI applications for Effective quantitation including automatic **AI-based segmentation**

Discovery

Diagnosis

Treatment

ESCO HEALTHCARE

"Discovery to Delivery"

Radiopharmacy Equipment

The Ultimate Solution for Your Radiopharmaceutical Needs

Esco Frontier® Radioisotope™ Fume Hood (EFI)

Cytoculture® Lead-Shielded Biological Safety Cabinet

Lead-shielded Biological Safety Cabinet

Streamline® Shielded Isolator

GMP-compliant Radioisotope Dispensing Isolator

Esco Philippines, Inc
Manila
Unit 707E, 7th floor, East Tower Four E-com Center,
Block 22 Seaside Cor Diokno Ave.
MOA Complex, Pasay City 1300
Tel: 0917 806 8026
Email: philippines@escolifesciences.com

www.escolifesciences.com

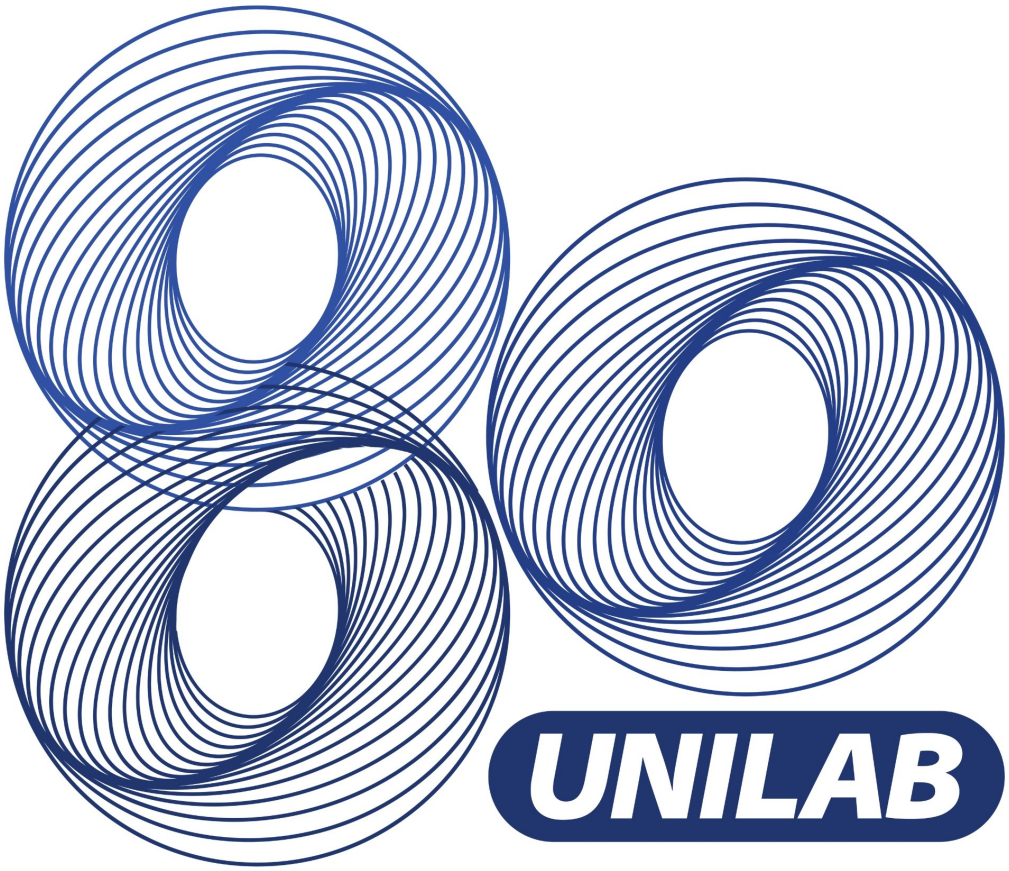

LRI-THERAPHARMA

The Cardio-Metabolic Subsidiaries of UNILAB

Levothyroxine

TFour

Higher Compliance Through Higher Savings

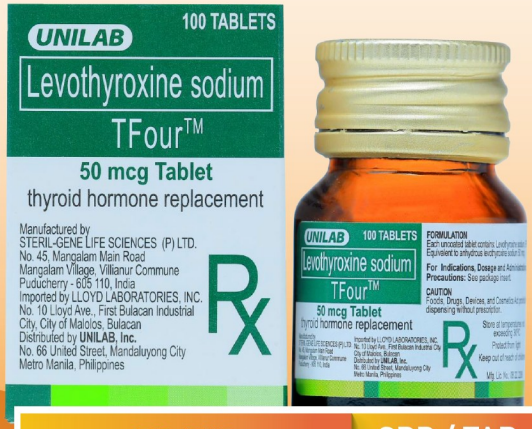

BRAND	SRP / TAB
TFOUR 50 MCG	₱7.50
BRAND E	₱10.45

28% LOWER IN PRICE THAN BRAND E*

BRAND	SRP / TAB
TFOUR 100 MCG	₱12.00
BRAND E	₱19.25

38% LOWER IN PRICE THAN BRAND E*

BASED ON PRICES AS OF FEBRUARY2025

Effects of Delayed Analysis of Serum Sample on the Stability of Thyroid Hormones Using Radioimmunoassay and Immunoradiometric Assay

Christian Dominique Sta. Cruz Yu, MD, Marcelino A. Tanquilut, MD, Wenceslao S. Llauderes, MD, Emelito O. Valdez-Tan, MD, Ivan Ray F. David, MD, Novy Jean B. Dela Cruz, RMT

Department of Nuclear Medicine, Jose R. Reyes Memorial Medical Center
E-mail address: christianyumd@gmail.com

ABSTRACT

Background:

Proper and accurate quantification of thyroid hormones are vital in the diagnosis of thyroid diseases. This study aims to determine if the duration of storage of serum samples affects the stability and levels of thyroid hormones using RIA and IRMA among OPD patients at Jose R. Reyes Memorial Medical Center .

Methodology:

A prospective study was done with the use of ANOVA on repeated measures to compare the values of the thyroid hormones from 24th(baseline), 72nd, and 168th hour. A total of 50 patients were included in the study wherein patient's blood sample of 10cc was divided into 3 aliquots and was processed in 3 different time points. The statistical significance was based on a value of $p < 0.05$ with a 95% confidence interval. In determining the stability of the hormones, if the results obtained at the 72nd and 168th hour period remained within the run-to-run precision of coefficient of variation of ≤ 10% then it would be considered the same as from the baseline value .

Results:

There was no significant change ($p > 0.05$) in the TSH levels from the baseline compared to the delayed samples, and the coefficient of variation was within the acceptable limit. Both FT3 and FT4 levels showed significant increase from baseline compared with the delayed samples ($p < 0.05$) ,and the coefficient of variation surpassed the acceptable limit .

Conclusion:

RIA and IRMA is a robust method allowing us to quantify the otherwise unmeasurable and aids our clinicians to accurately diagnose and manage patients with thyroid disorder. TSH holds stable and accurate despite delayed separation and sampling, while the FT3 and FT4 levels significantly increased in delayed sampling and separation compared to the baseline possibly due to pre-analytic artifacts caused by non-esterified fatty acids. To address this limitation, we recommend that samples requested with FT3 and FT4 be processed immediately, the sample be separated and be refrigerated immediately, or FT3 and FT4 be analyzed along with TSH levels. As for TSH, delayed separation and sampling can be routinely done due to its stability .

Keywords*: Thyroid hormones, Radioimmunoassay, Immunoradiometric assay*

INTRODUCTION

Thyroid disease is widespread and about 300 million people worldwide presents with thyroid dysfunction, such as hypothyroidism and hyperthyroidism [1,2] In such patients, analysis of the thyroid hormones is imperative to conclude a clear diagnosis and for monitoring of the said thyroid disorder, hence a reliable quantitation of thyroid hormone levels should be utilized [3, 4]. Serum TSH is used as the initial screening test since it has the highest sensitivity and specificity for evaluation of suspected thyroid disease. However, accuracy of the diagnosis improves when serum of FT3 and FT4 are analyzed along with the serum TSH [5, 6].

Various methods are used to measure the said hormones and among these methods are the radioimmunoassay (RIA) and immunoradiometric assay (IRMA) methods, methods that offer a technique to quantify the otherwise unmeasurable with high sensitivity and specificity and are the most reliable method for quantification of thyroid hormones, however it requires a long incubation period, specially trained staff, equipment, and radioactive materials [1].

Conventionally, due to long incubation period RIA and IRMA use the batch assay technique wherein pooled samples are analyzed or processed at the same time. A batch assay offers control over measurement errors resulting from variations in kits and batches, including the radiotracer's decay, radioactivity, incubation period, and laboratory conditions [7]. Because of the batch assay's practical simplicity and technical stability, this practice was preferred for RIA and IRMA. Another option is to send blood samples to a central laboratory, which would allow one facility to handle a large geographic area [8].

However, compared to the random assay technique, batch assay has restrictions regarding the relative lag of report time because it requires many samples to be more cost-effective [7]. Some studies recommend that the facilities offering such tests should make an effort to perform the analysis within 24 hours since thyroid hormones may not always be stable under storage condition at room temperature (20 - 25C) with delayed sample analysis [9].

For batch sampling, blood sample screening can be done at clinics or centers, and the unfrozen blood samples can be transported to storage laboratories. In developing countries, it is extremely difficult to process samples as quickly as possible because RIA and IRMA require measuring multiple subjects in order to be more cost-effective. Most middle-sized laboratories cannot afford to perform random sampling analysis on a daily basis. As a result, samples are kept in storage for a prolonged period [10].

The Philippines being a developing country also face the same predicaments in sample analysis using RIA and IRMA since there are also limited facilities that are capable of running and analyzing thyroid hormones using RIA and IRMA. As a result, batch sampling is utilized in order to accommodate multiple samples from different clinics, laboratories, and hospitals. The samples are sometime stored at room temperature as batches for several days before the analysis of the samples causing a lag in the report time. Currently there are no local data on the effects of long storage prior to sampling using RIA and IRMA .

OBJECTIVE

This study aims to determine if the duration of storage at room temperature of serum samples affects the stability of thyroid hormones using RIA and IRMA among patients at Jose R. Reyes Memorial Medical Center and contribute information about the changes in the values of the samples with delayed analysis to guide both our nuclear medicine physicians and clinicians in releasing accurate results.

METHODOLODY

This study is a prospective study where we aim to determine if there would be a significant difference in thyroid hormone levels (TSH, FT3, and FT4) if the same samples are processed on different time points using RIA and IRMA (DIAsource). The sample size computation considers the average blood of 121 based on of the study of Nye et al. (1975) [11]. Where the needed computed sample size was at least 45 at 95% confidence level and 80% power of test as shown in Figure 1. Convenience sampling was done for this study and patients that came to the OPD Nuclear Medicine Department requiring testing of thyroid function test were asked if they would like to participate in this study.

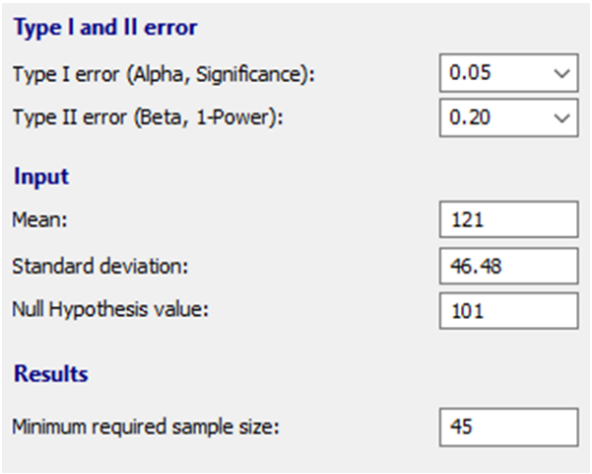

FIGURE 1. Computation for sample size

Each patient's blood sample of 10cc was divided into 3 aliquots in plain tubes. The 1st aliquot was processed on the same day. The 2nd and 3rd aliquot was stored at room temperature of (20-25C), clotted, and unseparated for 72nd and 168th hour, respectively before sample was processed by single technologist using RIA and IRMA. The serum from aliquots were analyzed by RIA/IRMA in different periods to compare the levels and changes of thyroid hormone. Data gathered was analyzed per patient, hormone, and day of processing .

Descriptive statistics such as mean, standard deviation, and coefficient of variation (CV) were used to present the thyroid hormone levels. In comparing the values from 24th, 72nd, and 168th hour, ANOVA on repeated measures was utilized. The statistical significance was based on a value of $p < 0.05$ with a 95% confidence interval.

Mean and standard deviation were computed per day of processing ,and pairwise comparison was done to identify the percent change and p-value of the same hormone from the different periods of processing. This study also employed the interpretation of Nye et al. (1975) and Kubasik et al. (1982), in determining the stability of the hormones [11, 12] If the results obtained at the 72nd and 168th hour period remained within the run-to-run precision of (CV of ≤ 10%), it would be considered the same as from the baseline value [11]. If the results obtained at the 72nd and 168th hour exceeds the coefficient of variation of 10%, the sample will be deemed not acceptable and will be considered different from the baseline value and would be statistically significant if the p-value was ≤ 0.05.

This research was conducted with the approval of Jose R. Reyes Memorial Medical Center Institutional Review Board. Identity of patients were not disclosed and confidentiality were ensured. Retrieval of medical records and patient information from the department was done in a systematic and organized manner to prevent untoward incidents. Patient information utilized were during the data collection period of January 2022 to December 2023.

RESULTS

A total of 50 patients consented and were included in the study. Table 1 shows the average of TSH levels per period. The coefficient of variation (9.12%) of TSH was within the acceptable limit of 10% (CV) and was considered the same with the baseline value. Table 2 shows that the percent change from the baseline TSH as compared with the 72nd hour (9.98%) and 168th hour (8.87%). This was not statistically significant with p value > 0.005.

TABLE 1. TSH (uIU/ml) Levels for the 24th, 72nd, and 168th hour

Hour	Mean ± SD	95% CI	CV
24^{th}	5.41 ± 12.36	(1.900, 8.927)	9.12%
72^{nd}	5.95 ± 14.71	(1.765, 10.126)	
168^{th}	5.89 ± 14.80	(1.686, 10.097)	

TABLE 2. Pairwise Comparison of TSH Levels for the 24th, 72nd, and 168th hour

Pairwise comparison		Percent Change	95% CI
24^{th}	72^{nd}	9.98%	(-1.428, 0.363) p = 0.338
	168^{th}	8.87%	(-1.706, 0.749) p = 1.000
72^{nd}	168^{th}	1.01%	(-0.705, 0.814) p = 1.000

Table 3 shows the average of FT3 levels per period. The coefficient of variation (14.39%) of FT3 exceeded the acceptable limit of 10% (CV), It was deemed not acceptable and was considered different from the baseline value. Table 4 shows significant increase in FT3 levels from baseline with a percent change at 72nd hour (13.25%) and 168th hour (10.54%) and a p-value of ≤ 0.005. The change (2.39%) between FT3 levels at 72nd and 168th hour was not significant (p = 0.8533).

Table 5 shows the average of FT4 levels per period. The coefficient of variation (11.78%) of FT4 exceeded the set limit of 10% (CV). It was deemed not acceptable and was considered different from the baseline value. Table 6 shows a significant increase in FT4 levels from baseline with a percent change at 72nd hour (10.57%) and 168th hour (14.40%) and a p-value of ≤ 0.005. The change (3.47%) between FT4 levels of 72nd and 168th hour was not significant (p = 0.6613).

TABLE 3. FT3 (pmol/L) Levels for the 24th, 72nd, and 168th hour

Hour	Mean ± SD	95% CI	CV
24th	3.32 ± 3.23	(2.406, 4.240)	14.39%
72nd	3.76 ± 3.78	(2.688, 4.835)	
168th	3.67 ± 3.42	(2.697, 4.640)	

TABLE 4. Pairwise Comparison of FT3 Levels for the 24th, 72nd, and 168th hour

Pairwise comparison		Percent Change	95% CI (p-value)
24th	72nd	13.25%	(-0.718, -0.160) p = 0.0009
	168th	10.54%	(-0.607, -0.084) p = 0.0050
72nd	168th	2.39%	(-0.120, 0.304) p = 0.8533

TABLE 5. FT4 (pmol/L) Levels for the 24th, 72nd, and 168th hour

Hour	Mean ± SD	95% CI	CV
24th	14.86 ± 8.51	(12.439, 17.273)	11.78%
72nd	16.43 ± 8.06	(14.139, 18.722)	
168th	17.00 ± 8.60	(14.559, 19.447)	

TABLE 6. Pairwise Comparison of FT4 Levels for the 24th, 72nd, and 168th hour

Pairwise comparison		Percent Change	95% CI (p-value)
24th	72nd	10.57%	(-2.443, -0.706) p = 0.0001
	168th	14.40%	(-2.776, -1.518) p = 0.0001
72nd	168th	3.47%	(-1.716, 0.571) p = 0.6613

DISCUSSION

The baseline for the TSH was compared with the TSH values of 72nd hour and values of 168th hour. It showed TSH to be stable and presented with no significant change even in delayed sampling (room temperature). In line with our result, the study of Basanta also showed stability of thyroid stimulating hormone (TSH) using ELISA, wherein the TSH levels also presented with no change despite delayed analysis and the samples being stored in varying temperatures [10]. The findings were similar with the study of Subhi wherein the TSH gave an acceptable concordance with respect to the fresh assay up to 3 days of refrigerated storage and found that TSH could be stored for up to 7 weeks with acceptable results [9]. These studies concluded that TSH may be resistant to degradation, immunologically stable, and reasonably insensitive to delayed sampling [9, 10].

On the other hand, our findings with the delayed sampling of FT3 and FT4 showed significant change as compared to the baseline. There was a significant increase in both FT3 and FT4 on the 72nd hour and on the 168th hour compared with the baseline. There were no significant change with the levels of both FT3 and FT4 between the 72nd and 168th hour. These findings were also similar to the study of Subhi where FT3 and FT4 using a chemiluminescent immunoassay. It showed a degree of discordance or coefficient of variation of the samples processed on the delayed days as compared to the initial result with CV values greater than 10% [9]. The FT4 had an unacceptable increase in variability in day 4 of refrigerated storage, while the free FT3 had an unacceptable increase in variability in day 3 of refrigerated storage.

A similar study conducted by Nishi showed similar results wherein samples were stored in a refrigerator with a temperature of (4-8C) and room temperature (20 - 25C). The FT4 and TSH values of the samples stored in an EDTA-tube were significantly lower than the samples stored in a serum tube. Serum and plasma FT4 values were decreased during the time that the samples were stored in a room temperature environment. With this finding, they concluded that TSH and Free T4 were not always stable under the storage condition at room temperature [13].

About 75% of the total circulating T4 concentration in normal human serum is carried on thyroxine-binding globulin (TBG), with the remaining 10%-15% linked to albumin and the other 10%-15% attached to transthyretin. Similarities exist in T3 carriage, with the exception that less of it is transthyretin-bound. The displacement of T4 and T3 from TBG may occur as a result of non-esterified fatty acids (NEFA). Both a high

blood triglyceride concentration and room temperature sample with delayed storage increase the amount of NEFA generated in vitro. Preanalytic artifacts caused by NEFA production in the sample could therefore cause an overestimation of free T4 and free T3 due to the displacement of the hormone from TBG that may explain the increase in the levels of our findings [15, 16].

With these findings, the hypothyroid values raised into the euthyroid range or euthyroid values raised to the thyrotoxic range, the changes in hormone levels could easily lead to a misdiagnosis. FT4 and FT3 should be correlated with the serum TSH concentration while paying attention to the assumptions that govern this connection [10]. It is appropriate to apply an alternative free thyroid hormone technique based on a different assay principle and correlate the result with an authentic total T4 measurement if an FT4 anomaly is still not explained after repeat sampling [13]. In addition, extended serum-clot contact may also result in pre-analytical variation. Thus, unless there is clear proof that longer contact times do not add to result inaccuracy, serum or plasma should be separated as soon as possible [10, 14].

With the studies presented along with our data, it showed that only TSH was stable even in delayed sampling while being stored at room temperature. Both FT3 and FT4 were not always stable under delayed sampling while stored at room temperature [10].

Since there are limited RIA/IRMA facilities in the Philippines, and most laboratories pool and delay their sampling in order to cater to more patients and be more cost-effective, it should be noted that the change in the stability of the thyroid hormone levels during delayed storage and sampling is critical in producing accurate results.

CONCLUSION

RIA and IRMA is a robust method allowing us to quantify the otherwise unmeasurable and aids our clinicians to accurately diagnose and manage patients with thyroid disorder. TSH holds stable and accurate despite delayed separation and sampling, while the FT3 and FT4 levels significantly increased in delayed separation and sampling compared to the baseline possibly due to pre-analytic artifacts caused by NEFA. To address this limitation, we recommend that samples requested with FT3 and FT4 be processed within 24 hours than later if possible, samples be separated and be refrigerated immediately, or FT3 and FT4 be analyzed along with TSH levels. As for TSH, delayed separation and sampling may be done considering its stability.

Due to the price of the radioimmunoassay kits, further analysis of a more prolonged period (2 weeks) in sampling was not achieved and only 1 brand of radioimmunoassay was used. We recommend to have a larger sample size, use several brands of RIA and IRMA kit with comparison of samples to other assay methods such as ELISA or chemiluminescent and to also compare samples stored in varying temperature.

DISCLOSURE

The authors of this study have no conflicts of interest to disclose.

REFERENCES

1. Shamsian, A.A., Ghazvini, K., Sokhtanloo, M. et al. Which quantitative method in determination of the thyroid hormone levels is more consistent with the clinical symptoms of the thyroid disorders?. Comp Clin Pathol 25, 101–106 (2016). https://doi.org/10.1007/s00580-015-2148-2.
2. Kasper, D. L., Fauci, A. S., Hauser, S. L., Longo, D. L., Jameson, J. L., & Loscalzo, J. (Eds.). (2015). Harrison's Principles of Internal Medicine, 19th Edition (Vol. 1 & 2) (ebook). McGraw-Hill Professional.
3. Kravets, I. Hyperthyroidism: Diagnosis and Treatment. AAFP American Academy of Family Physicians. (2016). https://www.aafp.org/afp/2016/0301/afp20160301p363.pdf
4. Mullur R, Liu YY, Brent GA. Thyroid hormone regulation of metabolism. Physiol Rev. 2014 Apr;94(2):355-82. doi: 10.1152/physrev.00030.2013. PMID: 24692351; PMCID: PMC4044302.
5. Ross DS, Burch HB, Cooper DS, Greenlee MC, Laurberg P, Maia AL, Rivkees SA, Samuels M, Sosa JA, Stan MN, Walter MA. 2016 American Thyroid Association Guidelines for Diagnosis and Management of Hyperthyroidism and Other Causes of Thyrotoxicosis. Thyroid. 2016 Oct;26(10):1343-1421. doi: 10.1089/thy.2016.0229. Erratum in: Thyroid. 2017 Nov;27(11):1462. doi: 10.1089/thy.2016.0229.correx. Erratum in: Thyroid. 2025 Sep;35(9):1097. doi: 10.1089/thy.2016.0229.correx2. PMID: 27521067.
6. Dayan CM. Interpretation of thyroid function tests. Lancet. 2001 Feb 24;357(9256):619-24. doi: 10.1016/S0140-6736(00)04060-5. PMID: 11558500.

7. Lee JM, Lee HH, Park S, Kim TS, Kim SK. Random Assay in Radioimmunoassay: Feasibility and Application Compared with Batch Assay. Nucl Med Mol Imaging. 2016 Dec;50 (4):337-343. doi: 10.1007/s13139-016-0436-7. Epub 2016 Jul 26. PMID: 27994689; PMCID: PMC5135698.
8. Piyasena, R. (1992). Radioimmunoassay in Developing Countries. nis.iaea.org/collection/NCLCollectionStore/_Public/29/049/29049611.pdf?r=1&r=1
9. Al-Jubori, H. A., & Al-Jumaily, H. M. Effect of storage temperature on the stability of free T4, free T3 and third generation TSH results by DPC Immulite 2000. Journal of the Bahrain Medical Society, 15(4), 204-207 (2003).
10. Basanta G, Gupta SP, Gautam S, Ashwini KN, Lal Das BK, et al. Effect of Delay Separation and Short Term Storage of Serum on Thyroid Stimulating Hormone (TSH). Open J Thyroid Res 1(1): 007-009 (2017). DOI: 10.17352/ojtr.000003.
11. Nye L, Yeo TH, Chan V, Goldie D, Landon J. Stability of thyroxine and triiodothyronine in biological fluids. J Clin Pathol. 1975 Nov;28(11):915-9. doi: 10.1136/jcp.28.11.915. PMID: 829832; PMCID: PMC475893.
12. Kubasik NP, Ricotta M, Hunter T, Sine HE. Effect of duration and temperature of storage on serum analyte stability: examination of 14 selected radioimmunoassay procedures. Clin Chem. 1982 Jan;28(1):164-5. PMID: 7034999.
13. Nishi I, Okada Y, Hayashi J, Takeoka K, Amino N, Miyai K. [Effect of various sampling condition on the measurement of circulating TSH and free thyroxine]. Rinsho Byori. 1992 Apr;40(4):417-22. Japanese. PMID: 1593766.
14. Wu, Z. (2022). Effect of Radioimmunoassay on accuracy of thyroid hormone detection. Publishing Open Access research journals & papers | Hindawi. https://doi.org/10.1155/2022/9206079.
15. Stockigt JR. Free thyroid hormone measurement. A critical appraisal. Endocrinol Metab Clin North Am. 2001 Jun;30 (2):265-89. doi: 10.1016/s0889-8529(05)70187-0. PMID: 11444163.
16. Hegstad-Davies RL. A review of sample handling considerations for reproductive and thyroid hormone measurement in serum or plasma. Theriogenology. 2006 Aug;66(3):592-8. doi: 10.1016/j.theriogenology.2006.05.004. Epub 2006 Jul 7. PMID: 16828859.

Liver, Kidney, and Urinary Bladder Metastases from Papillary Thyroid Cancer

Francis Manuel L. Resma, MD, Ruben V. Ogbac, MD, John Ricardo C. Solito, MD,
Benjamin Francis P. Rodriguez Jr., MD

Division of Nuclear Medicine Department of Medicine, Philippine General Hospital, University of the Philippines Manila
E-mail address: flresma@up.edu.ph

ABSTRACT

Metastasis to the liver, kidney, or urinary bladder from differentiated thyroid cancer is rare. Combined liver, kidney, and urinary bladder metastases are even rarer. Single-photon emission computed tomography with computed tomography (SPECT/CT) and other imaging modalities are vital in the detection and evaluation of such lesions. For patients with multiple distant metastases, surgical excision or external beam radiation therapy of all lesions is not practical. These patients can be treated with radioactive iodine (RAI) therapy if the lesions demonstrate iodine-131 (I-131) uptake. We report a case of papillary thyroid cancer with liver, kidney, and urinary bladder metastases (on top of lymph node, lung, and bone metastases) who received RAI therapy. To our knowledge, this is the first reported case.

Keywords*: Papillary thyroid cancer, liver metastasis, kidney metastasis, urinary bladder metastasis*

INTRODUCTION

Papillary thyroid carcinoma is the most common type of thyroid cancer, constituting 80% of cases [1]. It is two to four times more common in women than in men, and the average age of patients at the time of diagnosis is 40 years [2]. Regional lymph node metastasis is seen in 30 - 40% of patients with papillary thyroid cancer, while metastases to distant sites occur in 1 - 4% of cases. The most common sites of distant metastasis are the lungs and bones [3]. Metastasis to the liver, kidney, or urinary bladder from differentiated thyroid cancer is rare [4, 5, 6].

Case Presentation

A 65-year-old female with a 30-year history of a gradually enlarging anterior neck mass consulted in our institution with a chief complaint of worsening left hip pain, which began when she fell on her left hip 6 months prior. A radiograph of the pelvis was acquired which revealed an osteolytic focus in the proximal left femur, with an associated left hip fracture (Figure 1).

Bone scintigraphy was also ordered which demonstrated osteoblastic lesions in the skull, L3 vertebra, pelvis, and proximal left femur that were suggestive of bone metastases (Figure 2)

Because the anterior neck mass was suspected to be the primary malignancy, a neck ultrasound was performed which exhibited a TI-RADS 5 right thyroid lobe mass and cervical lymphadenopathy. A fine needle aspiration biopsy of the anterior neck mass was thus done, with findings suspicious for papillary thyroid carcinoma (Bethesda Category V). A neck, chest, and abdominal computed tomography (CT) scan with contrast was eventually requested which showed a 9.0 x 4.4 x 6.1 cm right thyroid lobe mass that was suspicious for malignancy, along with cervical and mediastinal lymphadenopathies, subcentimeter pulmonary nodules, and multiple lytic osseous foci with soft tissue components that were worrisome for metastases. Other findings included a 1.3 x 1.4 x 1.3 cm nodule in the right liver lobe, and a 1 x 1 cm nodule in the urinary bladder (Figure 3).

The patient then underwent proximal resection and cemented total arthroplasty of the left hip, with the final histopathologic diagnosis of metastatic carcinoma from a primary thyroid malignancy. Four months later, total thyroidectomy with central neck dissection was done, with the histopathologic diagnosis of papillary thyroid carcinoma, infiltrative follicular variant, 7.7 cm in greatest tumor dimension, involving the right lobe and isthmus, with microscopic strap muscle invasion and extensive angioinvasion. One of four lymph nodes was positive for tumor, with the largest metastatic deposit measuring 3.0 centimeters

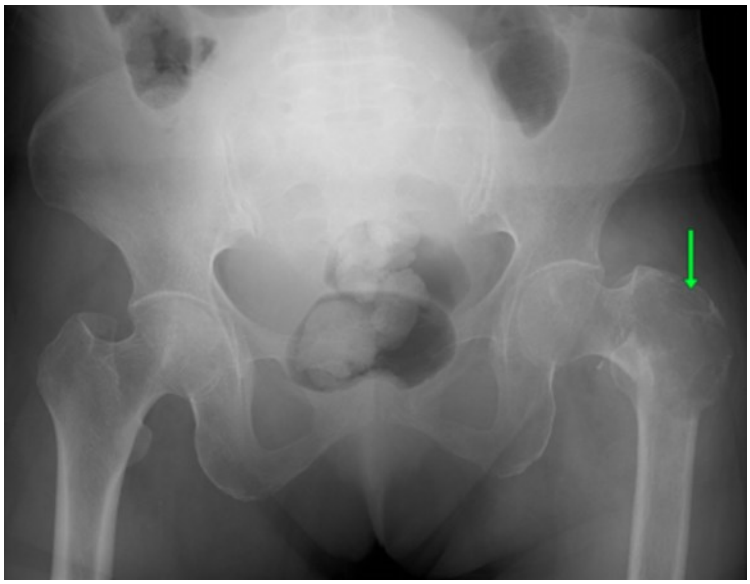

FIGURE 1. Radiograph of the pelvis. Expansile osteolytic focus in the greater trochanter of the left femur (light green arrow), associated with a fracture in the left femoral neck

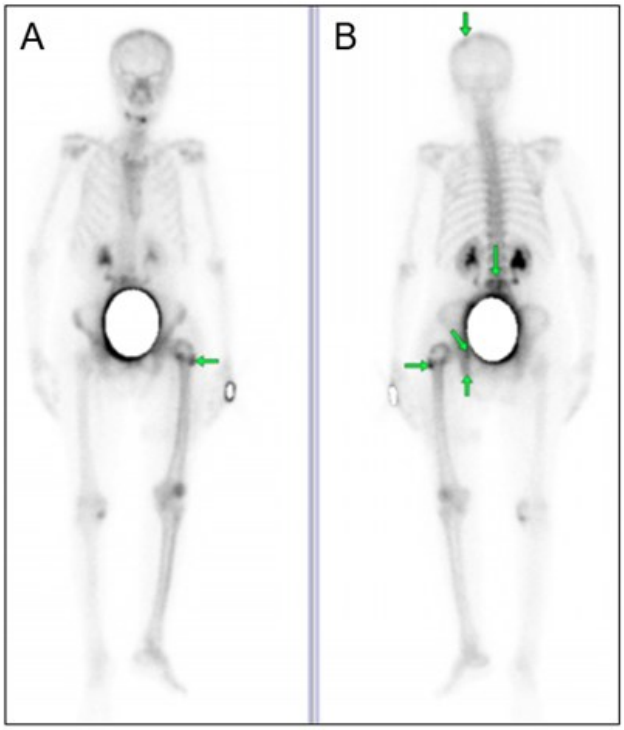

FIGURE 2. (A) Anterior and (B) posterior images of whole-body bone scintigraphy. Osteoblastic lesions in the left parietal bone, L3 vertebra, wall of the left acetabulum, left ischium, and proximal left femur (light green arrows), suggestive of bone metastases.

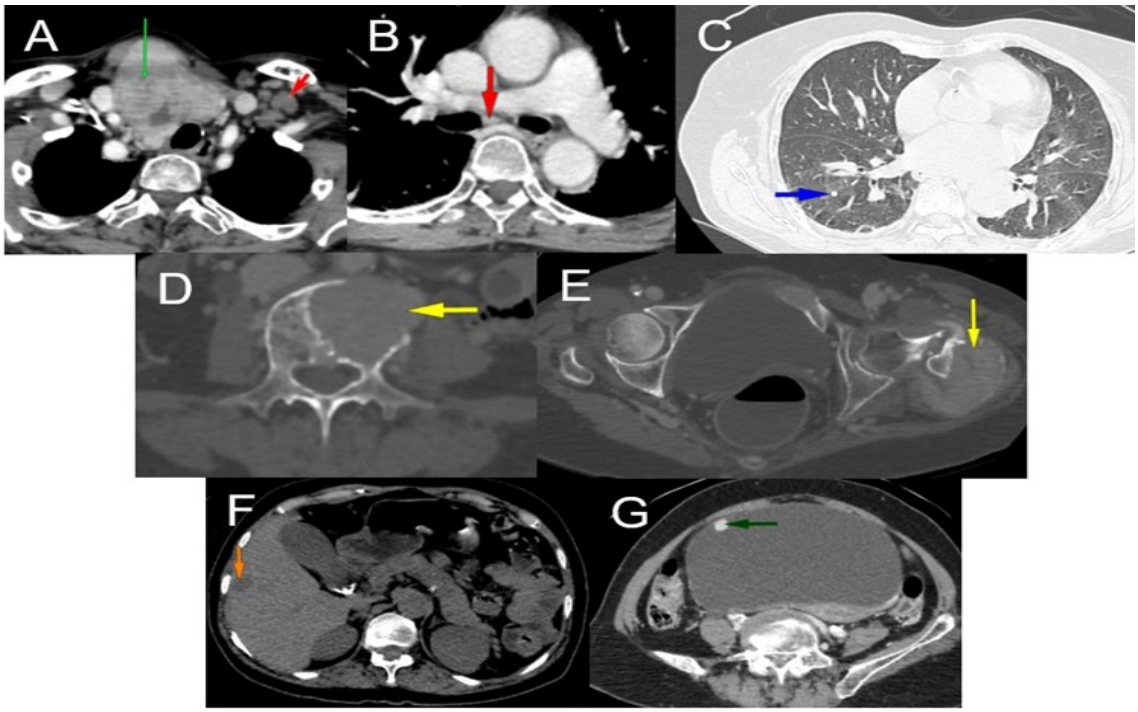

FIGURE 3. Neck, chest, and abdominal CT scan with contrast. (A) Large mass in the right thyroid lobe (light green arrow), and left supraclavicular lymphadenopathy (red arrow). (B) Subcarinal lymphadenopathy (red arrow). (C) Nodule in the lower lobe of the right lung (blue arrow). (D) Osteolytic lesion with soft tissue component in the L3 vertebra (yellow arrow). (E) Osteolytic lesion with soft tissue component in the proximal left femur (yellow arrow). (F) Nodule in the right lobe of the liver (orange arrow). (G) Nodule in the urinary bladder (dark green arrow).

Two months after neck surgery, the patient had hematuria. Whole abdomen ultrasound was performed which revealed a pedunculated solid mass within the urinary bladder. The patient was then referred to the Urology outpatient department clinic, eventually admitted in the hospital, and underwent cystoscopy and transurethral resection of the bladder tumor, which had a measurement of 2.4 cm x 1.6 cm x 1.6 cm. On histopathology, the bladder tumor was compatible with metastatic carcinoma from a primary thyroid malignancy. Immunohistochemistry study with TTF-1 showed diffuse, strong, nuclear staining in the cells of the urinary bladder tumor, supportive of a metastatic carcinoma from a primary thyroid malignancy.

Six months after resection of the bladder tumor, the patient received radioactive iodine (RAI) therapy with 5.55 GBq (150 mCi) of iodine-131 (I-131). Post-therapy whole-body I-131 scintigraphy with single-photon emission computed tomography and computed tomography (SPECT/CT) obtained 7 days later demonstrated functioning thyroid tissue remnants in the left thyroid bed, functioning lytic bone metastases with soft tissue components, RAI-avid foci in the right liver lobe and both kidneys, and non-RAI-avid nodules in both lungs (Figures 4 to 6). There were no RAI-avid lesions in the urinary bladder.

A triphasic contrast-enhanced abdominal CT scan was done for further evaluation of the lesions in the liver and kidneys. Images showed a 2.8 x 2.8 x 2.8 cm mass in the right liver lobe (Figure 8) compatible with hypervascular liver metastasis, which may arise from thyroid cancer. Heterogeneously enhancing, mixed solid and cystic nodules (Bosniak IV), with sizes ranging from 0.5 cm to 1.4 cm, were identified in both kidneys (Figure 9) and were also compatible with metastases. The mass in the right liver lobe and some of the nodules in both kidneys had corresponding I-131 uptake on post-therapy whole-body I-131 SPECT/CT (Figures 6 and 7), consistent with functioning liver and kidney metastases from papillary thyroid cancer. The nodule in the urinary bladder seen on the previous CT scan (Figure 3) was no longer visualized because it was already resected.

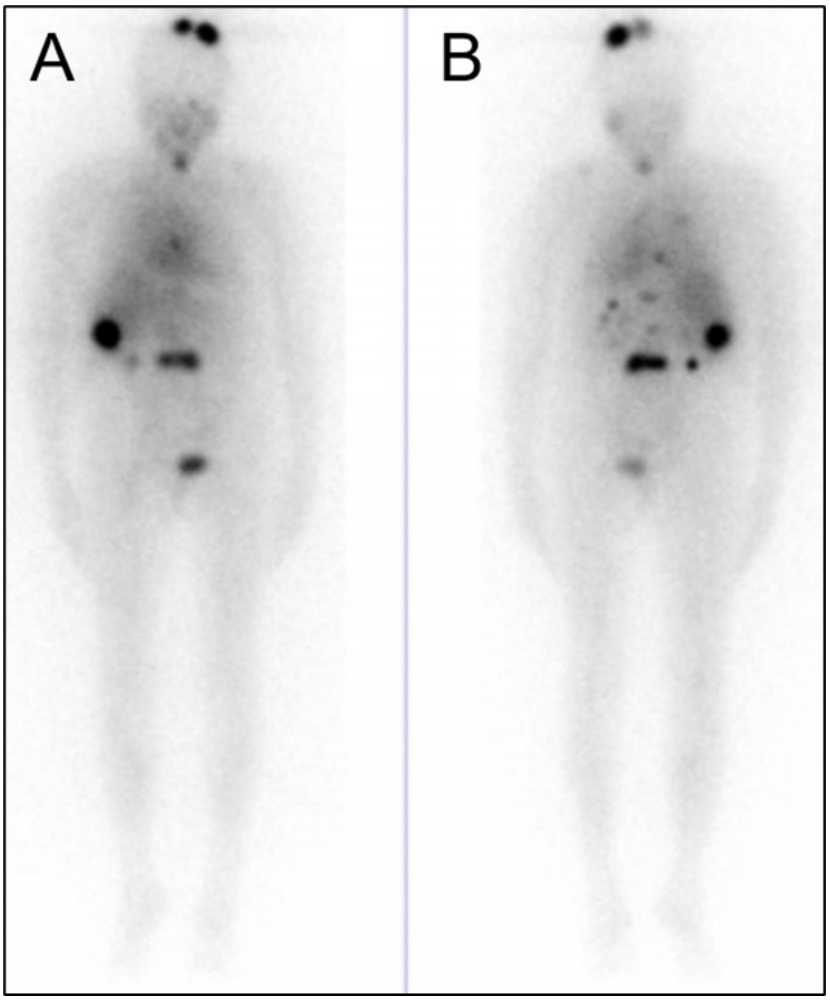

FIGURE 4. (A) Anterior and (B) posterior images of post-therapy whole-body I-131 scintigraphy. Multiple RAI-avid foci in the skull, left thyroid bed, vertebrae, left pubis, right liver lobe, and both kidneys.

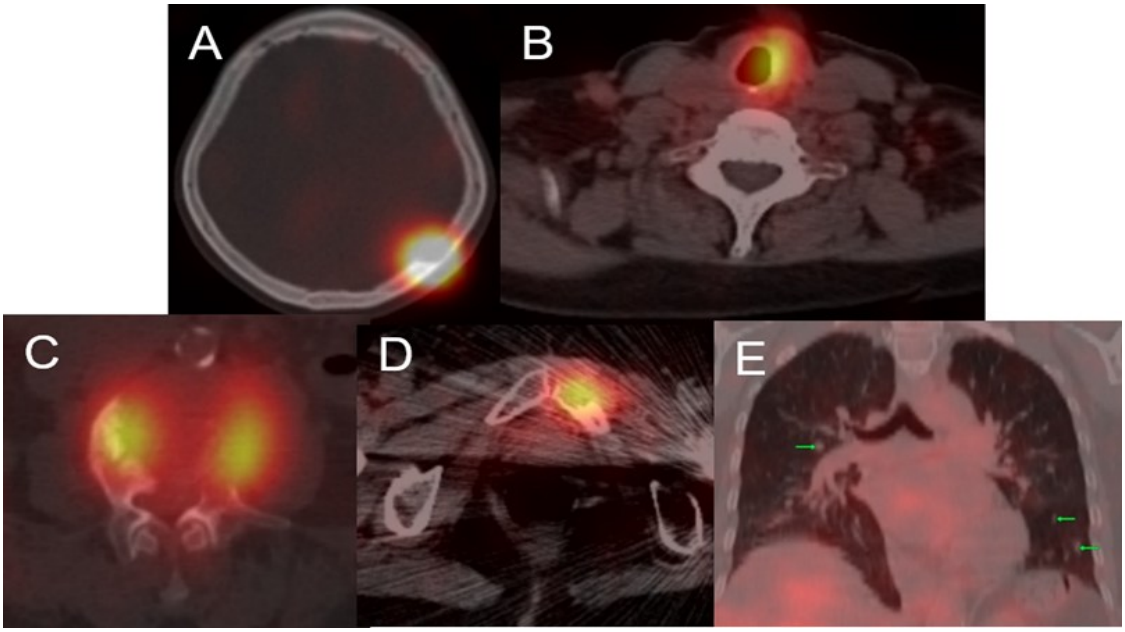

FIGURE 5. Post-therapy whole-body I-131 SPECT/CT. RAI-avid foci in the (A) left parietal bone, (B) left thyroid bed, (C) L3 vertebra, and (D) left pubis. (E) Nodules in both lungs with no significant I-131 uptake (light green arrows).

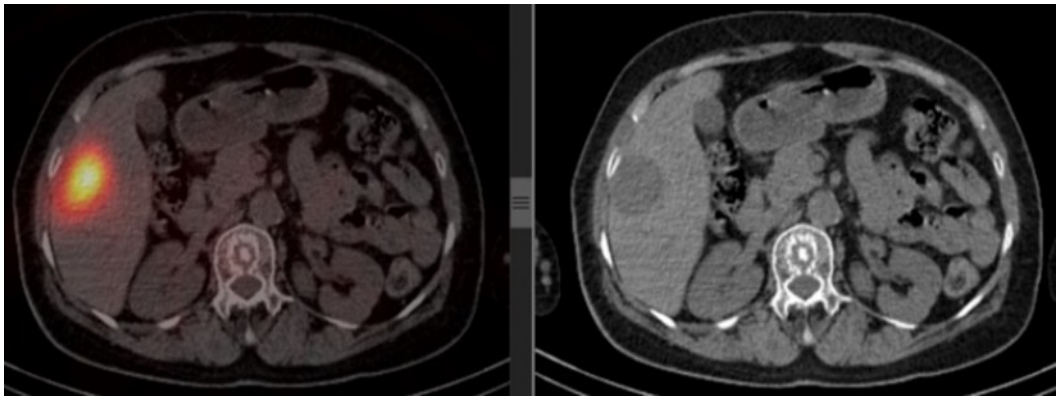

FIGURE 6. Post-therapy whole-body I-131 SPECT/CT. An RAI-avid focus in the right liver lobe

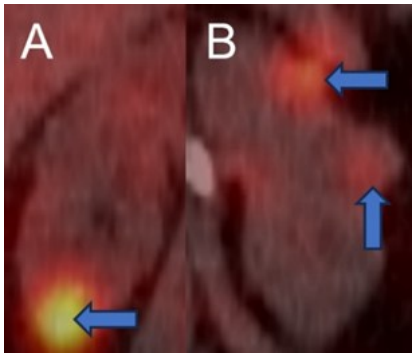

FIGURE 7. Post-therapy whole-body I-131 SPECT/CT. RAI-avid foci in the (A) inferior aspect of the right kidney and (B) lateral aspect of the left kidney (blue arrows).

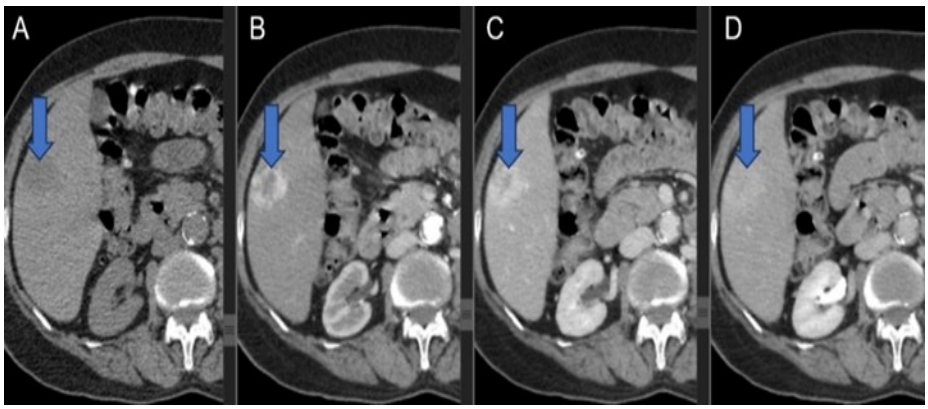

FIGURE 8. (A) Non-contrast-enhanced abdominal CT scan. (B) Late arterial, (C) portal venous, and (D) delayed phases of triphasic contrast-enhanced abdominal CT scan. The mass in the right lobe of the liver (blue arrow) was hypodense on non-contrast-enhanced CT, and had a continuous ring of contrast enhancement, compatible with hypervascular liver metastasis. Its central hypoenhancing component may represent an area of necrosis.

Other hypodense foci were seen in the right liver lobe on CT scan that were too small to characterize, but may represent tiny cysts versus metastases. Furthermore, there were some nodules in both kidneys on CT scan that did not have I-131 uptake on post-therapy whole-body I-131 scan (Figure 10).

DISCUSSION

Metastasis to the liver, kidney, or urinary bladder from differentiated thyroid cancer is rare, reported in only 0.5%, 0.47%, and <0.5% of patients, respectively [4, 5, 6]. Combined liver, kidney, or urinary bladder metastases are even rare. To our knowledge, this is the first reported case.

Risk factors for distant metastases from thyroid cancer include male sex, older age, histologic grade, adequacy of surgical removal of the primary thyroid mass, extrathyroidal extension, and lymph node metastasis [3]. One study concluded that among patients with the follicular variant of papillary thyroid carcinoma, the presence of angiolymphatic invasion, extrathyroidal extension, or nonencapsulation increased the risk of distant metastasis [7]. The infiltrative form of the follicular variant of papillary thyroid carcinoma also has a substantial risk of metastasis compared to the encapsulated form, with a different prognosis and molecular profile [8]. BRAF mutations are often found among the infiltrative subtype of papillary thyroid carcinoma follicular variant [9]. Another study found that a tumor size of ≥ 2 cm, the presence of nodal metastasis, and follicular thyroid cancer are correlated with a notably higher predilection for distant metastasis [10]. Our patient has the following risk factors for distant metastases: older age, extrathyroidal extension, lymph node metastasis, angiolymphatic invasion, non-encapsulation, infiltrative form of the follicular variant of papillary thyroid carcinoma, and a tumor size of ≥ 2 cm.

Liver metastases from differentiated thyroid cancer are often multiple or diffuse [11]. Although our patient only has one large RAI-avid lesion in the right liver lobe that is compatible with metastasis from thyroid cancer, there were other hypodense foci on CT scan that may represent metastases versus tiny cysts. Liver metastases from thyroid cancer usually do not have uptake of I-131 [12], in contrast to our patient who has I-131-avid liver metastasis.

Meanwhile, metastases to the kidney from thyroid cancer are seldom discovered, and most cases are only seen during autopsy [13]. When these lesions are detected during life, patients often do not have symptoms and are younger than 45 years [14], contrary to our patient who had hematuria and is older than 45 years. Kidney metastases from differentiated thyroid cancer may be missed on I - 131 whole - body scans

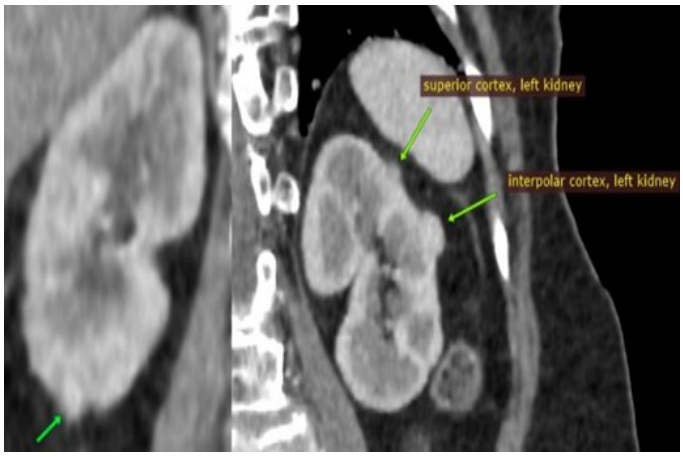

FIGURE 9. Contrast-enhanced abdominal CT scan. Heterogeneously enhancing, mixed solid and cystic nodules (Bosniak IV) in both kidneys, compatible with metastases (light green arrows).

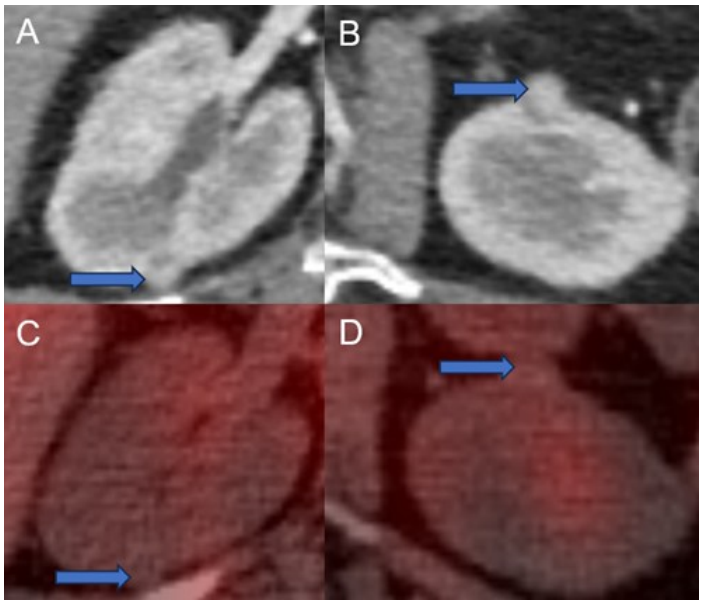

FIGURE 10. Contrast-enhanced abdominal CT revealed other nodules in the (A) right kidney and (B) left kidney (blue arrows). Upon review of the post-therapy whole-body I-131 SPECT/CT, these nodules in the (C) right kidney and (D) left kidney had no corresponding I-131 uptake.

because these lesions may be masked by normal kidney activity or interpreted as physiological bowel activity. Therefore, fusion imaging with SPECT/CT may add diagnostic value through accurate localization and characterization of areas with I-131 uptake. Other imaging modalities (such as ultrasound, enhanced CT, and MRI) are also crucial in the appropriate evaluation of kidney metastases from differentiated thyroid cancer [14].

For our patient, there were some nodules in both kidneys that did not have I-131 uptake. Non-RAI-avid lesions on whole-body I-131 scintigraphy may be caused by dedifferentiation which occurs in approximately 20 to 50% of metastatic differentiated thyroid cancers. Instead, these lesions have fluorine-18 fluorodeoxyglucose (F-18 FDG) uptake on positron emission tomography with computed tomography (PET/CT). This is called the flip-flop phenomenon [14]. Of note, the presence of F-18 FDG uptake in tumors implies a poor response to RAI therapy and an unfavorable prognosis [15]. The non-RAI-avid nodules in the kidneys of our patient may represent dedifferentiated metastases. These lesions are better evaluated using F-18 FDG PET/CT which is indicated for high-risk patients with a high serum thyroglobulin and a negative whole-body I-131 scan [14].

Because liver and kidney metastases from differentiated thyroid cancer are rare, patients with such lesions typically already have other distant metastases [11, 14]. This is consistent with our patient who has lymph node, bone, lung, and urinary bladder metastases.

Urinary bladder metastases may be caused by local extension from the retroperitoneum or implantation of venous emboli into the serosa [6]. Majority of urinary bladder metastases are identified only on autopsy [6]. Those that are detected during life usually cause hematuria or symptoms of urinary obstruction, similar to our patient who had hematuria.

Surgery, RAI therapy, and radiation therapy have been utilized in the management of distant metastases from papillary thyroid carcinoma [16]. Patients with low volume metastatic disease can be optimally managed with surgical resection and subsequent RAI therapy [16, 17]. However, for patients with metastases at multiple sites, surgical excision or even external beam radiation therapy of all lesions is not practical [14]. These patients can be given RAI therapy if the distant metastatic lesions have I-131 uptake on pre-therapy whole-body I-131 scintigraphy [11,14].

In patients with solitary liver metastasis from differentiated thyroid cancer, surgical resection has been associated with longer survival [12]. However, RAI therapy can still be effective for iodine-avid liver metastases [4]. Likewise, for kidney metastases that are iodine-avid, RAI therapy can drastically lower serum thyroglobulin, decrease the size, or prevent the progression of these lesions [14]. In one case report, solitary urinary bladder metastasis from thyroid cancer was managed by transurethral resection of the bladder tumor [6].

For advanced metastatic thyroid cancer that is refractory to I-131, tyrosine kinase inhibitors such as lenvatinib and sorafenib have been used [14, 16]. In some studies, patients with RAI-refractory liver and kidney metastases treated with tyrosine kinase inhibitors had better outcomes on survival [4,16]. However, challenges associated with tyrosine kinase inhibitors include their high cost and side effects [18].

Our patient with multiple distant metastases from papillary thyroid cancer received RAI therapy after she underwent left hip surgery, total thyroidectomy with central neck dissection, and resection of urinary bladder metastasis. Post-therapy whole-body I-131 SPECT/CT revealed I-131 uptake in multiple metastatic lesions. However, there were some lesions that did not demonstrate I-131 uptake. Therefore, close follow-up is recommended. Biochemical or structural incomplete response to therapy warrants monitoring with serum thyroglobulin and anti-thyroglobulin, neck ultrasound, diagnostic whole-body I-131 scintigraphy, and other imaging modalities, in accordance with guidelines. These are needed to assess response to RAI therapy and determine the next appropriate step in management.

Conclusion

We present a rare case of liver, kidney, and urinary bladder metastases from papillary thyroid cancer (on top of lymph node, lung, and bone metastases). These lesions can be treated with RAI therapy if they demonstrate I-131 uptake. However, such metastases may be missed on I-131 whole-body scans since their uptake can be masked by physiological uptake in the body. Therefore, the liver, kidneys, and urinary bladder must be carefully reviewed. In these cases, SPECT/CT and other imaging modalities are essential in the detection and evaluation of such lesions. After RAI therapy, follow-up and monitoring are needed to assess treatment response and guide subsequent management.

DISCLOSURE

The authors of this study have no conflicts of interest to disclose.

REFERENCES

1. Zhang D, Zhu XL, Jiang J. Papillary Thyroid Carcinoma With Breast and Bone Metastasis. Ear Nose Throat J. 2023 Apr;102(4):259-262. doi: 10.1177/01455613221145273. Epub 2022 Dec 7. PMID: 36476071.
2. Abdullah MI, Junit SM, Ng KL, Jayapalan JJ, Karikalan B, Hashim OH. Papillary Thyroid Cancer: Genetic Alterations and Molecular Biomarker Investigations. Int J Med Sci. 2019 Feb 28;16(3):450-460. doi: 10.7150/ijms.29935. PMID: 30911279; PMCID: PMC6428975.
3. Toraih EA, Hussein MH, Zerfaoui M, Attia AS, Marzouk Ellythy A, Mostafa A, Ruiz EML, Shama MA, Russell JO, Randolph GW, Kandil E. Site-Specific Metastasis and Survival in Papillary Thyroid Cancer: The Importance of Brain and Multi-Organ Disease. Cancers (Basel). 2021 Apr 1;13(7):1625. doi: 10.3390/cancers13071625. PMID: 33915699; PMCID: PMC8037301.
4. Brient C, Mucci S, Taïeb D, Mathonnet M, Menegaux F, Mirallié E, Meyer P, Sebag F, Triponez F, Hamy A. Differentiated thyroid cancer with liver metastases: lessons learned from managing a series of 14 patients. Int Surg. 2015 Mar;100(3):490-6. doi: 10.9738/INTSURG-D-14-00026.1. PMID: 25785333; PMCID: PMC4370541.
5. Yamazaki H, Kishida T, Noguchi G, Iwasaki H, Suganuma N, Masudo K, Nakayama H, Yamashita T, Yamanaka T, Sugawara Y, Matsubara Y, Kohagura K, Rino Y, Masuda M. Nephrectomy for Metastatic Kidney Tumor in Patients with Differentiated Thyroid Cancer: A Report of Two Cases. Case Rep Endocrinol. 2018 Nov 11;2018:7842792. doi: 10.1155/2018/7842792. PMID: 30534449; PMCID: PMC6252184.
6. Grivas N, Housianitis Z, Doukas M, Stavropoulos NE. Follicular thyroid cancer metastasis to the urinary bladder: report of a case and review of the literature. Case Rep Urol. 2012;2012:178915. doi: 10.1155/2012/178915. Epub 2012 Aug 1. PMID: 22900222; PMCID: PMC3415195.
7. Li YR, Chen ST, Hseuh C, Chao TC, Ho TY, Lin JD. Risk factors of distant metastasis in the follicular variant of papillary thyroid carcinoma. J Formos Med Assoc. 2016 Aug;115(8):665-71. doi: 10.1016/j.jfma.2015.07.002. Epub 2015 Aug 1. PMID: 26239193.
8. Vivero M, Kraft S, Barletta JA. Risk stratification of follicular variant of papillary thyroid carcinoma. Thyroid. 2013 Mar;23(3):273-9. doi: 10.1089/thy.2012.0369. PMID: 23025507.
9. Yu XM, Schneider DF, Leverson G, Chen H, Sippel RS. Follicular variant of papillary thyroid carcinoma is a unique clinical entity: a population-based study of 10,740 cases. Thyroid. 2013 Oct;23(10):1263-8. doi: 10.1089/thy.2012.0453. Epub 2013 Sep 11. PMID: 23477346; PMCID: PMC3787730.
10. Khan U, Al Afif A, Aldaihani A, MacKay C, Rigby MH, Rajaraman M, Imran SA, Bullock MJ, Taylor SM, Trites JRB, Hart RD. Patient and tumor factors contributing to distant metastasis in well-differentiated thyroid cancer: a retrospective cohort study. J Otolaryngol Head Neck Surg. 2020 Nov 16;49(1):78. doi: 10.1186/s40463-020-00469-8. PMID: 33198797; PMCID: PMC7667857.
11. Ostrovsky V, Bar-Zakai B, Miller R, Schiller T, Kirzhner A, Knobler H, Zornitzki T. Single liver metastasis of a follicular variant of papillary thyroid carcinoma: a rare pattern of organ spread. Endocrinol Diabetes Metab Case Rep. 2020 Aug 20;2020:20-0074. doi: 10.1530/EDM-20-0074. Epub ahead of print. PMID: 32820131; PMCID: PMC7487177.
12. Tsukagoshi M, Harimoto N, Araki K, Kubo N, Watanabe A, Igarashi T, Ishii N, Yajima T, Sano T, Shirabe K. Liver metastasis from papillary thyroid carcinoma treated by laparoscopic hepatectomy 43 years after resection of the primary tumor: a case report. Surg Case Rep. 2020 Jun 18;6(1):142. doi: 10.1186/s40792-020-00906-w. PMID: 32556940; PMCID: PMC7303250.
13. Smallridge RC, Castro MR, Morris JC, Young PR, Reynolds JC, Merino MJ, Sarlis NJ. Renal metastases from thyroid papillary carcinoma: study of sodium iodide symporter expression. Thyroid. 2001 Aug;11(8):795-804. doi: 10.1089/10507250152484664. PMID: 11525275.
14. Qiu ZL, Xue YL, Luo QY. Rare renal metastases from differentiated thyroid carcinoma: early clinical detection and treatment based on radioiodine. Arq Bras Endocrinol Metabol. 2014 Apr;58(3):260-9. doi: 10.1590/0004-2730000002913. PMID: 24863088.
15. Wang D, Bai Y, Huo Y, Ma C. FDG PET Predicts the Effects of 131I and Prognosis for Patients with Bone Metastases from Differentiated Thyroid Carcinoma. Cancer Manag Res. 2020 Dec 23;12:13223-13232. doi: 10.2147/CMAR.S284188. PMID: 33380830; PMCID: PMC7767715.
16. Yang J, Ma Y, Gong Y, Gong R, Li Z, Zhu J. Multiple Simultaneous Rare Distant Metastases as the Initial Presentation of Papillary Thyroid Carcinoma: A Case Report. Front Endocrinol (Lausanne). 2019 Nov 8;10:759. doi: 10.3389/fendo.2019.00759. PMID: 31781034; PMCID: PMC6856955.
17. Nair LM, Anila KR, Sreekumar A, Pradeep VM. Renal metastasis from papillary carcinoma thyroid detected by whole body iodine scan: A case report and review of the literature. Indian J Nucl Med. 2016 Jul-Sep;31(3):232-4. doi: 10.4103/0972-3919.183618. PMID: 27385900; PMCID: PMC4918493.
18. Sánchez-Garavito JE, Sanchez-Garcia J, Olsen D, Shorti RM, Lopez-Verdugo F, Rodriguez-Davalos MI. Liver resection for metastatic thyroid carcinoma. Case report and literature review. J Surg Case Rep. 2020 Sep 25;2020(9):rjaa370. doi: 10.1093/jscr/rjaa370. PMID: 33005326; PMCID: PMC7517888.

kHealth

CAREVIEW

Taking the Lead in PET/CT Imaging and Innovative Radiopharmaceuticals

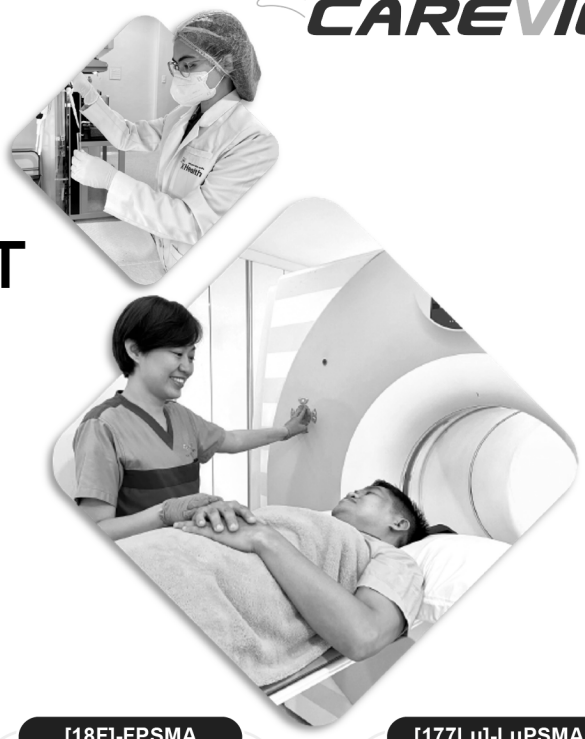

[18F]-FDG

A sugar analog used to detect **metabolically active malignant lesions**. A non-invasive approach to accurate diagnosis and staging for the optimal management of cancer patients

[18F]-FBB

Developed for routine clinical application to visualize beta amyloid neuritic plaque density. An effective tool to **differentiate Alzheimer's Disease** from other forms of Dementia

[18F]-FPSMA

Named as a top medical innovation by Cleveland Clinic in 2022. PSMA PET scan has greater sensitivity and can **detect prostate cancer metastases** sooner, allowing clinicians to better serve patients and make treatment decisions

[177Lu]-LuPSMA

Partnered with PSMA-directed PETCT scan, LuPSMA offers a **Theranostic approach** to treatment of metastatic castration-resistant prostate cancer (mCRPC)

NATIONAL KIDNEY AND TRANSPLANT INSTITUTE
East Ave., Diliman Quezon City

CENTURIA PET/CT CENTER
G/F Centuria Medical Makati, Kalayaan Ave., Cpr. Salamanca, Makati City

AUF MEDICAL CENTER
Angeles City, Philippines

ManilaMed
A MOUNT GRACE HOSPITAL
850 United Nations Ave, Paco, Manila

MARY MEDIATRIX MEDICAL CENTER
THE HUB OF HEALTHCARE EXPERTS
J.P. Laurel Highway, Lipa City Batangas

CAREVIEW Cancer Center BGC
31st Street Cor. Second Ave., Crescent Park West, BGC

Philippine General Hospital
Taft Ave, Ermita, Manila

CAREVIEW Cancer Center SM Valenzuela
McArthur Highway, Brgy. Karuhatan, Valenzuela City

PET/CT PATIENT SUPPORT

+63 998 323 5425
+63 917 714 4248
+63 917 714 4266
patientsupport@khealthcorp.com

SCAN THE QR CODE

PET/CT FINANCIAL ASSISTANCE

NEED A PET/CT SCAN?

Schedule it with us. Let CARE CALL Team call you


An established global key player in the radioisotope & radiopharmaceutical field.
Find out more about us and our products:
www.itm-radiopharma.com
Follow us:
itm
PASSION FOR PRECISION

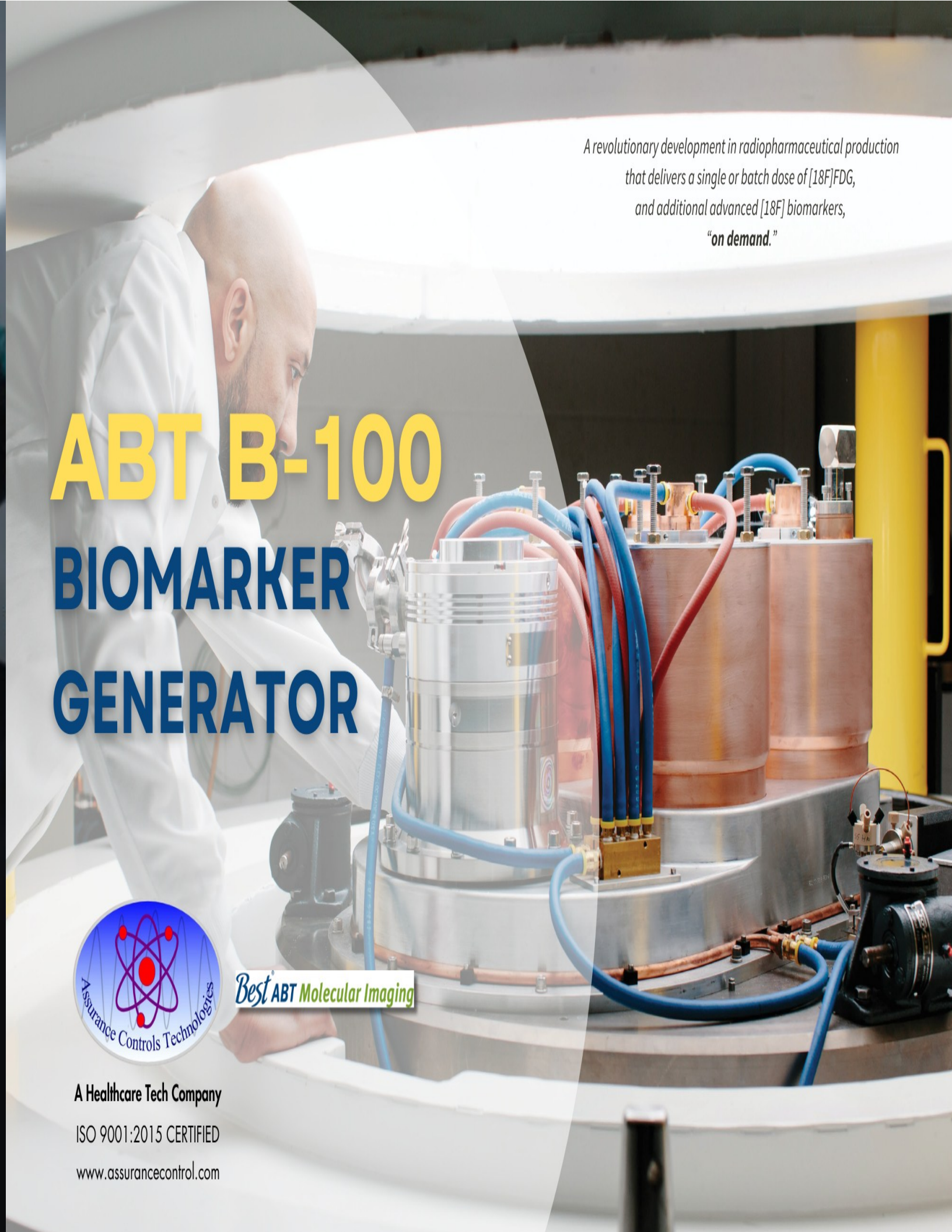

*A revolutionary development in radiopharmaceutical production that delivers a single or batch dose of [18F]FDG, and additional advanced [18F] biomarkers, "**on demand**."*

ABT B-100 BIOMARKER GENERATOR

Assurance Controls Technologies

Best ABT Molecular Imaging

A Healthcare Tech Company

ISO 9001:2015 CERTIFIED

www.assurancecontrol.com

RIA Instrument

Gamma Counter

Dispenser

Tube Washer

Incubator

Full Automatic

RIA KIT

ITEM		ITEM		ITEM		ITEM	
Hepatitis	HBsAg(1Step) Anti-HBs Anti-HBc IgG Anti-HBc IgM Anti-HBc (RIA) Anti-HAV IgG Anti-HAV IgM HBeAg/Ab Anti-HCV	Thyroid	T3 T4 Free T4 Free T3 T3-Uptake TSH Tg-s	Tumor	Free PSA Ultra PSA CA125 CA19-9 AFP CA15-3 Ferritin NSE SCC AFP CEA PSA	Hormones	B-HCG Insulin C-peptide Total IgE Testosterone 25-Vitamin D total 25-Vitamin D 3 FSH Prolactin LH

X3D

We Image Your Needs.

www.xddd.dk

CorCam™

SPECT Camera System
for Nuclear Cardiology Procedures

- Golden Standard Cardiac SPECT
- Fast Acquisition Time
- Prone & Supine Imaging
- Very Low Maintenence Cost
- Seamless Workflow & Small Footprint
- Made in Denmark

www.xddd.dk

UNITED IMAGING

Follow us on LinkedIn

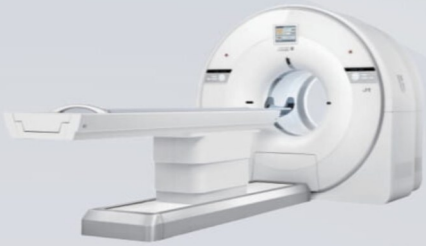

uMI 550
Digital. Attainable.

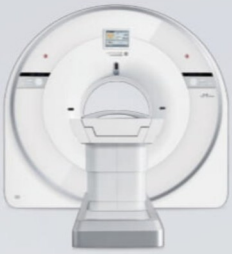

uMI Vista
Clarity. Profound.

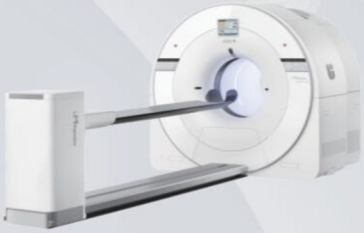

uMI Panvivo
Empowering Tomorrow for All

uMI Panorama
Digital High-Resolution PET/CT.

PASSION FOR *Change*

uEXPLORER
Total-body PET/CT.
Born to EXPLORE.

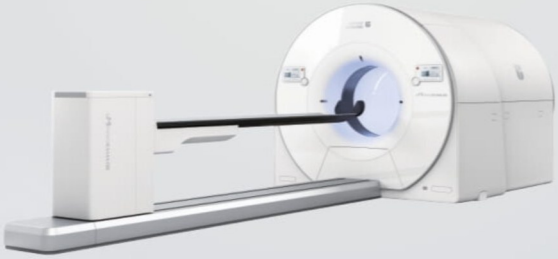

uMI Panorama GS
Next-Generation 148-cm
Whole-Body PET/CT.

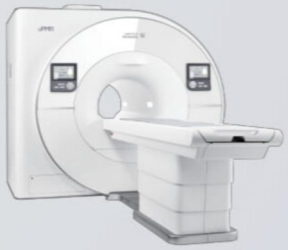

uPMR 790
Next Generation. Now Realized.

Leading innovations in molecular imaging, United Imaging has developed a complete portfolio of LYSO-based digital SiPM PET detector systems. Dedicated to revolutionizing user experiences from clinical applications to advanced research, our portfolio starts where others end. Together with our global customers, we're changing how we view Molecular Imaging today, and in the future.

UNITED IMAGING

uMI Panorama GS

Advancing Whole-Body Imaging

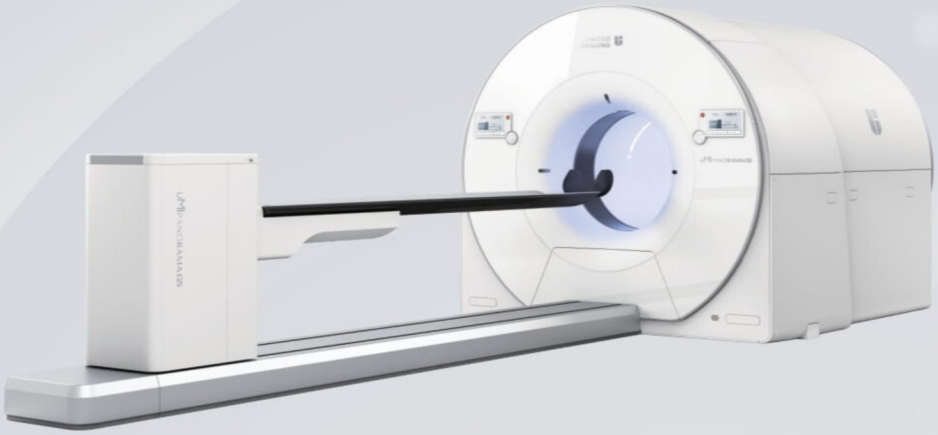

Expanding Whole-Body Imaging with 148 cm AFOV

- 148 cm axial FOV enables single-bed whole-body imaging, covering key nuclear medicine regions from the skull to the knees with high sensitivity.
- 25x sensitivity gain ensures precise line-of-response capture for unparalleled imaging clarity and superior sensitivity for diverse imaging needs, including low-dose, rapid scans for pediatrics and brain imaging.
- Fits within the footprint of standard FOV PET/CT systems.

Unlocking Precision without Compromise

- The 2.76 mm LYSO crystals provide a NEMA spatial resolution of 2.9 mm and 1.4 mm PSF+TOF spatial resolution with 100% SiPM coverage and ASIC technology, enabling sub-millimeter lesion detection and exceptional image clarity.
- Achieves 189 ps TOF and >3000 Peak-NECR, enhancing diagnostic accuracy with unparalleled details and contrast.
- AI-powered uExcel DPR and uExcel AIIR algorithms reduce noise and enhance contrast, while uExcel Focus corrects motion artifacts for improved quantification.

Enabling a Panoramic View for New Clinical and Research Dimensions

- Delivers precise PET imaging with ultra-low radiation through CT-Free attenuation correction (AC), ensuring safety without compromising quality.
- Supports advanced physiological and absolute quantitative analysis with innovative dynamic imaging technology (0.025/s Kernel Recon) and uKinetics.
- Achieves high-speed online reconstruction with average static scan times under 3 minutes, with options for parallel reconstruction and redundant acquisition.

UNITED IMAGING

uEXPLORER

Total-body PET/CT Born to Explore

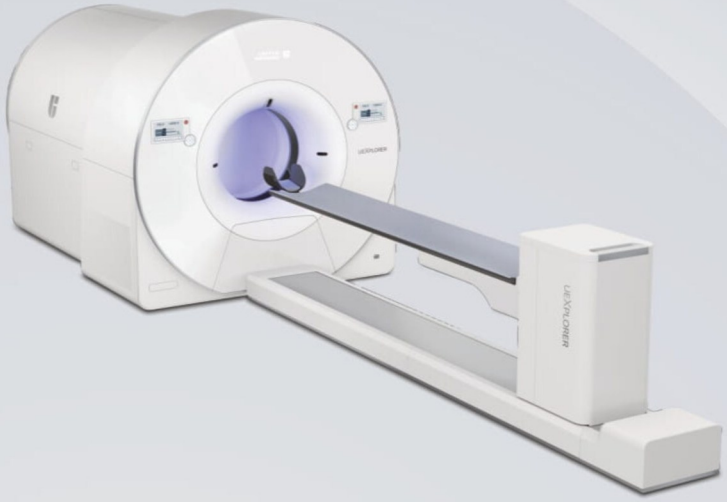

Unexplored Clinical Insight Became Tangible

- Industry-leading 194 cm single-bed AFOV for total-body coverage.
- The innovative cross-unit coincidence technology enables the capture of orders of magnitude more γ photons, giving a 40-fold overall sensitivity boost over conventional PET/CT systems.

Game-changer – Exceptional Precision to Explore

- Achieves 2.9 mm NEMA spatial resolution for sub-millimeter lesion detection and enhanced diagnostic accuracy.
- 1024×1024 PET matrix provides unprecedented image contrast and detail.
- A 76 cm PET aperture enhances patient comfort during scans.

Establish Total Body View for New Clinical and Research Dimensions

- Supports multifaceted research from diagnosis to theranostics for clinical complexity .
- High count rate performance allows for better detail visualization, particularly for theranostics tracers such as 68Ga/90Y.
- Comprehensive research tools are provided for personalized needs, such as uKinetics, which supports total-body dynamic studies.

UNITED IMAGING

uAI Solutions

uAI's multi-scenario solutions integrate multiple AI platforms and applications, building a digital healthcare ecosystem, and enabling precision clinical diagnosis and treatment. Furthermore, the integration of multiple AI technologies enables the entire process of diagnosis and treatment.

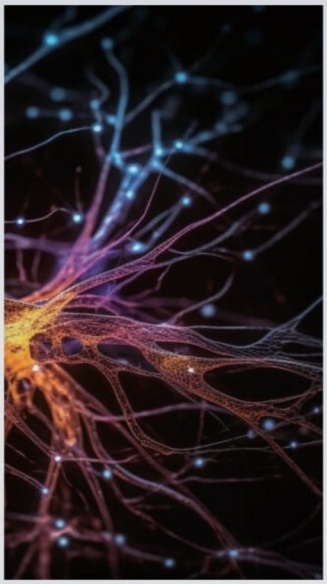

uAI Solution for Neuroradiology

ICH

Ischemic Stroke

Cerebral and Carotid Vessels

Cerebral CTP

Cerebral Collateral

PET/CT Neurology

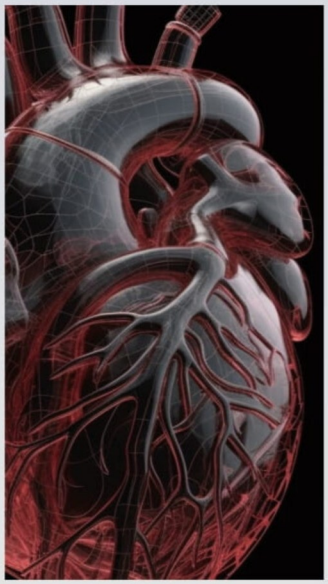

uAI Solution for Cardiology

CCTA

FFRct

Coronary Plaque

Aortic Dissection

Coronary CS

Non-gated Coronary CS

CCTP

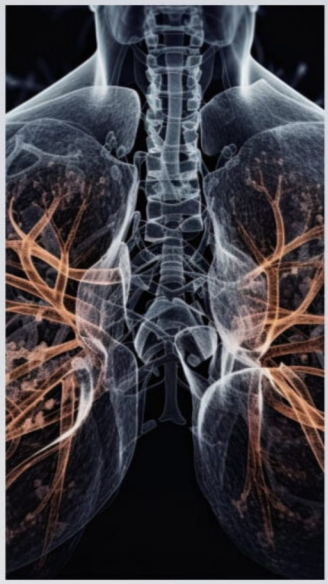

uAI Solution for Thoracic Radiology

Pulmonary Nodules

BMD

QCT Analysis

Bony Thorax Fractures

PE

Emphysema

Pneumonia

Lymph Nodes

Esophagus

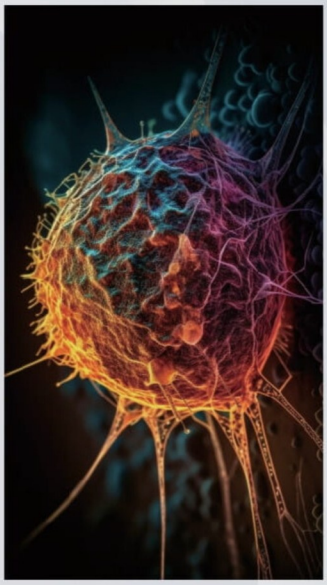

uAI Solution for Cancer Care Management

Pulmonary Nodule 3D

Abdominal CT

PET/CT Oncology

Sentinel Lymph Node Mapping by Planar Lymphoscintigraphy and Sentinel Lymph Node Biopsy with a Gamma Probe and Indocyanine Green in a Primary Malignant Melanoma of the Vulva: A Case Report

Christian Dominique S.C. Yu, MD, Marcelino A. Tanquilut, MD, Wenceslao S. Llauderes, MD, Emelito O. Valdez-Tan, MD, Ivan Ray F. David, MD

Department of Nuclear Medicine, Jose R. Reyes Memorial Medical Center
E-mail address: christianyumd@gmail.com

ABSTRACT

Malignant melanoma of the vulva is a rare and aggressive malignancy with a poor prognosis and has a high recurrence rate; the metastatic status of the regional lymph nodes plays a strong prognostic factor and powerful predictor of the survival outcome of the patient. To avoid morbidities from an extensive lymphadenectomy, a sentinel lymph node biopsy is ideal. The current gold standard for identifying sentinel lymph nodes is by mapping the lymphatic system with preoperative lymphoscintigraphy. The purpose of this paper is to present a case of a 56-year-old woman diagnosed with a rare case of a vulvar melanoma evaluated using preoperative sentinel lymph node mapping and intraoperative biopsy using a gamma probe. Lymphoscintigraphy mapping and gamma probe used in the identification of the sentinel lymph nodes spared the patient to undergo complete lymph node dissection and proceeded with adjuvant therapy in a short period. In this case, the lymphatic spread of malignant melanoma is unpredictable, and the planar images of the lymphoscintigraphy provided the lymphatic map of the tumor. With a noted low spatial resolution of a planar lymphoscintigraphy, the aid of the intraoperative biopsy with a gamma probe supplemented the identification and excision of the sentinel lymph nodes. In conclusion, sentinel lymph node mapping scintigraphy gives the surgeons the advantage to tailor a detailed surgical plan, and gamma probing aids to identify sentinel lymph nodes intraoperatively.

***Keywords**: Vulvar melanoma, Sentinel lymph node, Lymphoscintigraphy, Gamma probe*

INTRODUCTION

The sentinel lymph node (SLN) is known to be the first lymph node that directly drains from the primary tumor. The histological state of the SLN has been proven to be an indicator demonstrative of the entire lymph node basin, making it the first lymph node to be at risk to receive metastatic cells. It has proven to be the best indicator of survival and tumor recurrence. The gold standard for identification and excision of the SLN is the sentinel lymph node biopsy (SLNB) guided with lymphoscintigraphy using technetium Tc 99m [1, 2, 3].

The use of the detectable radioisotope is ideal since it mimics the natural migration of the metastatic cells retained in the SLN by macrophage phagocytosis or drains from the injection site via lymphatic capillaries and is accumulated due to its size in a short period. The idea with SLNB is to identify and excise the nodes that are likely to have metastasis to be pathologically assessed. A negative sentinel node with high accuracy can prognosticate the lack of tumor metastases in the local lymph nodes and a study found that technetium Tc 99m alone can have a 100% success rate in identifying sentinel lymph nodes [4, 5].

The earliest application of using radioisotopes for SLNB was done for staging breast cancer and cutaneous melanoma providing a lymphatic map of possible metastatic spread, hence serving as a guide for specific surgical procedures showing possible unexpected lymphatic drainage patterns that can be missed in a standard lymphadenectomy. Through time, SLN mapping and biopsy became a routine procedure for breast cancer and melanoma that contributed to minimizing extensive surgical procedures and avoiding morbidity from overtreatment as it provides prognostic information on the nodal status. Due to the success safety, and reproducibility of the procedure, the SLN mapping and biopsy were then applied to other malignant cases such as urologic and rare gynecologic malignancies such as vulvar melanoma [6, 7].

Ethical Considerations

The study was in compliance with the ethical standards of the Helsinki Declaration of 1975, as revised in 1983. Consent and assent forms were obtained from the guardian and the subject, respectively. No personal information of the patient was revealed in this paper.

OBJECTIVES

The key goal of this paper is to present a case of a 56-year-old woman diagnosed with a rare case of a vulvar melanoma evaluated recently using pre-operative sentinel lymph node mapping and intraoperative biopsy with gamma probe use. This also includes reviewing the epidemiology of the disease and the role of lymphoscintigraphy and gamma probe used in identifying the sentinel lymph node and how it affects the surgical plan, clinical staging, and management of the patient .

Case Report

A 56-year-old G3P3 (3003), married, from Caloocan with a past medical history of hypertension for 20 years, a family history of lung cancer on the paternal side, and an unremarkable personal and social history with a diagnosis of Vulvar Melanoma, T4aN0M0 Clinical Stage IIB, s/p Vulvar Mass Incisional Biopsy; s/p Colposcopic Guided Cervical Punch Biopsy with Endocervical Curettage was referred to our department for Sentinel lymph node mapping and biopsy.

The patient had a 4-month history of vaginal bleeding and a 1-month history of palpable vulvar mass. The patient had an incisional biopsy done revealing a positive S100 - nuclear and cytoplasmic, Melan A and HMB45 positive in the cells of interest while P16, Pancytokeratin, Synaptophysin, and Chromogranin were negative. ECOG performance score of 0. Unremarkable physical examination except for the vulvar mass. On inspection of the vulva, there are hyperpigmented mass with hemorrhagic areas measuring 3.0 x 3.0 cm at the left hymenal area at 11 o'clock position and another hyperpigmented mass in the right hymenal ring at 1 o'clock position measuring 1.0 x 1.0 cm (Figure 1).

The patient was then scheduled for Sentinel lymph node scintigraphy, cystourethroscopy, sentinel lymph Node probed biopsy (bilateral Inguinofemoral lymph node dissection) followed by wide local excision of the vulvar mass under spinal anesthesia.

Sentinel lymph node scintigraphy was started by first cleaning the site with an aseptic technique then intradermal injection of 0.5 mCi of filtered 99mTc Sulfur Colloid at the bilateral vulva (Figure 2), dynamic imaging of the pelvis in the anterior projection was done for 20 minutes (1 minute per frame, 256x256 matrix) with a single-head detector gamma camera, low-energy, high-resolution resolution collimator with an energy window of 20 % centered on the 140-keV photopeak. Additional early and delayed static views at the anterior and left lateral static images were also acquired at a 256 × 256 matrix over the lymph node basin. Truncation of the injection sites was done by covering the sites with a lead plate. A point source was also used to trace the outline of the body. Dynamic and static images show the multiple foci of intense radiotracer uptake located at the bilateral inguinal area (3 foci on the left and 2 foci on the right) which likely denotes the sentinel nodes. (Figures 3 and 4).

Intraoperatively, cystourethroscopy was done and was deemed unremarkable. We then proceeded with the sentinel lymph node mapping biopsy with the use of a gamma probe and handheld imager using indocyanine green dye (Figures 5 and 6). The sentinel lymph nodes were identified in the bilateral superficial and deep femoral lymph nodes. With the gamma probe, we were able to identify 6 sentinel lymph nodes. (Table 1)

On the histopathology report, malignant round cell neoplasm favors melanoma, Breslow level V with a thickness of 6.0 mm with skin ulceration present and anatomic Clark level IV. Lymphovascular space invasion was not demonstrated. Positive for tumor invasion was noted in the vulva, hymen, and vaginal floor. There was negative tumor invasion for all the noted sentinel lymph nodes.

DISCUSSION

Malignant melanoma of the female genital tracts such as vaginal and vulvar melanoma is rare and only represents 1% of all melanoma cases. Malignant melanoma of the vulva is aggressive with a high recurrence and metastatic rate and comes with a poor prognosis with only a 5-year overall survival rate of 27% - 54% [8, 9, 10]. Unlike cutaneous melanoma, vulvar melanoma is unrelated to ultraviolet light exposure and the pathogenesis is still unknown.

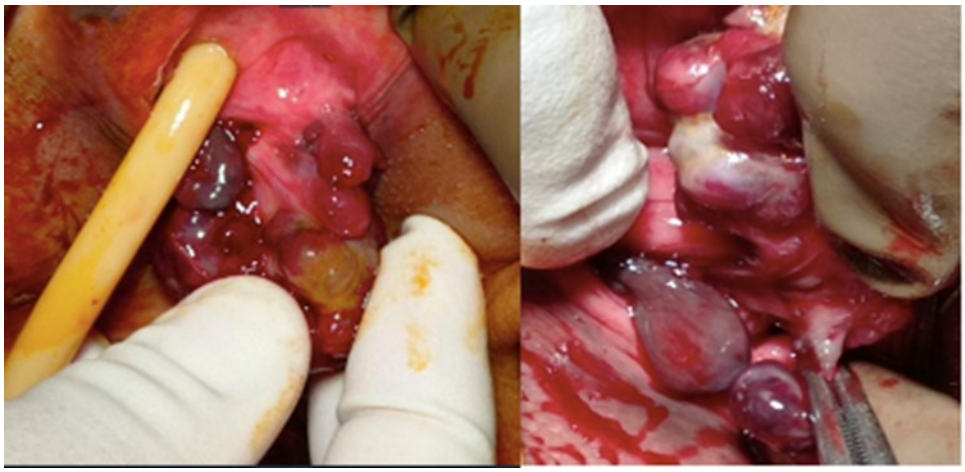

FIGURE 1. Hyperpigmented mass at 11' and 1'o clock position.

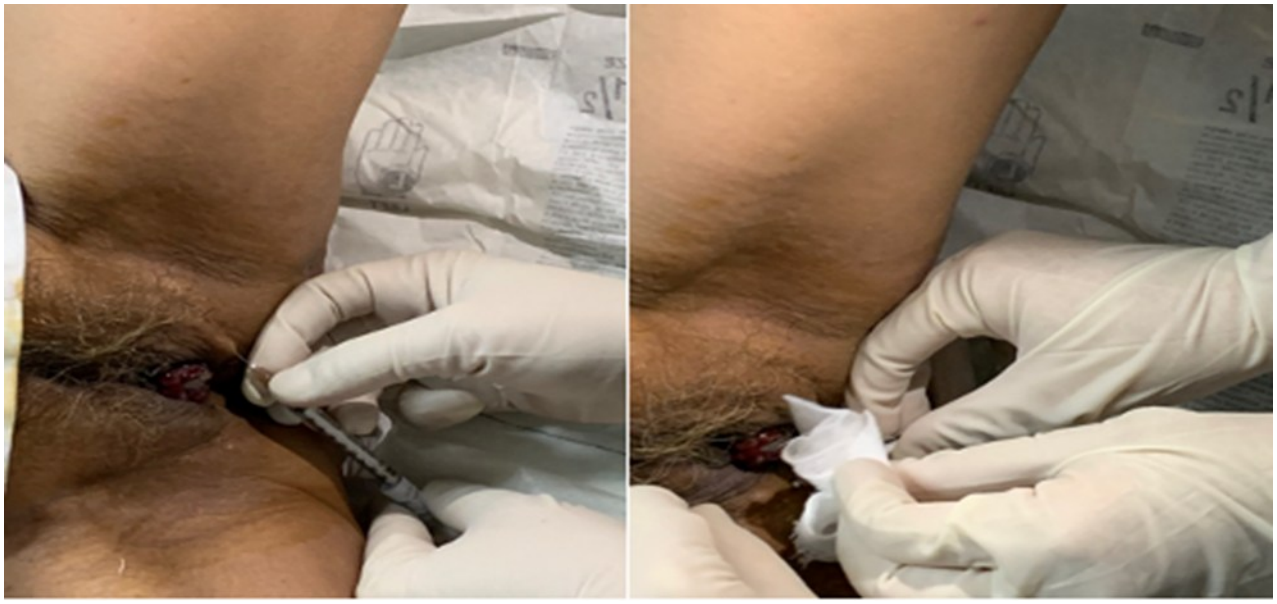

FIGURE 2. Intradermal injection of filtered Tc99m Sulfur colloid on the bilateral vulva

TABLE 1. Sentinel nodes identified with counts using a gamma probe

Location of Sentinel Lymph Node	Probe Recorded Counts
Background	54
Left Superficial Inguinal	65,535
Right Superficial Inguinal	17,688
Left Deep Inguinal Node	11,315
Left Deep Inguinal Node	2,997
Left Deep Inguinal Node	4,499
Right Deep Inguinal Node	11,140

FIGURE 3. Anterior Dynamic Images of the Pelvis for 20 minutes (1 minute per frame)

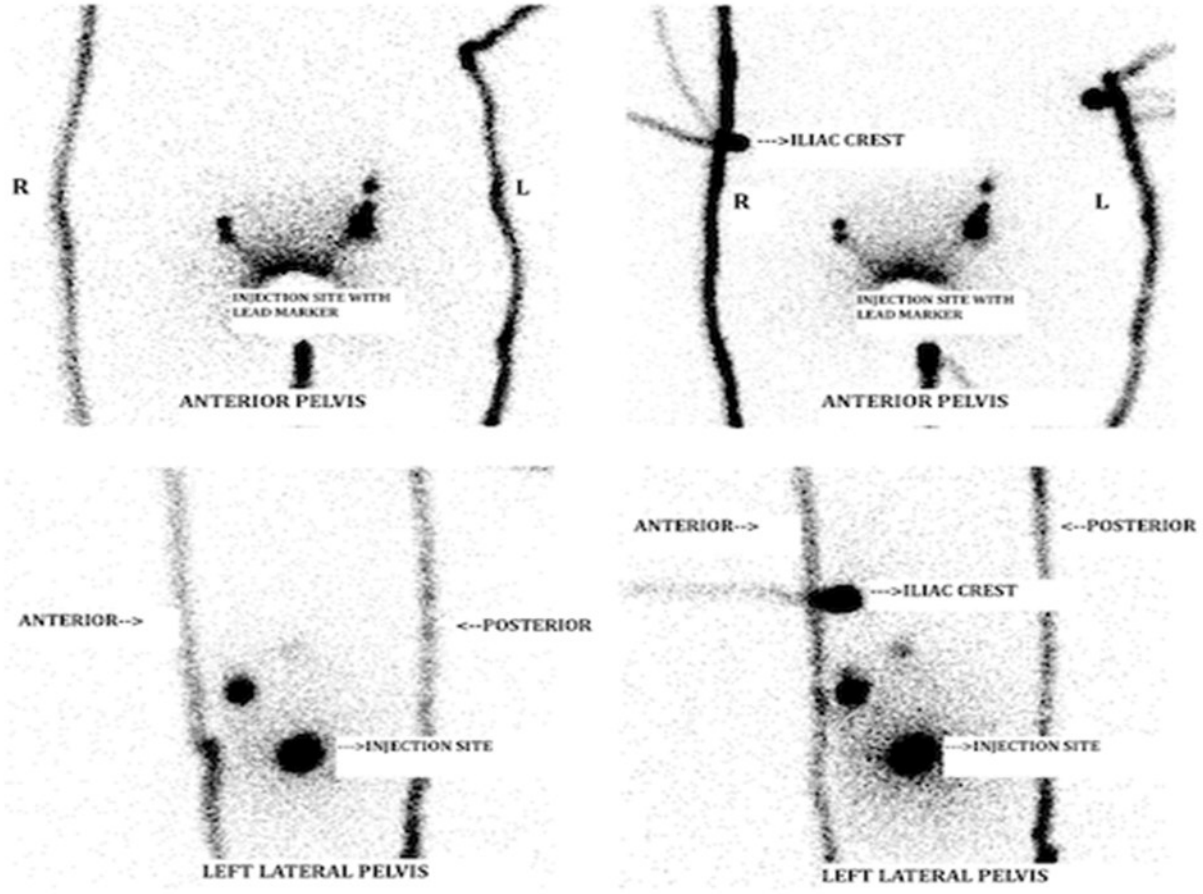

FIGURE 4. Early (left) and Delayed (right) Static images of the Anterior and left lateral view

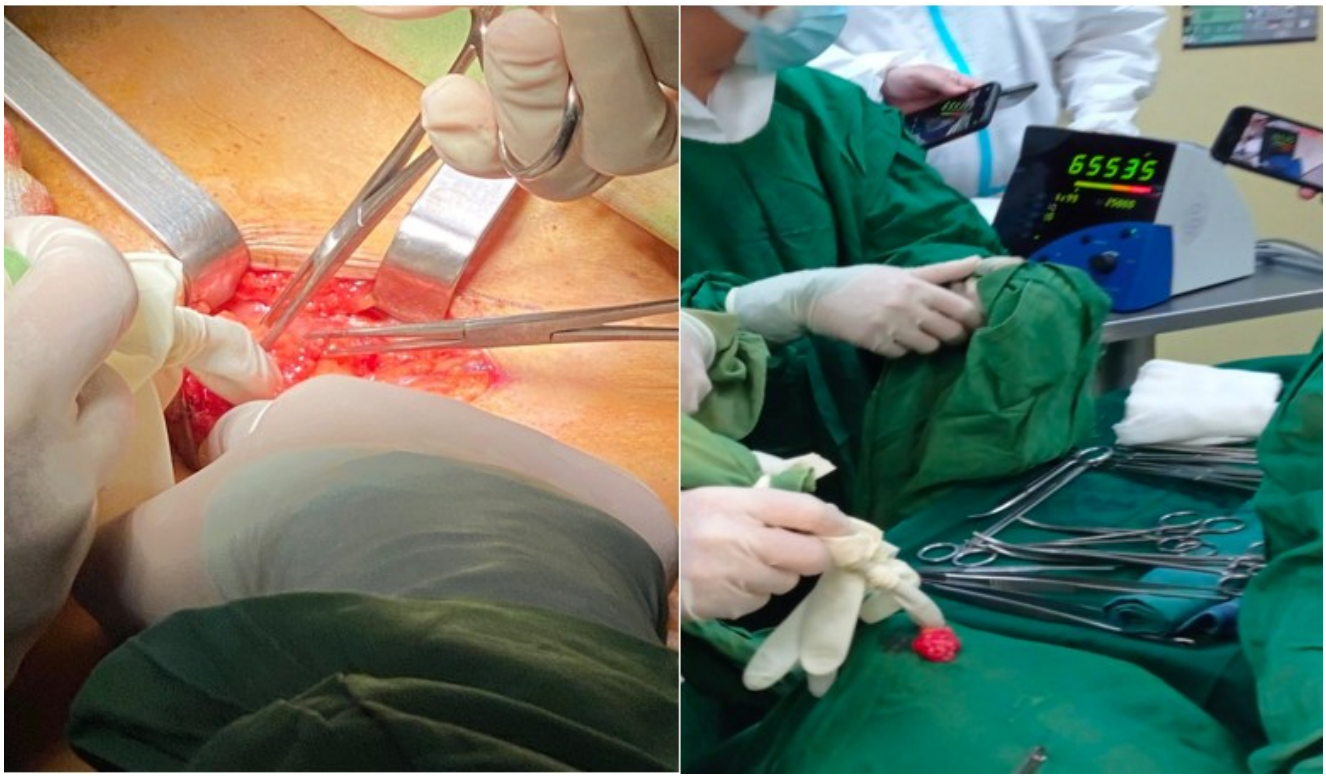

FIGURE 5. Sentinel lymph node mapping with the use of a gamma probe

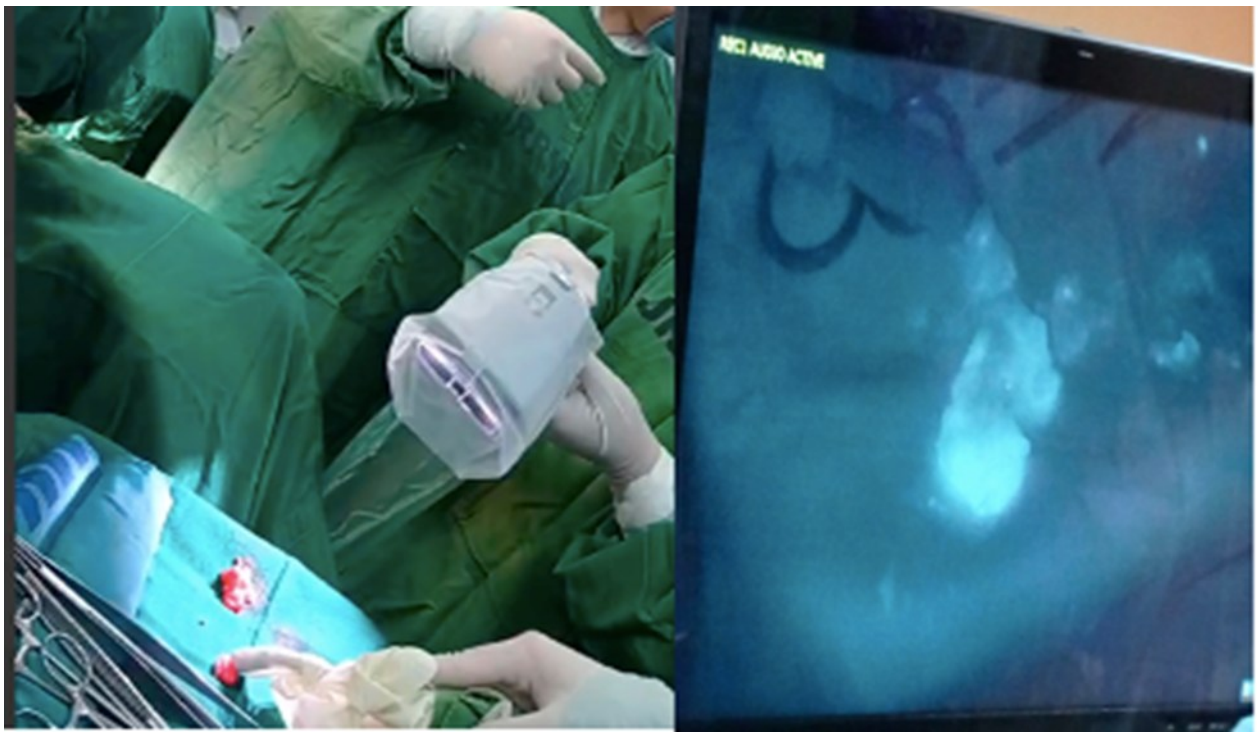

FIGURE 6. Sentinel lymph node mapping with the use of a handheld imager using indocyanine green dye

Vulvar melanoma behaves similarly to a cutaneous melanoma, hence, application of staging, diagnostics, and therapeutics for cutaneous melanoma can be considered for mucosal melanomas such as vulvar melanoma [11]. A primary melanoma is confirmed with immunohistochemical staining of S-100, Melan A, and HMB-45 [12] all of which were present in our patient [12].

There are two staging systems used for gynecologic malignancies: the International Federation of Gynecology and Obstetrics (FIGO) classification for clinical staging

the American Joint Committee on Cancer's (AJCC) TNM staging method for pathological staging [12]. At present, FIGO classification is predominantly used for gynecologic malignancies; however several studies suggest that the TNM staging having a detailed staging system and prognosis prediction was found to be superior for malignant vulva melanomas. The prognosis of malignant melanoma is not only determined by the tumor size but also by tumor invasion. In addition, lymph node status plays an important prognostic factor that can be used to assess the rate of recurrence and give physicians to institute a more appropriate management [5, 7].

The guidelines for the treatment of vulvar melanoma follow that of the cutaneous melanoma since there are limited data on genital tract lesions as a result surgical excision (wide local excision) which remains important in initial management for vulvar melanoma followed by other adjuvant treatment such as immunotherapy, chemotherapy, and radiation therapy [8, 12]. The overall survival is not significantly different among patients managed conservatively with wide local excision versus radical surgeries since the radicality of the procedure does not reduce the recurrence or improve survival, and it presents with more associated morbidities [5, 8, 11, 13].

Complete lymph node dissection (CLND) was the procedure of choice for malignant melanomas with metastasis seen in only about 15 - 20% [4]. As a result, sentinel node biopsy was included in the management of a patient with malignant melanoma to spare patients with no nodal metastasis from the morbidities that the CLND may hold [14, 15].

Gynecologic malignancies usually spread regionally and follow the normal drainage. To determine the extent of the disease, familiarity with the possible routes of nodal metastasis, analysis of lymph node characteristics, and treatment options are crucial [7]. Vulvar cancers usually spread in the unilateral superficial inguinal lymph nodes than into the deep femoro-inguinal lymph nodes and bilateral lymphatic spread is possible in midline lesions [16]. Melanoma may directly drain to one or several nodal basins which is why lymphatic drainage from melanoma sites is highly variable with unpredictable drainage patterns [6].

SLNB with the aid of lymphoscintigraphy helps the physician to plan the best surgical approach for the locoregional lymph node biopsy without compromising the identification of higher-risk patients where adjuvant therapy is ideal [2]. It also helps in establishing the best surgical approach if the patient would benefit from an extensive therapeutic lymphadenectomy and decrease the number of patients to undergo unnecessary extensive lymphadenectomy with a negative lymph node biopsy [11, 16, 17].

In the study of Bluemel et al. (2015) [6], SLNB can be used in patients in a patient with melanoma have a Breslow thickness of >1mm and <1 mm with ulceration, mitotic rate of > 0.6. Moncayo et al. (2017) also stated that the detection rates of SLNB using lymphoscintigraphy with thin or intermediate thickness melanomas are 100% [4]. Lymphoscintigraphy with SLNB is a robust technique with high reproducibility and accuracy in melanoma providing a lymphatic road map to assess the direct lymphatic flow of the tumor [2].

Lymphoscintigraphy with SLNB was applied in this case using Filtered Tc 99m Sulfur Colloid with preoperative planar imaging to assess the sentinel lymph nodes and their lymphatic drainage as vulvar melanoma has a high variability with unpredictable drainage patterns. The use of SLNB in Intermediate and thick-thickness melanomas does not demonstrate a survival benefit. Surgical oncologist still pursue SLNB due to its strong prognostic factor as specific survival is improved when CLND was performed immediately following SLNB with nodal involvement, and lastly, SLNB has a low morbidity and can stratify patients who are candidates for palliative or adjuvant therapy [4].

In addition, Giammarile et al. (2014) also stated that preoperative radiotracer lymphoscintigraphic mapping should be used whenever possible in vulvar cancer since it improves the accuracy in isolating the SLN and reduces morbidity along with a handheld gamma probe [1]. The use of the radiotracer along with methylene blue improves the detection rate at 95 - 100%.

Kraft et al. (2012) identified sentinel lymph nodes by identifying the lymphatic ducts, period of appearance, noted lymph node basin, and increased radiotracer uptake of the lymph node [18]. In some cases when there is non-visualization of nodes in planar images, adjacent nodes may be misinterpreted as one, injection site may masks the sentinel node, and limited radiotracer accumulation is noted due to alteration of the lymphatic drainage, a SPECT or SPECT/CT can be used to increase the sensitivity [6, 18]. In addition, SPECT/CT images can map and identify lymph nodes and drainage that are superimposed by the tumor. Due to the CT's anatomic component, increased localization precision is noted to be 70 - 100% [7].

Since the planar view of a gamma camera has limited spatial resolution, some nodes may appear as one. But after the removal of the said hot node, another node may still be detected and this usually occurs when the nodes are close together at around 15 - 20 mm [2, 4] This holds in our patient's case where we only identified 5 sentinel nodes in the preoperative SLN mapping and intraoperatively we identified 6 nodules with the aid of the gamma probe. After the excision of the SLN, a proper evaluation of the surgical bed was done to assess if there are other remaining SLN and the counts noted were unremarkable. In this case, the limiting spatial resolution of the preoperative Gamma Camera planar image was supplemented by the intraoperative biopsy using the gamma probe.

Along with the gamma probe, the indocyanine green fluorescence technique was also used. The nodes detected by the gamma probe also fluoresced under the hand-held infrared gun. However, some nodes did not fluoresce until it was excised out of the surgical bed. This was explained by the study of Bluemel et al. (2015) [6] that a limitation of the indocyanine green is that it has an optical penetration restriction of < 10 mm, as a result overlying structures or deep adipose tissue which can preclude the assessment of the specific node. Hence for reliability and effectiveness, gamma probing cannot be replaced by indocyanine green imaging intraoperatively for guided SLN biopsy. However the combination of the two techniques can be used to increase the accuracy of detecting the SLN [3].

CONCLUSION

Sentinel lymph node mapping scintigraphy gives the surgeons the advantage to tailor a detailed surgical plan, with intraoperative gamma probing helping to identify sentinel lymph nodes intraoperatively. With these, proper staging can be executed without risking morbidities, and adjuvant treatment can be started immediately. Especially for vulvar melanomas where it has a poor prognosis and a high recurrence rate. Proper staging can be done when sentinel lymph node mapping and biopsy are used. Over-treatment of lymphadenectomy can be avoided since sentinel lymph node status is vital in the prognosis of this disease.

DISCLOSURE

The authors of this study have no conflicts of interest to disclose.

REFERENCES

1. Giammarile F, Bozkurt MF, Cibula D, Pahisa J, Oyen WJ, Paredes P, Olmos RV, Sicart SV. The EANM clinical and technical guidelines for lymphoscintigraphy and sentinel node localization in gynaecological cancers. Eur J Nucl Med Mol Imaging. 2014 Jul;41(7):1463-77. doi: 10.1007/s00259-014-2732-8. Epub 2014 Mar 8. PMID: 24609929.
2. Kraft O, Havel M. Detection of Sentinel Lymph Nodes in Gynecologic Tumours by Planar Scintigraphy and SPECT/CT. Mol Imaging Radionucl Ther. 2012 Aug;21(2):47-55. doi: 10.4274/Mirt.236. Epub 2012 Aug 1. PMID: 23486989; PMCID: PMC3590971.
3. Stoffels I, Dissemond J, Pöppel T, Schadendorf D, Klode J. Intraoperative Fluorescence Imaging for Sentinel Lymph Node Detection: Prospective Clinical Trial to Compare the Usefulness of Indocyanine Green vs Technetium Tc 99m for Identification of Sentinel Lymph Nodes. JAMA Surg. 2015 Jul;150(7):617-23. doi: 10.1001/jamasurg.2014.3502. PMID: 26017057.
4. Moncayo VM, Alazraki AL, Alazraki NP, Aarsvold JN. Sentinel Lymph Node Biopsy Procedures. Semin Nucl Med. 2017 Nov;47(6):595-617. doi: 10.1053/j.semnuclmed.2017.06.004. Epub 2017 Sep 6. PMID: 28969759.
5. Zámbó K, Koppán M, Paál A, Schmidt E, Tinneberg HR, Bódis J. Sentinel lymph nodes in gynaecological malignancies: frontline between TNM and clinical staging systems? Eur J Nucl Med Mol Imaging. 2003 Dec;30(12):1684-8. doi: 10.1007/s00259-003-1264-4. Epub 2003 Sep 11. PMID: 13680196.
6. Bluemel C, Herrmann K, Giammarile F, Nieweg OE, Dubreuil J, Testori A, Audisio RA, Zoras O, Lassmann M, Chakera AH, Uren R, Chondrogiannis S, Colletti PM, Rubello D. EANM practice guidelines for lymphoscintigraphy and sentinel lymph node biopsy in melanoma. Eur J Nucl Med Mol Imaging. 2015 Oct; 42(11):1750-1766. doi: 10.1007/s00259-015-3135-1. Epub 2015 Jul 25. PMID: 26205952.
7. Paño B, Sebastià C, Ripoll E, Paredes P, Salvador R, Buñesch L, Nicolau C. Pathways of lymphatic spread in gynecologic malignancies. Radiographics. 2015 May-Jun;35(3):916-45. doi: 10.1148/rg.2015140086. PMID: 25969940.
8. Janco JM, Markovic SN, Weaver AL, Cliby WA. Vulvar and vaginal melanoma: case series and review of current management options including neoadjuvant chemotherapy. Gynecol Oncol. 2013 Jun;129(3):533-7. doi: 10.1016/j.ygyno.2013.02.028. Epub 2013 Feb 26. PMID: 23480869.
9. Sanchez A et al. (2016). Primary genitourinary melanoma: epidemiology and disease-specific survival in a large population-based cohort. PubMed. PMID: 26739672 DOI: 10.1016/j.urolonc.2015.11.009

10. Sinasac SE, Petrella TM, Rouzbahman M, Sade S, Ghazarian D, Vicus D. Melanoma of the Vulva and Vagina: Surgical Management and Outcomes Based on a Clinicopathologic Reviewof 68 Cases. J Obstet Gynaecol Can. 2019 Jun;41(6):762-771. doi: 10.1016/j.jogc.2018.07.011. Epub 2018 Nov 2. PMID: 30391279.
11. Trifirò G, Travaini LL, Sanvito F, Pacifici M, Mallia A, Ferrari ME, Vertua A, Maggioni A, Paganelli G, Sideri MG. Sentinel node detection by lymphoscintigraphy and sentinel lymph node biopsy in vulvar melanoma. Eur J Nucl Med Mol Imaging. 2010 Apr;37(4):736-41. doi: 10.1007/s00259-009-1358-8. Epub 2010 Jan 27. PMID: 20107788.
12. Kalampokas E, Kalampokas T, Damaskos C. Primary Vaginal Melanoma, A Rare and Aggressive Entity. A Case Report and Review of the Literature. In Vivo. 2017 Jan 2;31(1):133-139. doi: 10.21873/invivo.11036. PMID: 28064232; PMCID: PMC5354139.
13. Kobayashi K, Ramirez PT, Kim EE, Levenback CF, Rohren EM, Frumovitz M, Mar MV, Gayed IW. Sentinel node mapping in vulvovaginal melanoma using SPECT/CT lymphoscintigraphy. Clin Nucl Med. 2009 Dec;34(12):859-61. doi: 10.1097/RLU.0b013e3181becdaf. PMID: 20139817.
14. Bacalbasa N, Balescu I, Dimitriu M, Balalau C, Vilcu M, Brezean I. Does sentinel lymph node detection play a role in patients with vaginal cancer? J Clin Invest Surg. 2019; 4 (1): 1-4. DOI: 10.25083/2559.5555/4.1/1.4.
15. Jimenez-Heffernan A, Ellmann A, Sado H, Huić D, Bal C, Parameswaran R, Giammarile F, Pruzzo R, Kostadinova I, Vorster M, Almeida P, Santiago J, Gambhir S, Sergieva S, Calderon A, Young GO, Valdes-Olmos R, Zaknun J, Magboo VP, Pascual TN. Results of a Prospective Multicenter International Atomic Energy Agency Sentinel Node Trial on the Value of SPECT/CT Over Planar Imaging in Various Malignancies. J Nucl Med. 2015 Sep;56(9):1338-44. doi: 10.2967/jnumed.114.153643. Epub 2015 Jul 30. PMID: 26229148.
16. Skanjeti A, Dhomps A, Paschetta C, Tordo J, Giammarile F. Sentinel Node Mapping in Gynecologic Cancers: A Comprehensive Review. Semin Nucl Med. 2019 Nov;49 (6):521-533. doi: 10.1053/j.semnuclmed.2019.06.012. Epub 2019 Jun 29. PMID: 31630736.
17. Wechter ME, Gruber SB, Haefner HK, Lowe L, Schwartz JL, Reynolds KR, Johnston CM, Johnson TM. Vulvar melanoma: a report of 20 cases and review of the literature. J Am Acad Dermatol. 2004 Apr;50(4):554-62. doi: 10.1016/j.jaad.2003.07.026. PMID: 15034504.
18. Kraft O, Havel M. Localisation of sentinel lymph nodes in patients with melanomas by planar lymphoscintigraphic and hybrid SPECT/CT imaging. Nucl Med Rev Cent East Eur. 2012 Aug 27;15(2):101-7. PMID: 22936502.

Prevalence of Sarcopenia Among Filipinos with Breast Cancer Using Dual Energy X-ray Absorptiometry (DXA)

Iris Johanna S. Isip, MD, Raquel Marie R. Cabatu-Key, MD, Carl Joshua M. Chianpian, MD
Eduardo Erasto S. Ongkeko, MD, Irene S. Bandong, MD

Department of Nuclear Medicine and Theranostics, St. Luke's Medical Center - Quezon City
E-mail address: isip.md@yahoo.com

ABSTRACT

Introduction:

Sarcopenia is a new geriatric syndrome characterized by decreased muscle function or strength and low muscle mass. It has been observed to be a common parameter in many cancers with its presence showing a higher risk of morbidity and mortality. Currently, dual-energy X-ray absorptiometry (DXA) is the widely used method to measure muscle mass in sarcopenia research.

Objective:

This study aimed to determine the prevalence of sarcopenia and examine whether sarcopenia was associated with the risk for hip fracture and low bone mineral density among Filipinos with breast cancer. This study also determined the association of risk factors in the development of sarcopenia, osteoporosis, osteopenia and osteosarcopenia among Filipinos with breast cancer.

Methodology:

This is a cross sectional analytical study of 68 postmenopausal Filipinos diagnosed with breast carcinoma who underwent whole body bone densitometry from April 1, 2019 to August 31, 2023. A whole body composition analysis and whole body bone mineral density (BMD) was done to obtain bone mineral density and appendicular skeletal muscle mass. Height and weight were also measured to compute the body mass index. Skeletal muscle index was calculated by dividing the appendicular skeletal muscle mass by the height^2 and a cut -off value of 5.4 kg/m^2 was used to determine the presence of sarcopenia.

Results:

Among the 68 participants, 7 participants (10.3%) were diagnosed with sarcopenia. Sarcopenia was not associated with osteopenia, osteoporosis, and the risk of developing hip fracture. Normal body mass index showed a positive association with developing sarcopenia (p = 0.0) and osteosarcopenia (p = 0.001). Age proved to be a significant factor in the development of osteoporosis in our participants with the mean age of 63.63 years old (p = 0.03). Variables such as age, number of years diagnosed with breast cancer, type of surgery, histopathology, molecular types, and types of treatment received showed no significant association in the development of osteopenia.

Conclusion:

The study highlights the muscle-bone-fat tissue interaction in the development of both sarcopenia and osteosarcopenia. Though no statistically significant association was seen between sarcopenia and bone mineral density, the results suggest that patients with sarcopenia may be at higher risk for developing osteopenia and osteoporosis, especially those in the elderly population, and active screening should be considered.

.

Keywords*: Sarcopenia, Hip fracture, Breast Cancer, Philippines*

INTRODUCTION

Sarcopenia, a form of muscle atrophy and advanced disease, is a new geriatric syndrome common in people at the age of 50 with a prevalence of about 5 to 10% among people aged 65 years old and older. It is characterized as a decline in walking speed or grip strength associated with low muscle mass [1]. This may result in reduced physical capability, poorer quality of life, impaired cardiopulmonary performance, unfavorable metabolic effects, falls, disability, and mortality in older people, as well as high healthcare expenditure [2]. Breast cancer is the most frequent cancer in women and one of the most common causes of cancer-related death among women in the world. The disease, as well as its treatments, are associated with negative changes in body composition that may lead to sarcopenia which may impair quality of life, treatment completion, and survival outcomes. Evidence shows that sarcopenia and osteoporosis have similar pathways, including catabolic molecules released by the skeletal muscle [3]. Whole body bone densitometry (DXA) is most commonly used in diagnosing sarcopenia [4]. Asia, being the most populated and fastest-aging region in the world, may soon very well experience the effects of sarcopenia among its elderly population. Though experts and researchers of sarcopenia from China, Hong Kong, Japan, South Korea, Malaysia, Taiwan, and Thailand organized and updated the Asian Working Group for Sarcopenia (AWGS) last 2019 [5], local data from the Philippines and its association with breast cancer and hip fracture have yet to be fully investigated.

Significance and Rationale

Sarcopenia is a new geriatric syndrome that may be caused by multiple factors, including decreased caloric intake, poor blood flow to muscles, mitochondrial dysfunction, a decline in anabolic hormones, and an increase in proinflammatory cytokines (Figure 1).

Sarcopenia is a common finding in adults with cancer and has been associated with increased treatment-related toxicities and poor survival. The presence of sarcopenia in patients with hip fractures is 58% of the cases and results in lower functional ability. This may result in hip fracture complications, additional health source utilization, and a high probability of a contralateral hip fracture. The early detection of sarcopenia in adults with breast cancer is beneficial to initiate early treatment and avoid further complications [6]. The impact of sarcopenia has been quantified in several studies on morbidity, disability, high costs of healthcare, and mortality [7].

Sarcopenia and Breast Cancer

Sarcopenia is an important geriatric syndrome that increases the risk of negative consequences such as physical disability, poor quality of life, and death. In particular, a recent systematic review to assess the consequences of sarcopenia reported approximately six different types of adverse outcomes: mortality, functional decline, falls, fracture, length of hospital stay, and hospitalization [8]. Sarcopenia has emerged as a common parameter in many cancers. A recent study showed that 16% of breast cancer patients were sarcopenic and was independently associated with an overall higher risk for mortality compared to those non-sarcopenic breast cancer patients [9].

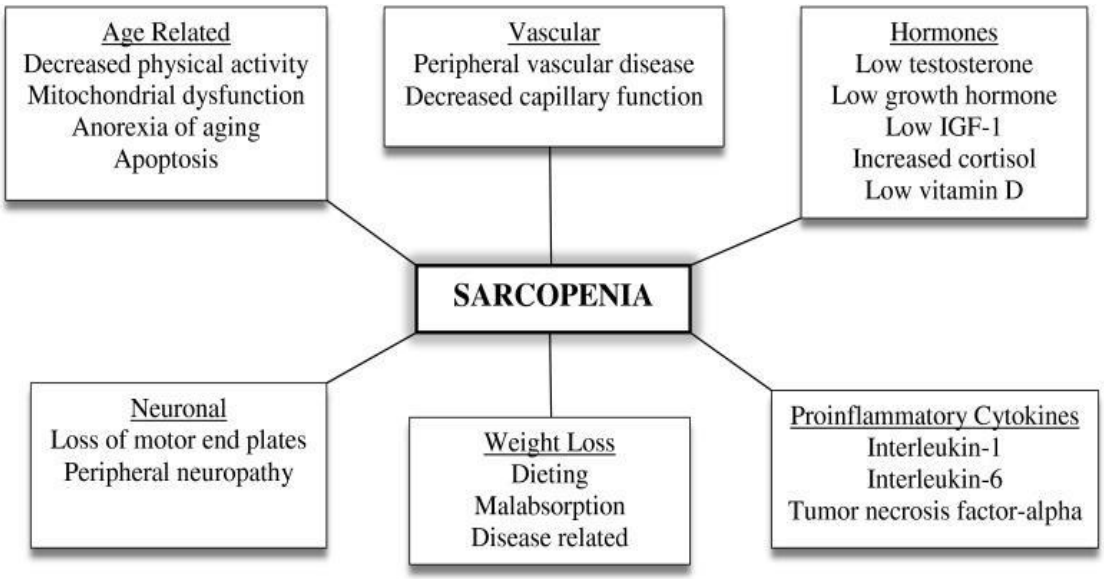

FIGURE 1. The causes of sarcopenia [1]

Dual Energy X-Ray Absorptiometry (DXA) and Sarcopenia

DXA is based on the physical principle of measurement of the X-ray transmission in crossing tissues of the human body at two different energy levels. The radiation energies are variably attenuated (absorbed or scattered) by anatomical structures, depending on the intensity of energy and the density and thickness of human tissues [10]. Currently, it is the most widely used method for muscle mass measurement in sarcopenia research. DXA provides absolute values for total muscle mass and regional muscle mass. Appendicular skeletal muscle mass (ASM) is defined as the sum of the muscle mass of both arms and legs and is generally used for the skeletal muscle mass index (SMI). However, muscle mass is fundamentally correlated with body size. Therefore, several studies have adjusted the absolute level of ASM for body size in different ways, namely using height squared (ASM/ht^2), weight (ASM/wt), or body mass index (ASM/BMI) [11]. These studies showed the following cut-off values, which will be the reference standards of this research [2, 12, 13].

TABLE 1. Mean cut-off values of ASM/ht for men and women in Japan and Korea

	AWGS ASM/ht	Japan ASM/ht		Korea ASM/ht		Korea ASM/ wt	
		Class I	Class II	Class I	Class II	Class I	Class II
Men	7.0	7.77	6.87	7.50	6.58	32.2	29.1
Women	5.4	6.12	5.46	5.38	4.59	25.6	23.0

Role of Sarcopenia in Osteoporotic Hip Fractures

Sarcopenia and osteoporosis which are major syndromes in elderly patients, which include weight loss, low muscle strength, decreased walking speed and instability, and more importantly, frequent falls and fractures. Both sarcopenia and osteoporosis are diseases characterized by a state of disequilibrium. Fall-related fractures are some of the most serious consequences of these two systemic pathologies, with hip fracture being a major complication affecting osteoporotic and sarcopenic elderly [14].

OBJECTIVES

General Objective

To determine the prevalence of sarcopenia among Filipinos with breast cancer.

Specific Objectives

1. To determine the association between sarcopenia and risk for hip fracture among Filipinos with breast cancer
2. To determine the association between bone mineral density and sarcopenia among Filipinos with breast cancer
3. To determine the association of risk factors in the development of sarcopenia among Filipinos with breast cancer
4. To determine the association of risk factors in the development of osteoporosis among Filipinos with breast cancer
5. To determine the association of risk factors in the development of osteopenia among Filipinos with breast cancer
6. To determine the association of risk factors in the development of osteosarcopenia among Filipinos with breast cancer

METHODOLOGY

Type of study, time period, and target population

This is a prospective cross-sectional analytical study on the prevalence of sarcopenia in post-menopausal Filipinas diagnosed with breast cancer who underwent whole body bone densitometry at a tertiary hospital in the Philippines from April 1, 2019 to August 31, 2023. Written informed consent was obtained from each participant and the study was approved by the Institutional Ethics Review Committee of the Research and Biotechnology Division of the said hospital. The study was conducted in compliance with Good Clinical Practice Guidelines Procedures (GCP) and complied with the Declaration of Helsinki.

Inclusion criteria

- Participants who provided informed consent
- Post-menopausal Filipina participants
- Participants with breast cancer for 2 to 3 years with or without treatment
- With or without history of hip fracture
- Participants who underwent whole bone densitometry

Exclusion criteria

- Pregnant participants
- Participants with metal implants and pacemakers
- Participants with musculoskeletal abnormalities
- Participants with metabolic abnormalities
- Participants who received bisphosphonates or anti-resorptive bone medications

Study Maneuver

All qualified participants who underwent whole body bone densitometry in a tertiary hospital in the Philippines from April 1, 2019 to August 31, 2023 were included in the study. The researchers obtained written consent using the consent to participate in the trial.

The participants' height, weight and BMI were determined. Relevant clinical history, such as histopathology, treatment received, history of hip fracture, were extracted. The lean mass of the four limbs were collected for sarcopenia computation and the bone mineral densities of the spine and bilateral hips were assessed for osteoporosis.

Measurement of Body Anthropometrics

The participants were asked to change into a hospital gown, and to remove shoes and accessories. Height and weight were measured twice and averaged to the nearest 0.1 kg and 0.5 cm, respectively.

Measurement of Body Composition Using GE Lunar iDXA

The participants were given written instructions before the procedure. A whole-body scan was performed in Thick Mode, as determined by GE's Lunar software enCORE for 13 minutes. Whole-body composition analysis provided data on different regions of interest, including the trunk, arms and legs. The machine was calibrated daily using a standardized phantom. Only one trained nuclear medicine technologist performed the whole body bone mineral density (BMD) and acquired the values of the lean mass and BMDs. Evaluation of the whole body composition analysis and whole body bone mineral density was done independently by two (2) nuclear medicine physicians of more than 5 years of experience who are blinded on the patient's information and clinical consideration. A third nuclear medicine physician of similar years of experience, also blinded regarding the patient's information, clinical consideration and the interpretation of the other 2 nuclear medicine physicians, evaluated the data in question to reach a consensus during the event of non-agreement.

Outcome Measures

A. Dependent variables

- Sarcopenia
- Risk for hip fracture

B. Independent variables

- Lean mass measurement
- Bone mineral densities in the spine and bilateral hips
- Height, weight and body mass index
- Histopathology

Operational definitions

1. Filipino patient – patient who is of Filipino descent in which both parents are Filipino
2. DXA – Dual-Energy X-ray Absorptiometry. A machine that measures the mass of a material (eg. muscle, fat, bone) by comparing the material's absorption of x-rays
3. Sarcopenia – a syndrome characterized by a decline in walking speed or grip strength associated with low muscle mass. AWGS recommends using 2 standard deviations below the skeletal muscle index (SMI) of young reference group or the lower quintile as the cutoff value determination. The group also recommends using height-adjusted skeletal muscle mass instead of weight-adjusted skeletal muscle mass, and the suggested cutoff values were 7.0 kg/m^2 in men and 5.4 kg/m^2 in women by using DXA. The equation for SMI is as follows:

$$SMI = \frac{appendicular\ skeletal\ muscle\ (ASM)}{height^2}$$

   where, ASM = sum of the muscle masses of the four limbs acquired using DXA.
4. Osteopenia – a decrease in bone mineral density defined by bone densitometry as a T score -1 to -2.5
5. Osteoporosis – a decrease in bone mineral density defined by bone densitometry as a T score < -2.5
6. Osteosarcopenia - the presence of both osteoporosis and sarcopenia
7. Geriatric syndrome – older age, cognitive impairment, functional impairment, and impaired mobility
8. Mitochondrial dysfunction – long-term, genetic, often inherited disorders that occur when the mitochondria fail to produce enough energy for the body to function properly
9. Anabolic hormones – hormones that stimulate protein synthesis and muscle growth
10. Proinflammatory cytokines – produced by activated macrophages; involved in up-regulation of inflammatory reactions in the body
11. Impaired cardiopulmonary performance – decreased oxygen uptake, heart rate, and pulse relative oxygen during an activity

12. Metabolic effects – changes in the body's metabolism
13. Bone mineral density (BMD) – measure of bone density, reflecting the strength of bones as represented by calcium content
14. Musculoskeletal abnormalities – decrease in muscle mass or leg atrophy secondary to poliomyelitis
15. Metabolic abnormalities – diseases that may affect bone mineral metabolism like hyperparathyroidism

Sample size estimation

Sample size was calculated based on the estimation of the prevalence of sarcopenia among breast cancer patients aged 50 years old and above, assumed to be 48.8% [6]. With a maximum allowable error of 10% and reliability of 90%, the calculated sample size was 68.

Statistical analysis

Data was encoded and tallied in SPSS version 23 for Windows. Descriptive statistics were generated for all variables. For nominal data, frequencies and percentages were computed. For numerical data, mean ± SD were generated. Analysis of the different variables was done using the following test statistics:

- Chi-square test – used to compare/associate nominal data
- T-test – used to compare two groups with numerical data
- Mann Whitney U test - a non-parametric equivalent of the t-test.

RESULTS

Among the 68 participants included in the study, 7 patients (10.3%) were found to have sarcopenia, while the remaining 61 patients (89.7%) did not. Table 2 shows the prevalence of sarcopenia and the distribution of patients according to BMD. No significant association was seen among sarcopenia and bone mineral density (p = 0.26), as well as in the risk of developing hip fracture (p = 0.98) (Table 3).

TABLE 2. Prevalence of Sarcopenia

	Frequency (%)
Sarcopenia	
Positive	7 (10.3%)
Negative	61 (89.7%)
BMD	
Osteoporosis	30 (44.1%)
Osteopenia	30 (44.1%)
Normal	8 (11.8%)

TABLE 3. Association of BMD and Risk for Hip Fracture with Sarcopenia

	Sarcopenia		Total	*p-value*
	Positive (n=7)	**Negative** (n=61)		
	Frequency (%) / Mean (SD)			
BMD				
Osteoporosis	5 (16.7%)	25 (83.3%)	30	0.26†
Osteopenia	2 (6.7%)	28 (93.3%)	30	
Normal	0	8 (100%)	8	
Risk for Hip Fracture	1.33 (1.18)	1.30 (2.88)	1.30 (2.75)	0.98‡

p > 0.05- NS (Not significant); p ≤ 0.05-(S) Significant;

† Chi-square test; ‡ t-test

Multiple variables such as bone mineral density, age, number of years diagnosed with breast cancer, type of surgery, histopathology, molecular types, and types of treatment received, were analyzed to identify their association in the development of sarcopenia, osteoporosis, osteopenia, as well osteosarcopenia (Tables 4 - 7). All of the patients with sarcopenia and osteosarcopenia have normal body mass index, showing statistically significant differences with the participants with no sarcopenia (p = 0.0) and no osteosarcopenia (p = 0.001). Age proved to be a significant factor in the development of osteoporosis in our participants with the mean age of 63.63 years old (p = 0.03). Among the aforementioned variables, no significant association was seen in the development of osteopenia.

DISCUSSION

Prevalence of sarcopenia among Filipinos with breast cancer

The study determined the prevalence of sarcopenia among Filipinos diagnosed with breast carcinoma. Seven out of 68 participants were diagnosed with sarcopenia (10.3%) which is relatively similar to the prevalence rate of 15.9% from the HEAL study describing the prevalence of breast cancer survivors using dual-energy X-ray absorptiometry to obtain appendicular lean muscle mass [9].

Multiple studies reported the prevalence of sarcopenia in breast cancer patients ranging from 11.5 to 17.3% utilizing bioelectrical impedance to measure appendicular skeletal muscle mass [15, 16, 17]. A higher prevalence of 30% was observed in a different study wherein they used the Computed Tomography scan to

TABLE 4. Association of the Different Variables with the Development of Sarcopenia Among Patients with Breast Cancer

	Sarcopenia		Total	*p-value*
	Positive (n=7)	**Negative**(n=61)		
	Frequency (%)/Mean (SD)			
BMI				
Obese	0	40 (65.6%)	40 (58.8%)	
Overweight	0	9 (14.8%)	9 (13.2%)	0.000†
Normal	7 (100%)	12 (19.7%)	19 (27.9%)	
Age (in years)	63.14 (7.88)	60.93 (8.66)	61.16 (8.55)	0.52‡
Number of Years Diagnosed with Breast cancer	9.00 (7.14)	8.61 (5.76)	8.65 (5.86)	0.86‡
Surgery				
Mastectomy	6 (85.7%)	52 (85.2%)	58 (85.3%)	
Lumpectomy	1 (14.3%)	2 (3.3%)	3 (4.4%)	0.28†
No Data	0	7 (11.5%)	7 (10.3%)	
Histopath				
Invasive Ductal CA	5 (83.3%)	30 (50.0%)	35 (53.0%)	
Invasive Breast CA	0	11 (18.3%)	11 (16.7%)	0.43†
Invasive Lobular CA	0	3 (5.0%)	3 (4.5%)	
No Data	1 (16.7%)	16 (26.7%)	17 (25.8%)	
ER				
Negative	2 (28.6%)	5 (8.3%)	7 (10.4%)	
Positive	4 (57.1%)	37 (61.7%)	41 (61.2%)	0.22†
No Data	1 (14.3%)	18 (30.0%)	19 (28.4%)	
PR				
Negative	2 (28.6%)	11 (18.3%)	13 (19.4%)	
Positive	4 (57.1%)	31 (51.7%)	35 (52.2%)	0.63†
No Data	1 (14.3%)	18 (30.0%)	19 (28.4%)	
HER2NEU				
Negative	3 (42.9%)	33 (54.1%)	36 (52.9%)	
Positive	3 (42.9%)	9 (14.8%)	12 (17.6%)	0.17†
No Data	1 (14.3%)	19 (31.1%)	20 (29.4%)	
Chemotherapy				
Negative	2 (28.6%)	16 (26.2%)	18 (26.5%)	
Positive	5 (71.4%)	41 (67.2%)	46 (67.6%)	0.78†
No Data	0	4 (6.6%)	4 (5.9%)	
Radiation				
Negative	5 (28.6%)	33 (54.1%)	38 (55.9%)	
Positive	2 (28.6%)	22 (36.1%)	24 (35.3%)	0.57†
No Data	0	6 (9.8%)	6 (8.8%)	
Hormonal Therapy				
Negative	2 (28.6%)	10 (16.4%)	12 (17.6%)	
Positive	5 (71.4%)	48 (78.7%)	53 (77.9%)	0.63†
No Data	0	3 (4.9%)	3 (4.4%)	

p > 0.05- NS (Not significant); p ≤ 0.05-(S) Significant;

† Chi-square test; ‡ t-test; §Mann Whitney U test

to measure skeletal muscle index [18]. Prevalences may vary from different studies due to the differences in the technique of evaluating skeletal muscle mass and by the operational definition of sarcopenia.

Association of sarcopenia with the risk for hip fracture among Filipinos with breast cancer

In the present study, the risk of hip fracture in sarcopenic participants was similar to the non-sarcopenic participants concluding that the presence of sarcopenia

TABLE 5. Association of the Different Variables with the Development of Osteoporosis Among Patients with Breast Cancer

	Osteoporosis		*p-value*
	Positive (n=30)	**Normal** (n=8)	
	Mean (SD); Frequency (%)		
BMI			
Obese	13 (43.3%)	7 (87.5%)	
Overweight	4 (13.3%)	0	0.08†
Normal	13 (43.3%)	1 (12.5%)	
Age (in years)	63.63 (8.19)	56.88 (4.76)	0.03‡
Number of Years Diagnosed with breast cancer	9.93 (6.30)	7.38 (3.85)	0.28‡
Surgery			
Mastectomy	26 (86.7%)	7 (87.5%)	
Lumpectomy	1 (3.3%)	0	0.85†
No Data	3 (10.0%)	1 (12.5%)	
Histopath			
Invasive Ductal CA	15 (50.0%)	5 (62.5%)	
Invasive Breast CA	5 (16.7%)	1 (12.5%)	0.57†
Invasive Lobular CA	1 (3.3%)	1 (12.5%)	
No Data	9 (30.0%)	1 (12.5%)	
ER			
Negative	4 (13.3%)	0	
Positive	17 (56.7%)	7 (87.5%)	0.25†
No Data	9 (30.0%)	1 (12.5%)	
PR			
Negative	6 (20.0%)	1 (12.5%)	
Positive	15 (50.0%)	6 (75.0%)	0.44†
No Data	9 (30.0%)	1 (12.5%)	
HER2NEU			
Negative	14 (46.7%)	7 (87.5%)	
Positive	7 (23.3%)	0	0.10†
No Data	9 (30.0%)	1 (12.5%)	
Chemotherapy			
Negative	8 (26.7%)	2 (25.0%)	
Positive	20 (66.7%)	6 (75.0%)	0.74†
No Data	2 (6.7%)	0	
Radiation			
Negative	14 (46.7%)	6 (75.0%)	
Positive	13 (43.3%)	2 (25.0%)	0.32†
No Data	3 (10.0%)	0	
Hormonal Therapy			
Negative	6 (20.0%)	0	
Positive	22 (73.3%)	8 (100%)	0.26†
No Data	2 (6.7%)	0	

p > 0.05- NS (Not significant); p ≤ 0.05-(S) Significant;

† Chi-square test; ‡ t-test; §Mann Whitney U test

is not a risk for developing hip fracture. This is similar to the previous studies wherein they observed that muscle mass alone was not associated with either hip or major fracture risk [19]. However, low bone mineral density with sarcopenia showed a greater risk for hip fracture compared to those with low bone mineral density and sarcopenia alone [20]. The study by He et al. (2019) suggested that appendicular lean muscle mass derived by DXA offers limited predictive value for the incidence of fractures in postmenopausal women when BMD is also considered [21].

TABLE 6. Association of the Different Variables with the Development of Osteopenia Among Patients with Breast Cancer

	Osteopenia		*p-value*
	Positive (n=30)	**Normal** (n=8)	
	Mean (SD); Frequency (%)		
BMI			
Obese	20 (66.7%)	7 (87.5%)	
Overweight	5 (16.7%)	0	0.40†
Normal	5 (16.7%)	1 (12.5%)	
Age (in years)	59.83 (9.12)	56.88 (4.76)	0.38‡
Number of Years Diagnosed with breast cancer	7.70 (5.80)	7.38 (3.85)	0.88‡
Surgery			
Mastectomy	25 (83.3%)	7 (87.5%)	
Lumpectomy	2 (6.7%)	0	0.75†
No Data	3 (10.0%)	1 (12.5%)	
Histopath			
Invasive Ductal CA	15 (50.0%)	5 (62.5%)	
Invasive Breast CA	5 (16.7%)	1 (12.5%)	0.57†
Invasive Lobular CA	1 (3.3%)	1 (12.5%)	
No Data	9 (30.0%)	1 (12.5%)	
ER			
Negative	3 (10.3%)	0	
Positive	17 (58.6%)	7 (87.5%)	0.30†
No Data	9 (31.0%)	1 (12.5%)	
PR			
Negative	6 (20.7%)	1 (12.5%)	
Positive	14 (48.3%)	6 (75.0%)	0.40†
No Data	9 (31.0%)	1 (12.5%)	
HER2NEU			
Negative	15 (51.7%)	7 (87.5%)	
Positive	5 (17.2%)	0	0.17†
No Data	9 (31.0%)	1 (12.5%)	
Chemotherapy			
Negative	8 (26.7%)	2 (25.0%)	
Positive	20 (66.7%)	6 (75.0%)	0.73†
No Data	2 (6.7%)	0	
Radiation			
Negative	18 (60.0%)	6 (75.0%)	
Positive	9 (30.0%)	2 (25.0%)	0.58†
No Data	3 (10.0%)	0	
Hormonal Therapy			
Negative	6 (20.0%)	0	
Positive	23 (76.7%)	8 (100%)	0.32†
No Data	1 (3.3%)	0	

p > 0.05- NS (Not significant); p ≤ 0.05-(S) Significant;

† Chi-square test; ‡ t-test; §Mann Whitney U test

Association of sarcopenia and bone mineral density among Filipinos with breast cancer

Previous studies showed the interrelationship of sarcopenia and bone mineral density with supportive findings such as sarcopenic patients having a higher osteoporosis risk, osteoporotic patients being more likely to suffer from sarcopenia, and that each standard deviation increase in relative appendicular skeletal muscle mass significantly decreased the risk of osteoporosis [21, 22]. There are similarities in the pathogenesis of sarcopenia and osteoporosis through biomechanics and biochemistry explaining their

TABLE 7. Association of the Different Variables with the Development of Osteosarcopenia Among Patients with Breast Cancer

	With Osteosarcopenia (n=5)	Without Osteosarcopenia (n=60)	Total	*p-value*
	Mean (SD); Frequency (%)			
BMI				
Obese	0	40 (63.5%)	40 (58.8%)	
Overweight	0	9 (14.3%)	9 (13.2%)	0.001†
Normal	5 (100%)	14 (22.2%)	19 (27.9%)	
Age (in years)	66.40 (6.80)	60.75 (8.58)	61.16 (8.55)	0.15‡
Years Diagnosed with Breast cancer	11.40 (7.12)	8.41 (5.76)	8.65 (5.86)	0.28‡
Surgery				
Mastectomy	4 (80.0%)	54 (85.7%)	58 (85.3%)	
Lumpectomy	1 (20.0%)	2 (3.2%)	3 (4.4%)	0.17†
No Data	0	7 (11.1%)	7 (10.3%)	
Histopath				
Invasive Ductal CA	4 (80.0%)	31 (49.2%)	35 (51.5%)	
Invasive Breast CA	0	11 (17.5%)	11 (16.2%)	0.56†
Invasive Lobular CA	0	3 (4.8%)	3 (4.4%)	
No Data	1 (20.0%)	18 (28.6%)	19 (27.9%)	
ER				
Negative	1 (20.0%)	6 (9.7%)	7 (10.4%)	
Positive	3 (60.0%)	38 (61.3%)	41 (61.2%)	0.74†
No Data	1 (20.0%)	18 (29.0%)	19 (28.4%)	
PR				
Negative	1 (20.0%)	12 (19.4%)	13 (19.4%)	
Positive	3 (60.0%)	32 (51.6%)	35 (52.2%)	0.90†
No Data	1 (20.0%)	18 (29.0%)	19 (28.4%)	
HER2NEU				
Negative	2 (40.0%)	34 (54.0%)	36 (52.9%)	
Positive	2 (40.0%)	10 (15.9%)	12 (17.6%)	0.39†
No Data	1 (20.0%)	19 (30.2%)	20 (29.4%)	
Chemotherapy				
Negative	1 (20.0%)	17 (27.0%)	18 (26.5%)	
Positive	4 (80.0%)	42 (66.7%)	46 (67.6%)	0.76†
No Data	0	4 (6.3%)	4 (5.9%)	
Radiation				
Negative	3 (60.0%)	35 (55.6%)	38 (55.9%)	
Positive	2 (40.0%)	22 (34.9%)	24 (35.3%)	0.76†
No Data	0	6 (9.5%)	6 (8.8%)	
Hormonal Therapy				
Negative	0	12 (19.0%)	12 (17.6%)	
Positive	5 (100%)	48 (76.2%)	53 (77.9%)	0.46†
No Data	0	3 (4.8%)	3 (4.4%)	

p > 0.05- NS (Not significant); p ≤ 0.05-(S) Significant;

† Chi-square test; ‡ t-test; § Mann Whitney U test

their symbiotic relationship.

This study showed no statistically significant association between the presence of sarcopenia and bone mineral density. However, we observed that among the 7 sarcopenic participants, 5 of them were osteoporotic (16.7%), 2 were osteopenic (6.7%), and none were observed to have normal BMDs. These findings suggest that clinicians should consider screening for sarcopenia in patients with low bone mineral density.

Risk factors in developing sarcopenia in breast cancer patients

The investigators observed that among the variables that may contribute to the development of sarcopenia, normal body mass index showed a significant association (p= 0.000). Other factors such as age, number of years diagnosed with breast cancer, type of surgery, histopathology, subtypes, and type of therapy showed no significant association. This finding is consistent with previous studies wherein they observed sarcopenic patients diagnosed with breast cancer had lower BMI (normal to underweight) compared to non-sarcopenic patients [15, 16, 23] despite the differences in determining skeletal muscle mass. One of the known causes of sarcopenia is weight loss which results in loss of both fat and muscle, and even when a person regains the weight, the majority will be fat rather than muscle [1]. Further studies stated that the increased likelihood of sarcopenia in individuals with low BMI may be a marker of malnutrition and warrants nutritional support or management [24].

Risk factors for developing osteoporosis or osteopenia among Filipinos with breast cancer

Advanced age appears to be a risk factor in developing osteoporosis among breast cancer patients. Previous studies observed that the incidence rate of osteoporosis was higher in older breast cancer patients [25, 26, 27]. In contrast to other studies [28] exposure to chemo- and hormonal therapies are not associated with developing either osteopenia or osteoporosis in breast cancer patients however the duration of treatment and specific treatment protocol were not taken into account.

Risk factors of osteosarcopenia among Filipinos with breast cancer

Bone, muscle, and adipose tissues interact with each other by mechanical and neuro-hormonal pathways and a problem in one aspect can greatly affect the other. Lower body mass index is identified as a positive risk factor in the development of osteosarcopenia among breast cancer patients. Our finding supports the previous study stating that a higher BMI is a protective factor against osteosarcopenia [29] whereas high-fat mass is a strongly associated factor in developing osteosarcopenia. This highlights the value of identifying body composition and differentiating fat from bone and muscle mass [30].

LIMITATION OF THE STUDY

The strengths of our study include a well characterized prospective cross-sectional design, consecutive sampling design and blinding of interpreters. The main limitation is the fact that this was done in a single institution and the sample population may not accurately represent the Filipino population with breast carcinoma. Future researchers should seek to confirm these findings in a larger and more diverse patient population. The study also lacks data regarding muscle strength and functional capacity of the participants to completely evaluate the presence of sarcopenia, as well as to grade the severity. Given the lack of a standardized definition for sarcopenia with multiple publications factoring in skeletal muscle mass, strength, functional capacity, BMI, height, weight, different methods of measurement, as well as conflicting cut-off values, the definition of sarcopenia that was adopted by the current investigation may have led to the underdetection of sarcopenia in the current participant pool.

RECOMMENDATIONS

Based on our findings, future researchers may want to focus on the following research topics.

1. Concordance with bioelectrical impedance, Computed tomography, and DXA, in measuring skeletal muscle mass.
2. Subgroup analyses such as cancer stage, molecular subtype, as well as the type and duration of the treatment regimen could also be explored to improve the predictive value of these tests.
3. Analysis of fat content through DEXA, determining its association with sarcopenia, as well as the prevalence of sarcopenic obesity is another area worth examining.

CONCLUSION

The prevalence of sarcopenia among Filipino breast cancer patients was 10.3%. Sarcopenia is not associated with osteopenia, osteoporosis, and the risk of developing hip fractures. The study highlights the muscle-bone-fat tissue interaction that supports our findings that low body mass index has a role in the development of both sarcopenia and osteosarcopenia. Though no statistically significant association was seen between sarcopenia and bone mineral density, the results suggest that patients with sarcopenia may be at higher risk for developing osteopenia and osteoporosis, especially those in the elderly population, and active screening should be considered in these individuals.

KEYPOINTS

The results of the study emphasizes the active screening for sarcopenia in patients with low bone mineral density and/or osteoporosis regardless of the presence of a concomitant malignancy or other co-morbidities, especially for post-menopausal women.

FUNDING

The authors extends their appreciation to the Research and Biotechnology Division for funding this work through a Research Project.

DISCLOSURE

The authors of this study have no conflicts of interest to disclose.

REFERENCES

1. Morley JE, Anker SD, von Haehling S. Prevalence, incidence, and clinical impact of sarcopenia: facts, numbers, and epidemiology-update 2014. J Cachexia Sarcopenia Muscle. 2014 Dec;5(4):253-9. doi: 10.1007/s13539-014-0161-y. Epub 2014 Oct 22. Erratum in: J Cachexia Sarcopenia Muscle. 2015 Jun;6(2):192. doi: 10.1002/jcsm.12038. PMID: 25425503; PMCID: PMC4248415.
2. Chen LK, Liu LK, Woo J, Assantachai P, Auyeung TW, Bahyah KS, Chou MY, Chen LY, Hsu PS, Krairit O, Lee JS, Lee WJ, Lee Y, Liang CK, Limpawattana P, Lin CS, Peng LN, Satake S, Suzuki T, Won CW, Wu CH, Wu SN, Zhang T, Zeng P, Akishita M, Arai H. Sarcopenia in Asia: consensus report of the Asian Working Group for Sarcopenia. J Am Med Dir Assoc. 2014 Feb;15(2):95-101. doi: 10.1016/j.jamda.2013.11.025. PMID: 24461239.
3. Reginster JY, Beaudart C, Buckinx F, Bruyère O. Osteoporosis and sarcopenia: two diseases or one? Curr Opin Clin Nutr Metab Care. 2016 Jan;19(1):31-6. doi: 10.1097/MCO.0000000000000230. PMID: 26418824; PMCID: PMC4888925.
4. Han A, Bokshan SL, Marcaccio SE, DePasse JM, Daniels AH. Diagnostic Criteria and Clinical Outcomes in Sarcopenia Research: A Literature Review. J Clin Med. 2018 Apr 8;7(4):70. doi: 10.3390/jcm7040070. PMID: 29642478; PMCID: PMC5920444.
5. Chen LK, Woo J, Assantachai P, Auyeung TW, Chou MY, Iijima K, Jang HC, Kang L, Kim M, Kim S, Kojima T, Kuzuya M, Lee JSW, Lee SY, Lee WJ, Lee Y, Liang CK, Lim JY, Lim WS, Peng LN, Sugimoto K, Tanaka T, Won CW, Yamada M, Zhang T, Akishita M, Arai H. Asian Working Group for Sarcopenia: 2019 Consensus Update on Sarcopenia Diagnosis and Treatment. J Am Med Dir Assoc. 2020 Mar;21(3):300-307.e2. doi: 10.1016/j.jamda.2019.12.012. Epub 2020 Feb 4. PMID: 32033882.
6. Deluche E, Leobon S, Desport JC, Venat-Bouvet L, Usseglio J, Tubiana-Mathieu N. Impact of body composition on outcome in patients with early breast cancer. Support Care Cancer. 2018 Mar;26(3):861-868. doi: 10.1007/s00520-017-3902-6. Epub 2017 Sep 25. PMID: 28948392; PMCID: PMC5785600.
7. Tee ML, Tee CA, Montemayor EB. Determination of normative reference for the definition of sarcopenia among Filipinos. Osteoporos Sarcopenia. 2016 Sep;2(3):186-190. doi: 10.1016/j.afos.2016.07.004. Epub 2016 Aug 23. Erratum in: Osteoporos Sarcopenia. 2016 Dec;2(4):259. doi: 10.1016/j.afos.2016.11.003. PMID: 30775486; PMCID: PMC6372749.
8. Liguori I, Russo G, Aran L, Bulli G, Curcio F, Della-Morte D, Gargiulo G, Testa G, Cacciatore F, Bonaduce D, Abete P. Sarcopenia: assessment of disease burden and strategies to improve outcomes. Clin Interv Aging. 2018 May 14;13:913-927. doi: 10.2147/CIA.S149232. PMID: 29785098; PMCID: PMC5957062.
9. Villaseñor A, Ballard-Barbash R, Baumgartner K, Baumgartner R, Bernstein L, McTiernan A, Neuhouser ML. Prevalence and prognostic effect of sarcopenia in breast cancer survivors: the HEAL Study. J Cancer Surviv. 2012 Dec;6(4):398-406. doi: 10.1007/s11764-012-0234-x. Epub 2012 Oct 4. PMID: 23054848; PMCID: PMC3747827.
10. Guglielmi G, Ponti F, Agostini M, Amadori M, Battista G, Bazzocchi A. The role of DXA in sarcopenia. Aging Clin Exp Res. 2016 Dec;28(6):1047-1060. doi: 10.1007/s40520-016-0589-3. Epub 2016 Jun 2. PMID: 27256078.
11. Kim KM, Jang HC, Lim S. Differences among skeletal muscle mass indices derived from height-, weight-, and body mass index-adjusted models in assessing sarcopenia. Korean J Intern Med. 2016 Jul;31(4):643-50. doi: 10.3904/kjim.2016.015. Epub 2016 Jun 22. PMID: 27334763; PMCID: PMC4939509.
12. Sanada K, Miyachi M, Tanimoto M, Yamamoto K, Murakami H, Okumura S, Gando Y, Suzuki K, Tabata I, Higuchi M. A cross - sectional study of sarcopenia in

Japanese men and women: reference values and association with cardiovascular risk factors. Eur J Appl Physiol. 2010 Sep;110(1):57-65. doi: 10.1007/s00421-010-1473-z. PMID: 20390291.

13. Kim YS, Lee Y, Chung YS, Lee DJ, Joo NS, Hong D, Song Ge, Kim HJ, Choi YJ, Kim KM. Prevalence of sarcopenia and sarcopenic obesity in the Korean population based on the Fourth Korean National Health and Nutritional Examination Surveys. J Gerontol A Biol Sci Med Sci. 2012 Oct;67(10):1107-13. doi: 10.1093/gerona/gls071. Epub 2012 Mar 19. PMID: 22431554.

14. Oliveira A, Vaz C. The role of sarcopenia in the risk of osteoporotic hip fracture. Clin Rheumatol. 2015 Oct;34 (10):1673-80. doi: 10.1007/s10067-015-2943-9. Epub 2015 Apr 26. PMID: 25912213.

15. Liu X, Zhang E, Wang S, Shen Y, Xi K, Fang Q. Association of body composition with clinical outcome in Chinese women diagnosed with breast cancer. Front Oncol. 2022 Sep 20;12:957527. doi: 10.3389/fonc.2022.957527. PMID: 36203426; PMCID: PMC9530819.

16. Morlino D, Marra M, Cioffi I, Santarpia L, De Placido P, Giuliano M, De Angelis C, Carrano S, Verrazzo A, Buono G, Naccarato M, Di Vincenzo O, Speranza E, De Placido S, Arpino G, Pasanisi F. Prevalence of Sarcopenia in Women with Breast Cancer. Nutrients. 2022 Apr 28;14(9):1839. doi: 10.3390/nu14091839. PMID: 35565806; PMCID: PMC9099516.

17. Oflazoglu U, Alacacioglu A, Varol U, Kucukzeybek Y, Salman T, Taskaynatan H, Yildiz Y, Ozdemir O, Tarhan M. Prevalence and related factors of sarcopenia in newly diagnosed cancer patients. Support Care Cancer. 2020 Feb;28(2):837-843. doi: 10.1007/s00520-019-04880-4. Epub 2019 Jun 3. PMID: 31161438.

18. Kayalı İ, Habiboğlu R. Prevalence and Presence of Sarcopenia and Sarcopenic Obesity in Female Breast Cancer Patients". Clinical Science of Nutrition, vol. 6, no. 1, Apr. 2024, pp. 1-10, https://doi.org/10.62210/ClinSciNutr.2024.81.

19. de Almeida Marques Bernabé R, de Souza Vieira M, Felício de Souza V, Gomes Fontana L, Albergaria BH, Marques-Rocha JL, Guandalini VR. Muscle strength is associated with fracture risk obtained by fracture risk assessment tool (FRAX) in women with breast cancer. BMC Cancer. 2022 Nov 1;22(1):1115. doi: 10.1186/s12885-022-10203-4. PMID: 36320019; PMCID: PMC9623985.

20. Harris R, Chang Y, Beavers K, Laddu-Patel D, Bea J, Johnson K, LeBoff M, Womack C, Wallace R, Li W, Crandall C, Cauley J. Risk of Fracture in Women with Sarcopenia, Low Bone Mass, or Both. J Am Geriatr Soc. 2017 Dec;65 (12):2673-2678. doi: 10.1111/jgs.15050. Epub 2017 Sep 27. PMID: 28960230; PMCID: PMC5729083.

21. He H, Liu Y, Tian Q, Papasian CJ, Hu T, Deng HW. Relationship of sarcopenia and body composition with osteoporosis. Osteoporos Int. 2016 Feb;27(2):473-82. doi: 10.1007/s00198-015-3241-8. Epub 2015 Aug 5. PMID: 26243357.

22. Yu X, Sun S, Zhang S, Hao Q, Zhu B, Teng Y, Long Q, Li S, Lv Y, Yue Q, Lu S, Teng Z. A pooled analysis of the association between sarcopenia and osteoporosis. Medicine (Baltimore). 2022 Nov 18;101(46):e31692. doi: 10.1097/MD.0000000000031692. PMID: 36401390; PMCID: PMC9678526.

23. Del Fabbro E, Parsons H, Warneke CL, Pulivarthi K, Litton JK, Dev R, Palla SL, Brewster A, Bruera E. The relationship between body composition and response to neoadjuvant chemotherapy in women with operable breast cancer. Oncologist. 2012;17(10):1240-5. doi: 10.1634/theoncologist.2012-0169. Epub 2012 Aug 17. PMID: 22903527; PMCID: PMC3481889.

24. Curtis M, Swan L, Fox R, Warters A, O'Sullivan M. Associations between Body Mass Index and Probable Sarcopenia in Community-Dwelling Older Adults. Nutrients. 2023 Mar 21;15(6):1505. doi: 10.3390/nu15061505. PMID: 36986233; PMCID: PMC10059806.

25. Ramin C, May BJ, Roden RBS, Orellana MM, Hogan BC, McCullough MS, Petry D, Armstrong DK, Visvanathan K. Evaluation of osteopenia and osteoporosis in younger breast cancer survivors compared with cancer-free women: a prospective cohort study. Breast Cancer Res. 2018 Nov 13;20(1):134. doi: 10.1186/s13058-018-1061-4. PMID: 30424783; PMCID: PMC6234595.

26. Chen Z, Maricic M, Pettinger M, Ritenbaugh C, Lopez AM, Barad DH, Gass M, Leboff MS, Bassford TL. Osteoporosis and rate of bone loss among postmenopausal survivors of breast cancer. Cancer. 2005 Oct 1;104(7):1520-30. doi: 10.1002/cncr.21335. PMID: 16110508.

27. Huang JF, Tan QC, Bai H, Wang J, Bergman M, Wu Z. Bone mineral density, osteopenia and osteoporosis among US adults with cancer. QJM. 2022 Oct 25;115(10):653-660. doi: 10.1093/qjmed/hcac015. PMID: 35092293.

28. Shapiro CL. Osteoporosis: A Long-Term and Late-Effect of Breast Cancer Treatments. Cancers (Basel). 2020 Oct 23;12(11):3094. doi: 10.3390/cancers12113094. PMID: 33114141; PMCID: PMC7690788.

29. Moreno-Aguilar M, Molina MM, Hernandez MFH. Inverse Association Between Body Mass Index and Osteosarcopenia in Community Dwelling Elderly. Surgery for Obesity and Related Diseases. 2017 13(10) Supplement, S190. https://doi.org/10.1016/j.soard.2017.09.419.

30. Fahimfar N, Zahedi Tajrishi F, Gharibzadeh S, Shafiee G, Tanha K, Heshmat R, Nabipour I, Raeisi A, Jalili A, Larijani B, Ostovar A. Prevalence of Osteosarcopenia and Its Association with Cardiovascular Risk Factors in Iranian Older People: Bushehr Elderly Health (BEH) Program. Calcif Tissue Int. 2020 Apr;106(4):364-370. doi: 10.1007/s00223-019-00646-6. Epub 2019 Dec 17. PMID: 31848645.

Skeletal Muscle Mass among Postmenopausal Filipino Women and its Relationship with Bone Mineral Density and FRAX-based Fracture Risks

Francis Manuel L. Resma, MD, Arnel E. Pauco, MD

Division of Nuclear Medicine, Department of Medicine, University of the Philippines - Philippine General Hospital
E-mail address: flresma@up.edu.ph

ABSTRACT

Background:

Decreased skeletal muscle mass is one of the components of sarcopenia. Sarcopenia and osteoporosis, which are both common in the elderly, are associated with increased morbidity and mortality. This study examined the relationship of total body skeletal muscle mass (SMM) and appendicular skeletal muscle mass (ASM) with bone mineral density (BMD) and FRAX-based fracture risks in postmenopausal Filipino women.

Methodology:

A total of 123 postmenopausal Filipino women who underwent whole-body bone densitometry scans using dual -energy X-ray absorptiometry (DXA) in the Philippine General Hospital from January 1, 2017 to December 31, 2019 were included in this study. Significant differences between patients with low ASM and patients with normal ASM were determined using Student t test, Mann-Whitney U test, and Fisher exact test. Pairwise correlations between the different numerical variables were determined using Spearman rank-correlation coefficient analysis .

Results:

Among the 123 study subjects, 110 (89.43%) had normal ASM, while 13 (10.57%) had low ASM. Meanwhile, 6 (4.88%) had normal BMD, 40 (32.52%) had osteopenia, and 77 (62.60%) had osteoporosis. Compared to study subjects with normal ASM, study subjects with low ASM had significantly lower median lumbar spine BMD, lower mean femoral neck BMD, lower mean total hip BMD, higher median FRAX (major osteoporotic fracture), and higher median FRAX (hip fracture). There was no sufficient evidence that study subjects with low ASM and study subjects with normal ASM had a significant difference in BMD category. Both SMM and ASM had positive moderate correlations with BMD in all three sites (lumbar spine, femoral neck, and total hip). Moreover, both SMM and ASM had inverse moderate correlations with FRAX (major osteoporotic fracture) and FRAX (hip fracture).

Conclusion:

Our study showed that both low SMM and low ASM are associated with lower BMD and higher FRAX-based fracture risks among postmenopausal Filipino women. However, larger studies incorporating muscle strength and physical performance are recommended to further analyze the relationship between sarcopenia and osteoporosis .

Keywords*: Skeletal muscle mass, appendicular skeletal muscle mass, bone mineral density, FRAX*

INTRODUCTION

Skeletal muscle mass contributes 30 to 40% of the total body mass and is thus a key constituent of body composition. It is related to physical functions and the health status of individuals. Approximately 75% of skeletal muscle mass is situated at the limbs (also known as appendicular skeletal muscle mass). Decreased muscle mass in the appendicular skeleton results in adverse health consequences, including weakness, disability, poor quality of life, and mortality [1].

Low appendicular skeletal muscle mass is part of the three criteria to diagnose sarcopenia. According to the Asian Working Group for Sarcopenia (AWGS), sarcopenia is the loss of skeletal muscle mass with increasing age, together with decreased muscle strength and/or physical performance. The pathophysiology of sarcopenia may involve motor neuron loss,

decreased activity of neuromuscular junctions, hormonal changes, cytokines that promote inflammation, decreased function of mitochondria, abnormal production of myokines, and decreased weight due to reduced appetite [2] .

Sarcopenia is common in older people, as is osteoporosis. According to the WHO, osteoporosis is the disease wherein low bone mass as well as microarchitectural decline of bone tissue result in fragile bones, resulting in an higher probability of fracture [3]. Sarcopenia and osteoporosis are both linked to substantial morbidity and mortality [4], as sarcopenia is linked to a greater probability of falls, which further predisposes osteoporotic individuals to sustain low-impact or fragility fractures such as in the hip [5]. Sarcopenia and hip/vertebral fractures have also been shown to predict future mortality in older individuals. Studies likewise reveal that muscle health may be linked to bone health. A possible explanation for this link is the mechanostat hypothesis which states that muscle contraction provides a direct mechanical stimulus for osteogenesis. Hormones, including growth hormone, can also enhance the growth of muscles and bones. Genetics may also contribute to muscle and bone health [4]. There are also factors that cause both loss of skeletal muscle mass and loss of bone mass. These include changes associated with aging such as the decline in the levels of sex steroid hormones, as well as impaired signaling and activity of growth hormone and IGF-1 [5]. Therefore, muscle mass may have a relationship with bone mineral density (BMD) and the probability of fractures.

Dual-energy x-ray absorptiometry, or DXA, is a widely utilized test to diagnose osteoporosis using BMD measurements in the spine as well as the proximal femur, which are the two most frequent sites of osteoporotic fractures [6]. Osteoporosis is diagnosed among postmenopausal women and males at least 50 years old if the BMD values in the lumbar spine, total hip, or femoral neck are at least 2.5 standard deviations below the reference standard (white female, 20 to 29 years old, NHANES III database). The 33% radius (1/3 radius) of the non-dominant forearm may be used to diagnose osteoporosis if the hip and/or spine cannot be measured or interpreted, in patients with hyperparathyroidism, and in severely obese patients whose weight is greater than the maximum weight that the DXA table can carry [7].

Aside from initial diagnosis and monitoring of osteoporosis using BMD, another application of DXA includes the measurement of body composition (divided into bone, lean or muscle, and fat) [6]. DXA can be used to measure total body lean tissue mass (total body skeletal muscle mass or SMM) and appendicular skeletal muscle mass or ASM. Because individuals with a bigger body size usually have a higher muscle mass, either height, weight, or BMI can be used to adjust for the measured SMM and ASM [8]. The AWGS 2019 recommends using either DXA or multifrequency bioelectrical impedance analysis (BIA) for the measurement of muscle mass in the diagnosis of sarcopenia. The AWGS 2019 cutoffs for low ASM (height-adjusted) in the diagnosis of sarcopenia using DXA are: less than 7.0 kg/m^2 in males and <5.4 kg/m2 in females [2].

BMD alone may not be sensitive for predicting fracture risk [9]. Hence, the Fracture Risk Assessment Tool or FRAX algorithm was created. The FRAX algorithm utilizes clinical risk factors and fracture and mortality data specific to each country to measure an individual's probability of a hip or major osteoporotic fracture in 10 years. The FRAX algorithm guides clinicians in determining which patients have a higher probability of developing fragility fractures. These patients require treatment to improve their bone health. The National Osteoporosis Foundation recommends that aside from patients with hip/vertebral fractures and osteoporosis, treatment should also be commenced in postmenopausal women as well as males at least 50 years old with low bone mass (defined as a T-score of -1.1 to -2.4 in the femoral neck, total hip, or spine) in combination with a ≥ 3% probability of hip fracture or ≥ 20% probability of major osteoporotic fracture in 10 years, measured using the FRAX algorithm [10].

Osteopenic and osteoporotic patients who have a low ASM may have a higher fracture risk than osteopenic or osteoporotic women with normal ASM. It has been proposed that screening for low ASM during BMD examinations by DXA may be useful in detecting osteopenic or osteoporotic women who have a low ASM because these patients may require interventions to increase both muscle mass and BMD [5].

OBJECTIVE

General objective

To measure the skeletal muscle mass of postmenopausal Filipino women and its relationship with bone mineral density (BMD) and FRAX-based fracture risks

Specific objectives

1. To measure the total body skeletal muscle mass (SMM) and appendicular skeletal muscle mass (ASM) of postmenopausal Filipino women
2. To measure the prevalence of low ASM among postmenopausal Filipino women
3. To measure the relationship of SMM and ASM with BMD (at the lumbar spine, at the femoral neck, and at the total hip) and FRAX-based fracture risks (major osteoporotic and hip fracture risks)

METHODOLOGY

Research design

Retrospective analytical study that utilized a review of medical records

Study site

This study was conducted at the Radioisotope Laboratory, located inside the Philippine General Hospital.

Sampling design

All postmenopausal Filipino women who had whole-body bone mineral densitometry scans using DXA during the period January 1, 2017 to December 31, 2019 who fulfilled the inclusion criteria but did not satisfy the exclusion criteria were involved in this study. With confidence level at 95%, 5% error, and the prevalence of sarcopenia which was 6.10% in a study done in the Philippines [11], the computed sample size for this study was 89.

Inclusion criteria

All postmenopausal Filipino women (no menstruation for at least 1 year) who had whole-body bone mineral densitometry scans using DXA during the period January 1, 2017 and December 31, 2019.

Exclusion criteria

1. Patients with prosthetic or metal implants because these affect the values calculated by the DXA machine
2. Patients under 40 years old because FRAX-based fracture risks were not available for these younger patients
3. Patients with diseases associated with secondary osteoporosis and other disorders that may affect the musculoskeletal system such as rheumatoid arthritis, type 1 diabetes mellitus, osteogenesis imperfecta, thyrotoxicosis, hypogonadism, early menopause (before 45 years of age), nutritional disorders, heart failure, chronic lung disease, chronic liver disease, chronic kidney disease, growth hormone deficiency, gigantism, acromegaly, hypothyroidism, hyperparathyroidism, Cushing syndrome, vitamin D deficiency, other bone metabolic disorders, malignancy, neurologic diseases, paralysis or immobilization, myopathy, other diseases associated with a lower muscle mass, or a history of taking medications known to affect skeletal muscle mass or bone mineral density (including levothyroxine, estrogen, progesterone, anti-osteoporosis drugs, and chronic steroid use)

Data collection and outcomes

The principal investigator collected the following data: age, BMI, SMM, ASM, BMD at the lumbar spine, BMD at the femoral neck, BMD at the total hip, FRAX with BMD for major osteoporotic fracture, and FRAX with BMD for hip fracture. These values were obtained from the whole-body bone densitometry scans performed by trained technicians using the DXA machine (Stratos dR, DMS Group, France). For the BMD at the femoral neck and total hip, the lower value among the bilateral femora was used. For the FRAX with BMD for major osteoporotic fracture and hip fracture, the higher value among the two femora was used.

The ISCD guidelines [7] were followed. The L1-L4 vertebrae were used to calculate the lumbar spine BMD; however, if a vertebra had structural changes or artifacts, it was excluded, with at least two vertebrae remaining. Anatomically abnormal vertebrae were excluded from analysis if they were grossly abnormal and unable to be evaluated by the resolution of the system, and if the difference in the T-score between one vertebra and its adjacent vertebrae was greater than 1.0. The WHO criteria for normal BMD (T-score of -1.0 or higher), osteopenia (T-score of -1.1 to -2.4), and osteoporosis (T-score of -2.5 or lower) were used [3]. The AWGS 2019 cutoff for low ASM in women by DXA (<5.4 kg/m^2) was applied [2].

Data handling, processing, and storage

Data was handled, processed, and stored in adherence to the Data Privacy Act of 2012. The principal investigator encoded the data in a Microsoft Excel file, locked using a password, that was accessible to the principal investigator only. For the protection of privacy and confidentiality of research information, patients were anonymized using code numbers. Data stored will be kept for five (5) years. Subsequently, the data will be erased.

Statistical analysis

For numerical variables that were normally distributed, means and standard deviations were applied to summarize the data. For numerical variables not following the normal distribution, median and interquartile range were utilized. Finally, for categorical variables, frequency and percentage were applied. Significant differences between patients with low ASM and patients with normal ASM were determined by Student t test, Mann-Whitney U test, and Fisher exact test for numerical variables that followed the normal distribution, non-normally distributed numerical variables, and categorical variables, respectively. Pairwise correlations between the different numerical variables were determined by Spearman rank-correlation coefficient analysis. Data analysis was accomplished via Stata 17. There were no missing values in this dataset. The Shapiro-Wilk test of normality was employed to evaluate if numerical variables followed the normal distribution. Tests of hypothesis were evaluated with significance level established at $p = 0.05$.

Ethical considerations

Approval from the University of the Philippines Manila Research Ethics Board (UPMREB) was obtained before the initiation of this study. The study subjects did not receive incentives or compensation.

Conflict of interest

The authors declare no conflicts of interest relevant to the preparation of this study.

RESULTS

Table 1 summarizes the characteristics of the 123 study subjects. The mean SMM was 33.44 kg, while the median ASM was 6.5 kg/m2. Among the 123 study subjects, 110 (89.43%) had normal ASM, while 13 (10.57%) had low ASM. Furthermore, 6 (4.88%) had normal BMD, 40 (32.52%) had osteopenia, and 77 (62.60%) had osteoporosis.

TABLE 1. Characteristics of the 123 study subjects.

Characteristic	Value
Age (years), *mean (SD)*	66.59 (8.39)
BMI (kg/m^2), *median (IQR)*	24.9 (4.5)
SMM (kg), *mean (SD)*	33.44 (4.79)
ASM (kg/m^2), *median (IQR)*	6.5 (1.3)
ASM Category	
Normal ASM, *frequency (%)*	110 (89.43%)
Low ASM, *frequency (%)*	13 (10.57%)
Lumbar spine BMD (g/cm^2), *median (IQR)*	0.74 (0.19)
Femoral neck BMD (g/cm^2), *mean (SD)*	0.70 (0.13)
Total hip BMD (g/cm^2), *mean (SD)*	0.84 (0.14)
BMD Category	
Normal BMD, *frequency (%)*	6 (4.88%)
Osteopenia, *frequency (%)*	40 (32.52%)
Osteoporosis, *frequency (%)*	77 (62.60%)
FRAX (major osteoporotic fracture) (%), *median (IQR)*	2.88 (1.7)
FRAX (hip fracture) (%), *median (IQR)*	0.7 (1.23)

Table 2 shows the comparisons between study subjects with normal ASM and study subjects with low ASM. Study subjects with low ASM were found to have significantly lower mean BMI, lower median lumbar spine BMD, lower mean femoral neck BMD, lower mean total hip BMD, higher median FRAX (major osteoporotic fracture), and higher median FRAX (hip fracture) in comparison to study subjects with normal ASM. The group with low ASM was revealed to have a higher incidence of osteoporosis (84.62%) than the group with normal ASM (60.00%). However, no sufficient evidence was acquired to conclude that the study subjects with low ASM and the study subjects with normal ASM had a significant difference in BMD category. There was also no sufficient evidence to conclude that there was a significant difference in the mean age between study subjects with low ASM and study subjects with normal ASM.

The correlations between the variables are listed in Table 3. Both SMM and ASM had positive moderate correlations with BMD in all three sites (lumbar spine, femoral neck, and total hip). Moreover, both SMM and ASM had inverse moderate correlations with FRAX (major osteoporotic fracture) and FRAX (hip fracture).

TABLE 2. Comparisons between study subjects with normal ASM and study subjects with low ASM

Variable	Normal ASM (n = 110)	Low ASM (n = 13)	*p*-value
Age (years), *mean (SD)*	66.45 (8.46)	67.69 (7.94)	0.617
BMI (kg/m^2), *median (IQR)*	25.3 (3.7)	19.5 (1.5)	< 0.001
Lumbar spine BMD (g/cm^2), *median (IQR)*	0.76 (0.17)	0.65 (0.16)	< 0.001
Femoral neck BMD (g/cm^2), *mean (SD)*	0.72 (0.13)	0.61 (0.12)	0.003
Total hip BMD (g/cm^2), *mean (SD)*	0.85 (0.13)	0.73 (0.11)	0.003
BMD Category			0.310
Normal BMD, *frequency (%)*	6 (5.45%)	0	
Osteopenia, *frequency (%)*	38 (34.55%)	2 (15.38%)	
Osteoporosis, *frequency (%)*	66 (60.00%)	11 (84.62%)	
FRAX (major osteoporotic fracture) (%), *median (IQR)*	2.69 (1.57)	3.74 (2.22)	< 0.001
FRAX (hip fracture) (%), *median (IQR)*	0.68 (1.06)	1.53 (1.34)	< 0.001

TABLE 3. Correlation of age, BMI, SMM, ASM, BMD, and FRAX, with Spearman's rank correlation coefficient r_s. Correlations with p--value < 0.05 are marked with asterisks.

	Age	BMI	SMM	ASM	Lumbar spine BMD	Femoral neck BMD	Total hip BMD	FRAX (major osteoporotic fracture)	FRAX (hip fracture)
Age	---	0.0383	-0.1401	-0.0599	-0.0789	-0.3526*	-0.3497*	0.5081*	0.5219*
BMI	---	---	0.6981*	0.9110*	0.2612*	0.4253*	0.4257*	-0.2791*	-0.3579*
SMM	---	---	---	0.7903*	0.3409*	0.5168*	0.4832*	-0.4020*	-0.4727*
ASM	---	---	---	---	0.3045*	0.4702*	0.4733*	-0.3339*	-0.4070*
Lumbar spine BMD	---	---	---	---	---	0.6035*	0.5935*	-0.5919*	-0.5563*
Femoral neck BMD	---	---	---	---	---	---	0.8998*	-0.9324*	-0.9668*
Total hip BMD	---	---	---	---	---	---	---	-0.8605*	-0.8828*
FRAX (major osteoporotic fracture)	---	---	---	---	---	---	---	---	0.9639*
FRAX (hip fracture)	---	---	---	---	---	---	---	---	---

DISCUSSION

In this study, the prevalence of low height-adjusted appendicular skeletal muscle mass (low ASM) measured using DXA among postmenopausal women was 10.57%. This is consistent with other studies wherein the prevalence ranged from 4% to 19.5% [12, 13, 14]. However, these studies defined low ASM as a value of less than 5.45 kg/m^2, with the study of Walsh et al. (2006) [14] explaining that this cutoff value was more than 2 standard deviations under the mean of a reference population of healthy young women. Our study used a cutoff value of < 5.4 kg/m^2, based on the AWGS 2019 definition of low ASM in women when measured using DXA [2]. Other criteria for low ASM exist, such as a cutoff value of less than 5.5 kg/m^2 in the EWGSOP2 study in 2019 [8]. Differences in the cutoff values used for defining low ASM among studies may contribute to these studies' differences in the prevalence of low ASM. Disparities in the prevalence of low ASM among studies may also be due to the varying characteristics of the population included in each study, including age, home setting, and ethnicity [15]. Sarcopenia was more prevalent in studies involving women above 80 years and in nursing homes and hospitalized women compared to community-dwelling women [15, 16]. Finally, sarcopenia was more prevalent in non-Asians compared to Asians [15].

Our study revealed that postmenopausal women with low ASM had a significantly lower median lumbar spine BMD, mean femoral neck BMD, and mean total hip BMD compared to postmenopausal with normal ASM. This is contrary to the study of Sherk et al. (2009) [12] wherein there was no statistically significant difference in the mean BMD at the lumbar spine, total hip, and femoral neck between postmenopausal women with low ASM and postmenopausal women with normal ASM. The smaller sample size in the study of Sherk et al. (2009) [12], wherein only 7 postmenopausal women with low ASM and 48 postmenopausal women with normal ASM were included, possibly did not have enough statistical power to reveal significant differences between the two groups, whereas our study included 13 patients with low ASM and 110 patients with normal ASM. Meanwhile, in the study of Saddik et al. (2020) [17], postmenopausal women with low ASM had a significantly lower mean total hip BMD and mean femoral neck BMD compared to postmenopausal women with normal ASM, similar to our study. However, contrary to our study, no statistically significant difference was found in the mean lumbar spine BMD between postmenopausal women with low ASM and postmenopausal women with normal ASM. These conflicting findings may be due to differences in the severity of lumbar spine degenerative changes between patients among various studies. Degenerative lumbar spine changes are linked to increased lumbar spine BMD [5]. This may affect the correlation of lumbar spine BMD with ASM.

Other studies have investigated the relationship of total body skeletal muscle mass (SMM) and ASM with BMD in postmenopausal women. Similar with our study, Ilesanmi-Oyelere et al. (2018) [18] and Sotunde et al. (2015) [19] noted that in postmenopausal women, SMM was discovered to have significant positive correlations with BMD in the lumbar spine, femoral neck, and total hip. Gillette-Guyonett [20] also observed a significantly positive correlation between SMM and femoral neck BMD in postmenopausal women. On the contrary, in the study of Lee et al. (2016) [21], SMM was not significantly correlated with the BMD at the femoral neck or total hip among postmenopausal women. Akin to our study, Sornay-Rendu et al. (2017) [22] detected that in postmenopausal women, both SMM and ASM had positive correlations with BMD at the femoral neck. Meanwhile, Sherk et al. [12] found that in postmenopausal women, both SMM and ASM had positive correlations with BMD in the total hip and femoral neck, but not in the lumbar spine. However, in our study, both SMM and ASM had positive moderate correlations with the BMD at all three sites. Finally, in the study of Saddik et al. (2020) [17], both SMM and ASM had a positive correlation with total hip BMD and femoral neck BMD in postmenopausal women, but only SMM was positively correlated with lumbar spine BMD. These discrepancies in the relationship of SMM and ASM with BMD in postmenopausal women among studies are possibly due to differences in study designs, study populations, and DXA machines used [19].

Similar to our study, Gillette-Guyonett et al. (2000) [20] and Walsh et al. (2006) [14] did not find a correlation between low ASM and osteoporosis in postmenopausal women. One possible explanation for this is that low ASM by itself may not be enough to promote osteoporosis. There are other contributory factors to the occurrence of osteoporosis in postmenopausal women, such as genetics, older age, race, duration of estrogen deprivation, nutritional status, sedentary lifestyle, body composition, weight, smoking, chronic steroid intake, excessive alcohol intake, coffee intake, and vitamin D deficiency [23, 24]. Furthermore, aside from muscle mass, sarcopenia has two other components: muscle strength and muscle performance. One study showed that compared to muscle mass, grip strength was more significantly associated with osteoporosis in postmenopausal women [25]. Moreover, they demonstrated that the combination of ASM, grip strength, and physical performance had a stronger relationship with osteoporosis compared to the relationship of each component with osteoporosis.

Our study exhibited that in postmenopausal women, SMM and ASM had an inverse moderate correlation with median FRAX (major osteoporotic fracture) and median FRAX (hip fracture). Likewise, in the study of Zhang et al. (2012) [26], SMM displayed a negative linear correlation with the calculated probability of major osteoporotic and hip fractures in 10 years among postmenopausal women. Meanwhile, Sornay-Rendu [22] concluded that lower values of ASM correlated with a significantly increased risk of major osteoporotic fractures, along with other fractures. Similarly, in the study of Harvey et al. (2021) [27], lower values of ASM were correlated with a higher risk of incident fracture, whether clinical, osteoporotic, major osteoporotic, or at the hip.

The positive correlation of muscle mass with BMD, as well as the negative correlation of muscle mass with fracture risk, may be explained by the fact that in

postmenopausal women, muscles contribute 25 to 30 % of the extragonadal conversion of androgens to estrogen, while fat contributes only 10 to 15% [26]. The hormone estrogen promotes bone growth and prevents bone remodeling [18]. In the postmenopausal state, there is a continuous reduction in estrogen, causing bone resorption to surpass bone formation, leading to faster bone loss as well as lower bone mass [28]. Therefore, in postmenopausal women with a greater muscle mass, the higher levels of estrogen converted from androgens in their muscles may contribute to increased BMD and decreased risk of fractures. Another hypothesis that may explain the relationship of muscle mass with BMD is that higher muscle mass contributes to mechanical loading, stimulating bone growth and leading to increased BMD [29].

Postmenopausal women who are more physically active have been shown to have greater ASM compared to postmenopausal women who are sedentary or less physically active [13]. According to the study of Walsh et al. (2006) [14], physical activity had a positive correlation with both ASM and BMD in postmenopausal women. Aside from increasing muscle mass, physical activity also promotes balance, coordination, muscle strength, and reaction time, which may provide protection against fractures [26]. Muscles, which surround bones, may provide protection or padding to bones; therefore, increased muscle mass may reduce the force of impact on bones during a fall [14]. Thus, studies recommend exercise because it can increase muscle mass and consequently, decrease the risk of fractures [14, 26].

According to current guidelines, some of the indications for BMD testing include women 65 years old and above, younger postmenopausal women who have a risk factor for low bone mass, and perimenopausal women possessing clinical factors associated with an increased probability of fractures [7]. Because sarcopenia is accompanied by a greater risk of falls and fractures, measuring ASM and BMD simultaneously using DXA is recommended by Walsh et al. (2006) [14]. According to Miyakoshi et al. (2013) [5], screening for low ASM using DXA should be considered because sarcopenia is a major reason for disability and increased health costs, especially among the elderly. Moreover, concurrent measurement of ASM and BMD using DXA may be helpful in detecting women with both sarcopenia and osteoporosis, because these patients may benefit the most from physical activity and exercise programs to increase both muscle mass and BMD [5, 14].

However, our study had limitations. One limitation is that the sample size in our study was relatively small. Furthermore, our study may have suffered selection bias because only patients who visited our hospital were included. Therefore, the results of our study cannot be applied to the entire population of postmenopausal Filipino women. Larger studies with multiple centers, including communities across the country, are needed to validate the results of our study. Another limitation is that according to the AWGS 2019 criteria, sarcopenia is diagnosed by the presence of low ASM in combination with either low muscle strength (evaluated using handgrip strength) or low physical performance (measured using 6-meter walk, 5-time chair stand test, or Short Physical Performance Battery). Our study only had data on ASM and did not have data on the muscle strength and physical performance of patients. Future studies with these data are essential to further analyze the relationship between sarcopenia and osteoporosis.

CONCLUSIONS

Our study showed that lower SMM and lower ASM are both associated with lower BMD and higher FRAX-based fracture risks among postmenopausal Filipino women. Although there was no sufficient evidence to conclude that low ASM had a correlation with osteopenia or osteoporosis among postmenopausal women, measuring ASM and BMD concurrently using DXA may still be helpful because it can detect postmenopausal women with both sarcopenia and osteoporosis, a group that may be the most in need of exercise interventions to increase their ASM and BMD, as well as decrease their risk of fractures. However, larger studies are needed to validate these findings.

REFERENCES

1. Rathnayake N, Alwis G, Lenora J, Lekamwasam S. Concordance between appendicular skeletal muscle mass measured with DXA and estimated with mathematical models in middle-aged women. J Physiol Anthropol. 2018 Jul 31;37(1):19. doi: 10.1186/s40101-018-0179-5. PMID: 30064499; PMCID: PMC6069740.
2. Chen LK, Woo J, Assantachai P, Auyeung TW, Chou MY, Iijima K, Jang HC, Kang L, Kim M, Kim S, Kojima T, Kuzuya M, Lee JSW, Lee SY, Lee WJ, Lee Y, Liang CK, Lim JY, Lim WS, Peng LN, Sugimoto K, Tanaka T, Won CW, Yamada M, Zhang T, Akishita M, Arai H. Asian Working Group for Sarcopenia: 2019 Consensus Update on Sarcopenia Diagnosis and Treatment. J Am Med Dir Assoc. 2020

Mar;21(3):300-307.e2. doi: 10.1016/j.jamda.2019.12.012. Epub 2020 Feb 4. PMID: 32033882.

3. Assessment of fracture risk and its application to screening for postmenopausal osteoporosis. Report of a WHO Study Group. World Health Organ Tech Rep Ser. 1994;843:1-129. PMID: 7941614.
4. Edwards MH, Dennison EM, Aihie Sayer A, Fielding R, Cooper C. Osteoporosis and sarcopenia in older age. Bone. 2015 Nov;80:126-130. doi: 10.1016/j.bone.2015.04.016. Epub 2015 Apr 14. PMID: 25886902; PMCID: PMC4601530.
5. Miyakoshi N, Hongo M, Mizutani Y, Shimada Y. Prevalence of sarcopenia in Japanese women with osteopenia and osteoporosis. J Bone Miner Metab. 2013 Sep;31(5):556-61. doi: 10.1007/s00774-013-0443-z. Epub 2013 Mar 21. PMID: 23515924.
6. Blake GM, Fogelman I. Technical principles of dual energy x-ray absorptiometry. Semin Nucl Med. 1997 Jul;27(3):210-28. doi: 10.1016/s0001-2998(97)80025-6. PMID: 9224663.
7. Adult Positions. ISCD. Accessed July 14, 2024. https://iscd.org/learn/official-positions/adult-positions/
8. Cruz-Jentoft AJ, Bahat G, Bauer J, Boirie Y, Bruyère O, Cederholm T, Cooper C, Landi F, Rolland Y, Sayer AA, Schneider SM, Sieber CC, Topinkova E, Vandewoude M, Visser M, Zamboni M; Writing Group for the European Working Group on Sarcopenia in Older People 2 (EWGSOP2), and the Extended Group for EWGSOP2. Sarcopenia: revised European consensus on definition and diagnosis. Age Ageing. 2019 Jan 1;48(1):16-31. doi: 10.1093/ageing/afy169. Erratum in: Age Ageing. 2019 Jul 1;48(4):601. doi: 10.1093/ageing/afz046. PMID: 30312372; PMCID: PMC6322506.
9. Silverman SL, Calderon AD. The utility and limitations of FRAX: A US perspective. Curr Osteoporos Rep. 2010 Dec;8(4):192-7. doi: 10.1007/s11914-010-0032-1. PMID: 20811963; PMCID: PMC2947011.
10. Cosman F, de Beur SJ, LeBoff MS, Lewiecki EM, Tanner B, Randall S, Lindsay R; National Osteoporosis Foundation. Clinician's Guide to Prevention and Treatment of O steoporosis. Osteoporos Int. 2014 Oct;25(10):2359-81. doi: 10.1007/s00198-014-2794-2. Epub 2014 Aug 15. Erratum in: Osteoporos Int. 2015 Jul;26(7):2045-7. doi: 10.1007/s00198-015-3037-x. PMID: 25182228; PMCID: PMC4176573.
11. Gabat JAL, Faltado AL Jr, Sedurante MB, Tee ML. Association of obesity and sarcopenia among adult Filipinos. Osteoporos Sarcopenia. 2018 Sep;4(3):109-113. doi: 10.1016/j.afos.2018.08.001. Epub 2018 Sep 13. PMID: 30775552; PMCID: PMC6362942.
12. Sherk VD, Palmer IJ, Bemben MG, Bemben DA. Relationships between body composition, muscular strength, and bone mineral density in estrogen-deficient postmenopausal women. J Clin Densitom. 2009 Jul-Sep;12(3):292-8. doi: 10.1016/j.jocd.2008.12.002. Epub 2009 Jan 19. PMID: 19155180.
13. Sipilä S, Törmäkangas T, Sillanpää E, Aukee P, Kujala UM, Kovanen V, Laakkonen EK. Muscle and bone mass in middle-aged women: role of menopausal status and physical activity. J Cachexia Sarcopenia Muscle. 2020 Jun;11(3):698-709. doi: 10.1002/jcsm.12547. Epub 2020 Feb 3. PMID: 32017473; PMCID: PMC7296268.
14. Walsh MC, Hunter GR, Livingstone MB. Sarcopenia in premenopausal and postmenopausal women with osteopenia, osteoporosis and normal bone mineral density. Osteoporos Int. 2006 Jan;17(1):61-7. doi: 10.1007/s00198-005-1900-x. Epub 2005 Jul 2. PMID: 15995793.
15. Buckinx F, Aubertin-Leheudre M. Sarcopenia in Menopausal Women: Current Perspectives. Int J Womens Health. 2022 Jun 23;14:805-819. doi: 10.2147/IJWH.S340537. PMID: 35769543; PMCID: PMC9235827.
16. Okayama A, Nakayama N, Kashiwa K, Horinouchi Y, Fukusaki H, Nakamura H, Katayama S. Prevalence of Sarcopenia and Its Association with Quality of Life, Postural Stability, and Past Incidence of Falls in Postmenopausal Women with Osteoporosis: A Cross-Sectional Study. Healthcare (Basel). 2022 Jan 19;10(2):192. doi: 10.3390/healthcare10020192. PMID: 35206807; PMCID: PMC8872599.
17. Saddik H, Nasr R, Pinti A, Watelain E, Fayad I, Baddoura R, Berro AJ, Al Rassy N, Lespessailles E, Toumi H, El Hage R. Sarcopenia negatively affects hip structure analysis variables in a group of Lebanese postmenopausal women. BMC Bioinformatics. 2020 Mar 11;21(Suppl 2):86. doi: 10.1186/s12859-020-3353-9. PMID: 32164524; PMCID: PMC7068911.
18. Ilesanmi-Oyelere BL, Coad J, Roy N, Kruger MC. Lean Body Mass in the Prediction of Bone Mineral Density in Postmenopausal Women. Biores Open Access. 2018 Oct 10;7(1):150-158. doi: 10.1089/biores.2018.0025. PMID: 30327744; PMCID: PMC6188582.
19. Sotunde OF, Kruger HS, Wright HH, Havemann-Nel L, Kruger IM, Wentzel-Viljoen E, Kruger A, Tieland M. Lean Mass Appears to Be More Strongly Associated with Bone Health than Fat Mass in Urban Black South African Women. J Nutr Health Aging. 2015 Jun;19(6):628-36. doi: 10.1007/s12603-015-0492-1. PMID: 26054499.
20. Gillette-Guyonnet S, Nourhashemi F, Lauque S, Grandjean H, Vellas B. Body composition and osteoporosis in elderly women. Gerontology. 2000 Jul-Aug;46(4):189-93. doi: 10.1159/000022158. PMID: 10859457.
21. Lee I, Cho J, Jin Y, Ha C, Kim T, Kang H. Body Fat and Physical Activity Modulate the Association Between Sarcopenia and Osteoporosis in Elderly Korean Women. J Sports Sci Med. 2016 Aug 5;15(3):477-482. PMID: 27803626; PMCID: PMC4974860.
22. Sornay-Rendu E, Duboeuf F, Boutroy S, Chapurlat RD. Muscle mass is associated with incident fracture in postmenopausal women: The OFELY study. Bone. 2017 Jan;94:108-113. doi: 10.1016/j.bone.2016.10.024. Epub 2016 Oct 27. PMID: 27989649.

23. Dogu B, Sirzai H, Usen A, Yilmaz F, Kuran B. Comparison of body composition, nutritional status, functional status, and quality of life between osteoporotic and osteopenic postmenopausal women. Medicina (Kaunas). 2015;51 (3):173-179. doi: 10.1016/j.medici.2015.05.003. Epub 2015 Jul 5. PMID: 28705480.
24. Chiu CT, Lee JI, Lu CC, Huang SP, Chen SC, Geng JH. The association between body mass index and osteoporosis in a Taiwanese population: a cross-sectional and longitudinal study. Sci Rep. 2024 Apr 12;14(1):8509. doi: 10.1038/s41598-024-59159-4. PMID: 38605101; PMCID: PMC11009266.
25. Sjöblom S, Suuronen J, Rikkonen T, Honkanen R, Kröger H, Sirola J. Relationship between postmenopausal osteoporosis and the components of clinical sarcopenia. Maturitas. 2013 Jun;75(2):175-80. doi: 10.1016/j.maturitas.2013.03.016. Epub 2013 Apr 28. PMID: 23628279.
26. Zhang Z, Shen X, Zhang H, Li S, Zhou H, Wu X, Sheng Z, Liao E. The relationship between body composition and fracture risk using the FRAX model in central south Chinese postmenopausal women. Clin Endocrinol (Oxf). 2012 Oct;77(4):524-30. doi: 10.1111/j.1365-2265.2012.04399.x. PMID: 22469329.
27. Harvey NC, Kanis JA, Liu E, Cooper C, Lorentzon M, Bea JW, Carbone L, Cespedes Feliciano EM, Laddu DR, Schnatz PF, Shadyab AH, Stefanick ML, Wactawski-Wende J, Crandall CJ, Johansson H, McCloskey E. Predictive Value of DXA Appendicular Lean Mass for Incident Fractures, Falls, and Mortality, Independent of Prior Falls, FRAX, and BMD: Findings from the Women's Health Initiative (WHI). J Bone Miner Res. 2021 Apr;36(4):654-661. doi: 10.1002/jbmr.4239. Epub 2021 Jan 28. PMID: 33450071; PMCID: PMC7610603.
28. Zhou Z, Zheng L, Wei D, Ye M, Li X. Muscular strength measurements indicate bone mineral density loss in postmenopausal women. Clin Interv Aging. 2013;8:1451-9. doi: 10.2147/CIA.S48447. Epub 2013 Oct 25. PMID: 24187494; PMCID: PMC3810326.
29. Ho-Pham LT, Nguyen UD, Nguyen TV. Association between lean mass, fat mass, and bone mineral density: a meta-analysis. J Clin Endocrinol Metab. 2014 Jan;99(1):30-8. doi: 10.1210/jc.2014-v99i12-30A. Epub 2013 Jan 1. PMID: 24384013.

Mediso

AnyScan® TRIO Product Line
SPECT, SPECT/CT and SPECT/CT/PET *Molecular Imaging Scanners*

Triple-NaI-Detector SPECT/CT for quantitative and high-performance 360° PET-Like imaging and workflow for diagnostic and theranostic applications.

The AnyScan® triple modality platform uniquely integrates SPECT, CT and PET for clinical NM imaging in a single scanner for dual- and triple-detector systems.

HOLOGIC®

Horizon™ DXA System
An Innovative Solution for Accurate Diagnosis

Hologic, the pioneer in X-ray based bone densitometry, takes advanced health assessment to a new level with the Horizon DXA System. This multi-faceted system can help clinicians assess bone health, body composition and cardiovascular risk — critical elements that will help patients keep life in motion.

RADIO PHARMA SOLUTIONS

iba

Find your solution for your radiopharmaceutical production

IBA offers complete solutions for your radiopharmaceutical production.
You can extend your tracer production for programs beyond oncology, such as cardiology and neurology.

COMECER
an ATS company

VDC-606 Touch Screen Dose Calibrator

- 10" touch screen medical ceritfed PC
- Easy to use
- IBC-LITE software included
- Accurate and fast measurements
- FDA approved and Medical Device
- Available for vials and syringes
- VIK-202 or VIK-203 ionisation chamber

EUROMEDICAL
INSTRUMENTS

Gamma and Fluorescence bi-modal detection

With a single readout module and numerous gamma probe options, the Europrobe 3.2 is a unique system that fulfills all needs of per and post-operative detection as well as per-cutaneous localisation within 7 major clinical fields.

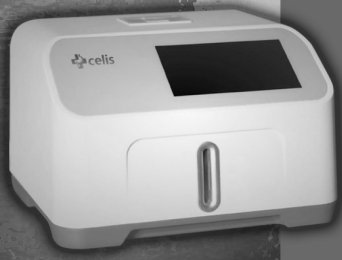

celis

Urea Breath Test Innovator

14C Urea Breath Test is used for primary diagnosis and post-treatment follow-up of H. pylori infections. The individual to be tested simply swallows 14C-urea. If H pylori presents, the enzyme urease produced by H pylori will metabolize 14C-urea to 14CO2 and ammonia. Then 14CO2 is transported in the blood to the lungs. When the patient exhales after a defined time this 14CO2 is captured in a breath collection card.

CAPINTEC
A MIRION MEDICAL COMPANY

Captus® 4000e Thyroid Uptake System

A comprehensive Nuclear Medicine Measurement System, with specific software modules for thyroid uptake, bioassay, wipe tests, automated quality assurance tests, and isotope library. Includes a fully functional 1024 channel MCA with auto and manual calibration. Timed activity mode features a programmable repetitive timed measurement program.

l'acn scientific laboratories
HOSMAN
HOSPITAL MANAGING

Particle counter VIDEOGAMMA RACK

The first apparatus of a new generation of gamma counters. It is the first device at all that allows measurements without needing to download the tubes from their rack. It is the first instrument in the world designed for carrying automatically tubes from their rack to the detection system. For the first time the area where measurement takes place and the area where tubes are positioned are separated. In this way any kind of interference is exclud-

GMS
PHILIPPINES
GLOBAL MEDICAL SOLUTIONS

3/F 14 Economia St., Bagumbayan, 1110 Quezon City, Philippines
Telephone No.: 8633-2051/53 | Fax: 8633-1840
www.globalmedicalsolutions.com

PHILIPPINE SOCIETY OF NUCLEAR MEDICINE

41st ANNUAL CONVENTION

FEBRUARY 7-8, 2026 • BORACAY

Save the date!

Celebrating 60 years of PSNM

Biograph Trinion PET/CT

Future-forward by design

siemens-healthineers.com/en-ph/biograph-trinion

Launch your future forward with a PET/CT that puts you confidently ahead of the curve and easily adapts to evolving clinical possibilities: Biograph Trinion™ with myExam Companion™.

Biograph Trinion PET/CT fully integrates best-in-class hardware and software to create one high-performance platform. A brand-new imaging experience puts patients more at ease, while users gain efficiency from a modern design and AI-supported workflow. Always the right fit, Biograph Trinion provides a sustainable investment from today onward—delivering reduced costs through its compact footprint, automated energy-saving features, and on-site scalability.

SIEMENS Healthineers

Symbia Pro.specta SPECT/CT
with myExam Companion

Modernize to MAXIMIZE

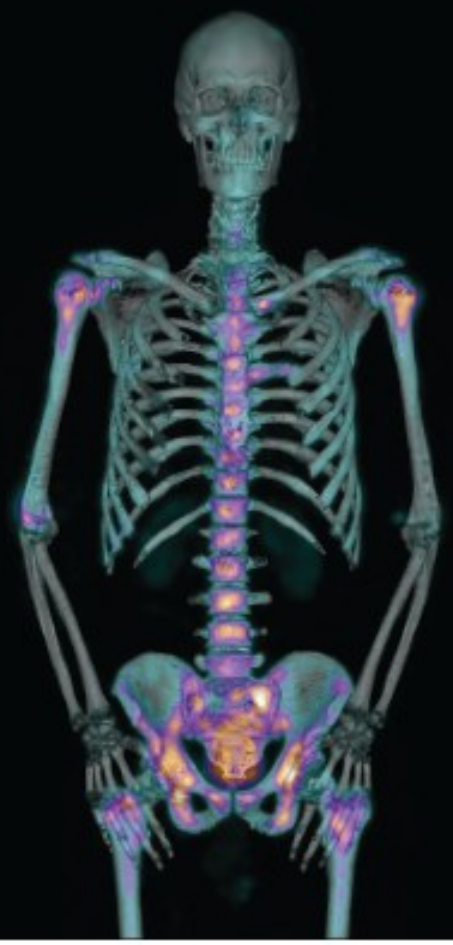

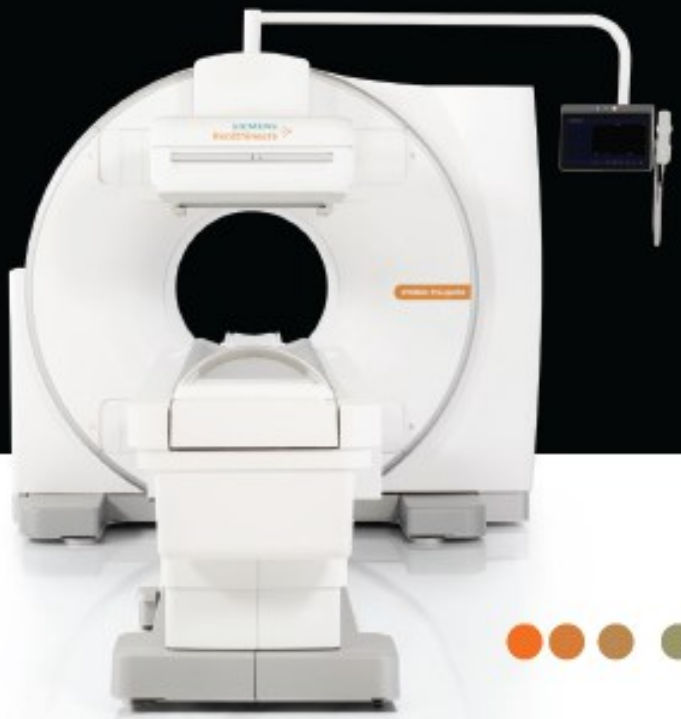

Take your nuclear medicine department into the future with intelligent SPECT/CT imaging. Symbia Pro.specta™ with myExam Companion™ gives you the power of more.

Redefine performance with new standards for SPECT/CT

Automatic SPECT motion correction and up to 64-slice CT enable faster scanning at the highest image quality.[1]

Reach your full potential with a smart workflow

A single, intuitive interface automates steps across the entire workflow—helping you achieve high-quality, reproducible results.

Achieve optimized imaging from dedicated clinical tools

A multi-purpose SPECT/CT that transforms into a specialized camera for cardiology, neurology, oncology, theranostics, and more.

[1] *Based on competitive literature at time of publication. Data on file.*

Symbia Pro.specta SPECT/CT is not commercially available in all countries. Future availability cannot be guaranteed. Please contact your local Siemens Healthineers organization for further details.

Learn more at siemens-healthineers.com/symbia-prospecta

SIEMENS Healthineers